

Exclusive photoproduction of $\chi_c\gamma$ pairs

Marat Siddikov¹, Ivan Zemlyakov^{1,2}

¹Departamento de Física, Universidad Técnica Federico Santa María,

y Centro Científico - Tecnológico de Valparaíso, Casilla 110-V, Valparaíso, Chile and

²Instituto de Física, Pontificia Universidad Católica de Valparaíso, Av. Brasil 2950, Valparaíso, Chile

In this manuscript we study the exclusive photoproduction of $\chi_c\gamma$ pairs in the collinear factorization framework. We found the coefficient functions for all possible spins and helicity projections of χ_c mesons and final-state photons in the leading order in the strong coupling α_s . In our analysis we focused on the contribution of the leading twist chiral even GPDs, and found that for all spin states of χ_c the suggested process is determined by the behavior of the gluon GPDs H_g in the ERBL kinematics. Using the phenomenological parametrizations of the GPDs from the literature, we estimated numerically the photoproduction cross-sections and the expected counting rates in the kinematics of middle-energy photoproduction experiments that could be realized at the Electron-Ion Collider. We observed that the χ_{c1} , χ_{c2} mesons are produced predominantly with the same polarization as the incoming photon, and the expected counting rates of $\chi_{c1}\gamma$ and $\chi_{c2}\gamma$ pairs are sufficiently large for their experimental study. We also analyzed the angular distribution of χ_c mesons in *electroproduction* experiments, and noticed that for some helicity components there are sizable angular asymmetries, which can be used as complementary observables for experimental study. Finally, we estimated the role of this process as a potential background to χ_c photoproduction, which has been recently suggested as a tool for studies of odderons. We found that the contribution of $\chi_c\gamma$ (with undetected photon) is on par with expected contributions of odderons and Primakoff mechanisms in the kinematics of small momentum transfer $|t| \lesssim 1 \text{ GeV}^2$, but becomes negligible at larger $|t|$.

I. INTRODUCTION

At present the Generalized Parton Distributions (GPDs) are being used as standard tools to describe the nonperturbative dynamics of partons in the hadronic target [1–9]. Nowadays *ab initio* computations of the GPDs are not feasible, and for this reason phenomenological extractions from experimental data remain the main way to access these objects. At present the available parametrizations of the GPDs largely rely on experimental data for $2 \rightarrow 2$ processes, such as Deeply Virtual Meson Production or Compton Scattering (DVMP and DVCS respectively). However, these channels have low sensitivity to some kinematic domains, and for this reason do not fix uniquely the GPDs of the target (the so-called “*shadow GPD problem*”) [10–12]. Although the experimental data provide reasonable constraints for some of the GPDs, currently, these constraints remain quite weak for the transversity GPDs and the gluon GPDs in the Efremov-Radyushkin-Brodsky-Lepage (ERBL) kinematics [13]. This stimulated a search of new channels that could complement existing $2 \rightarrow 2$ data, and several novel $2 \rightarrow 3$ processes have been proposed as possible instruments for phenomenological extractions of the GPDs [14–28]. All these channels inherently complement one another due to sensitivity to a unique flavor combination of the GPD flavors. The conditions for applicability of the factorization in such processes are usually satisfied in presence of hard scales which guarantee a good kinematic separation of the final-state hadrons [29, 30]. The aforementioned studies largely focused on the production of light meson or photon pairs, with their amplitudes primarily controlled by quark GPDs in both chiral-odd and chiral-even sectors. While gluon GPDs can also contribute in some of these channels, their contribution is typically intertwined with that of quarks, making the phenomenological analysis more complex. Furthermore, as was discussed in [31, 32], the presence of massless quarks and gluons in the theory may lead to nontrivial overlapping singularities which challenge the applicability of the collinear factorization unless the distribution amplitude of produced light meson vanishes rapidly enough at the endpoints.

Recently in [33] we suggested that the gluonic GPDs can be studied in exclusive photoproduction processes which include a quarkonium and a photon in the final state. The process $\gamma p \rightarrow J/\psi \gamma p$ is strongly suppressed, since it requires C -odd exchanges in t -channel. For this reason, in our previous study we focused on $\eta_c\gamma$ production. In this manuscript we extend those studies and analyze $\chi_c\gamma$ photoproduction, which also proceeds without C -odd exchanges in t -channel. In contrast to η_c mesons, the χ_c mesons are the lightest P -wave quarkonia, and thus can be used as independent tools for study of GPDs. Due to large branching fractions of the radiative decays $\chi_{cJ} \rightarrow J/\psi \gamma$ ($J = 1, 2$) and very clean experimental signature of J/ψ mesons (an $\ell^+\ell^-$ lepton pair with appropriate mass), we expect that it will be possible to distinguish experimentally the events which correspond to this process. The sufficiently heavy mass of χ_c and the fact that it is an excited state implies that feed-down contributions (from decays of heavier quarkonia) should be negligible. The mass of this quarkonium also serves as a natural hard scale, which justifies the perturbative treatment even for the photoproduction [34, 35], and allows to avoid many collinear and soft singularities which may appear in diagrams with massless quarks. Finally, the heavy quark and quarkonia masses justify the application of

NRQCD approach for description of the $\bar{Q}Q$ pair hadronization into final state quarkonium [36–42]. We expect that the suggested process can be studied in low- and middle-energy photon-proton collisions in ultraperipheral kinematics at LHC, as well as in electron-proton collisions at the future Electron Ion Collider (EIC) [7–9].

The proposed process $\gamma p \rightarrow \chi_c \gamma p$ (with unobserved photon) also deserves attention as a possible background to the exclusive χ_c photoproduction $\gamma p \rightarrow \chi_c p$. The latter process has been proposed recently in [43] for study of odderons. Since the $\gamma p \rightarrow \chi_c \gamma p$ process does not require C -odd exchanges in t -channel, its cross-section in certain kinematics is sufficiently large and can lead to a substantial background for odderon searches via χ_c photoproduction.

The subsequent sections are organized as follows. In the following Section II we explain in detail the kinematics of the process and describe the theoretical approach used for evaluation of the partonic amplitudes (coefficient functions) of the process. However, due to a large number of similarly looking expressions for helicity components, which occupy a lot of space, the final expressions for these objects are relocated to Appendix B. The Section III includes our numerical estimates for the cross-sections and counting rates obtained with some commonly used parametrizations of the GPDs. In its subsection III C we compare the cross-sections of the odderon-mediated $\gamma p \rightarrow \chi_c p$ and the proposed $\gamma p \rightarrow \chi_c p \gamma$ with unobserved photon. In the final Section IV we summarize our findings and draw conclusions.

II. THEORETICAL FRAMEWORK

The choice of the reference frame and light-cone parametrization of the particles' momenta for $\chi_c \gamma$ -photoproduction largely coincide with what was done in [33] for analysis of $\eta_c \gamma$ production. In the limit of massless quarkonium (but fixed invariant mass of quarkonium) this parametrization reduces to the expressions obtained in [14, 15] for exclusive photoproduction of *light* meson-photon pairs $\gamma\pi$, $\gamma\rho$ with large invariant mass. In what follows we will consider that the mass of the quarkonium M_{χ_c} is a large parameter, parametrically of the same order as the invariant mass $M_{\chi_c \gamma}$. At the same time, we will explicitly exclude the kinematics where the emitted photon is soft, and thus $M_{\chi_c \gamma} \approx M_{\chi_c}$. Since the spectrum of equivalent photons in ep and pp collisions is dominated by quasi-real photons with small virtuality $Q \approx 0$, in what follows we will focus only on the photoproduction by transversely polarized real photons. Below in the subsections II A, II B we describe the kinematic variables used to describe the 4-momenta of all particles and explain the main steps used for evaluation of the partonic amplitudes .

A. Kinematics of the process

For our evaluations we will work in the photon-proton collision frame, where the colliding proton and the incoming quasireal photon move along the axis z in opposite directions. In what follows we will use a notation q for the 4-momentum of the incoming photon, $P_{\text{in}}, P_{\text{out}}$ for the momenta of the target before and after interaction, k for the momentum of the final-state photon, and p_{χ_c} for the momentum of produced χ_c meson. For the light-cone components of all the vectors, we will use the Kogut-Soper convention [44], and bold-face letters with subindex \perp for the transverse (1,2)-components, namely

$$v^\mu = (v^+, \quad v^-, \quad \boldsymbol{v}_\perp) = v^+ n_+ + v^- n_- + \boldsymbol{v}_\perp, \quad v^\pm = \frac{v^0 \pm v^3}{\sqrt{2}}, \quad \boldsymbol{v}_\perp = v_x \hat{\mathbf{x}} + v_y \hat{\mathbf{y}}, \quad (1)$$

where the light-cone vectors n_\pm are defined as $n_+ = (1, 0, \mathbf{0}_\perp)$ and $n_- = (0, 1, \mathbf{0}_\perp)$. The square of the vector in this convention is given by

$$v^2 \equiv v^\mu v_\mu = 2v^+ v^- - \boldsymbol{v}_\perp^2, \quad (2)$$

and the convolution with Dirac γ -matrix reads as

$$\hat{v} = \gamma^\mu v_\mu = \gamma^+ v^- + \gamma^- v^+ - \boldsymbol{\gamma}_\perp \cdot \boldsymbol{v}_\perp. \quad (3)$$

The light-cone decomposition of the particles' momenta may be written as [14, 15]

$$q^\mu = \left(0, \sqrt{\frac{s}{2}}, \mathbf{0}_\perp \right) \quad (4)$$

$$P_{\text{in}}^\mu = \left((1 + \xi) \sqrt{\frac{s}{2}}, \frac{m_N^2}{\sqrt{2s}(1 + \xi)}, \mathbf{0}_\perp \right), \quad (5)$$

$$P_{\text{out}}^\mu = \left((1 - \xi) \sqrt{\frac{s}{2}}, \frac{m_N^2 + \Delta_\perp^2}{\sqrt{2s}(1 - \xi)}, \boldsymbol{\Delta}_\perp \right), \quad (6)$$

$$\Delta^\mu = P_{\text{out}}^\mu - P_{\text{in}}^\mu = \left(-2\xi \sqrt{\frac{s}{2}}, \frac{2\xi m_N^2 + (1+\xi) \Delta_\perp^2}{\sqrt{2s}(1-\xi^2)}, \boldsymbol{\Delta}_\perp \right) \quad (7)$$

$$p_{\chi_c}^\mu = \left(\frac{(\mathbf{p}_\perp^{\chi_c})^2 + M_{\chi_c}^2}{\alpha_{\chi_c} \sqrt{2s}}, \alpha_{\chi_c} \sqrt{\frac{s}{2}}, \mathbf{p}_\perp^{\chi_c} \right), \quad \mathbf{p}_\perp^{\chi_c} := -\mathbf{p}_\perp - \frac{\boldsymbol{\Delta}_\perp}{2} \quad (8)$$

$$k^\mu = \left(\frac{(\mathbf{k}_\perp^\gamma)^2}{(1-\alpha_{\chi_c}) \sqrt{2s}}, (1-\alpha_{\chi_c}) \sqrt{\frac{s}{2}}, \mathbf{k}_\perp^\gamma \right), \quad \mathbf{k}_\perp^\gamma := \mathbf{p}_\perp - \frac{\boldsymbol{\Delta}_\perp}{2} \quad (9)$$

$$\mathbf{p}_\perp \equiv (\mathbf{k}_\perp^\gamma - \mathbf{p}_\perp^{\chi_c}) / 2 \quad (10)$$

We may rewrite the invariant Mandelstam variables $S_{\gamma N}, t$ in terms of these variables as

$$S_{\gamma N} \equiv W^2 = (q + P_{\text{in}})^2 = s(1+\xi) + m_N^2, \quad (11)$$

$$t = (P_{\text{out}} - P_{\text{in}})^2 = -\frac{1+\xi}{1-\xi} \Delta_\perp^2 - \frac{4\xi^2 m_N^2}{1-\xi^2}. \quad (12)$$

From Eq. (12) we can see that at given ξ , the invariant momentum transfer t is bound by

$$t \leq t_{\min} = -\frac{4\xi^2 m_N^2}{1-\xi^2}.$$

In order to characterize the kinematics of the final-state quarkonium and photon, we also define the invariants

$$u' = (p_{\chi_c} - q)^2, \quad t' = (k - q)^2, \quad M_{\gamma\chi_c}^2 = (k + p_{\chi_c})^2, \quad (13)$$

which correspond to invariant momentum transfer from the incoming photon to the χ_c meson, momentum transfer to the final-state (outgoing) photon, and the invariant mass of the $\gamma\chi_c$ pair. These variables are related with each other as

$$-u' - t' = M_{\gamma\chi_c}^2 - M_{\chi_c}^2 - t. \quad (14)$$

Rewriting the variable u' in the rest frame of the quarkonium, we may obtain an additional constraint

$$u' = M_{\chi_c}^2 - 2E_\gamma M_{\chi_c} \leq M_{\chi_c}^2 \quad \Rightarrow \quad -t' \leq M_{\gamma\chi_c}^2 - t. \quad (15)$$

The polarization vectors of the incoming and outgoing real photons with momenta \mathbf{k} are chosen in the light-cone gauge as

$$\varepsilon_T^{(\lambda=\pm 1)}(\mathbf{k}) = \left(\frac{\mathbf{e}_\lambda^\perp \cdot \mathbf{k}_\perp}{k^-}, 0, \mathbf{e}_\lambda^\perp \right), \quad \mathbf{e}_\lambda^\perp = \frac{1}{\sqrt{2}} \begin{pmatrix} 1 \\ i\lambda \end{pmatrix}, \quad (16)$$

namely they satisfy the gauge condition $A^- = 0$. As we discuss in Appendix A, this choice is preferable since it allows to avoid evaluation of additional contributions which stem from coupling of the external photons to the gauge link in the χ_c meson.

The parametrization (4-9) satisfies various nontrivial constraints on momenta of the produced particles, such as onshellness, conservation of the energy-momentum, etc. In order to clarify the physical meaning of the introduced variables and the role of the aforementioned constraints, in the Figures 1 and 2 we have shown the values of transverse momenta $\mathbf{p}_{\chi_c}^\perp = -\mathbf{p}_\perp - \boldsymbol{\Delta}_\perp$, $\mathbf{p}_\gamma^\perp = \mathbf{p}_\perp - \boldsymbol{\Delta}_\perp/2$ which may be achieved at fixed rapidities of the final-state particles in the kinematically allowed domains (colored bands). The color of each pixel in the Figure (1) in the left and right panels illustrates the value of the azimuthal angle ϕ between the transverse momenta of χ_c, γ and the invariant mass $M_{\gamma\chi_c}$, respectively. In the Figure 2 we also have shown the relation of the variables ξ, α_{χ_c} to rapidities y_{χ_c}, y_γ .

In what follows we will focus on the kinematics where the variables $m_N, |\boldsymbol{\Delta}_\perp|, t$ are negligibly small, whereas all the other variables are parametrically large, $\sim M_{\chi_c}$. In this kinematics it is possible to simplify the light-cone decomposition (4-9) and obtain approximate relations of the above-mentioned variables with $\alpha_{\chi_c}, \mathbf{p}_\perp$, viz:

$$-t' \approx \alpha_{\chi_c} M_{\gamma\chi_c}^2 - M_{\chi_c}^2, \quad -u' \approx (1 - \alpha_{\chi_c}) M_{\gamma\chi_c}^2, \quad (17)$$

$$\mathbf{p}_\perp^2 \approx (1 - \alpha_{\chi_c}) (\alpha_{\chi_c} M_{\gamma\chi_c}^2 - M_{\chi_c}^2) = -t' (1 - \alpha_{\chi_c}), \quad M_{\gamma\chi_c}^2 \approx 2s\xi \quad (18)$$

The physical constraint for the momenta of real (on shell) photons

$$t' = (q - k)^2 = -2q \cdot k = -2|\mathbf{q}| |\mathbf{k}| (1 - \cos \theta_{\mathbf{q}, \mathbf{k}}) \leq 0, \quad (19)$$

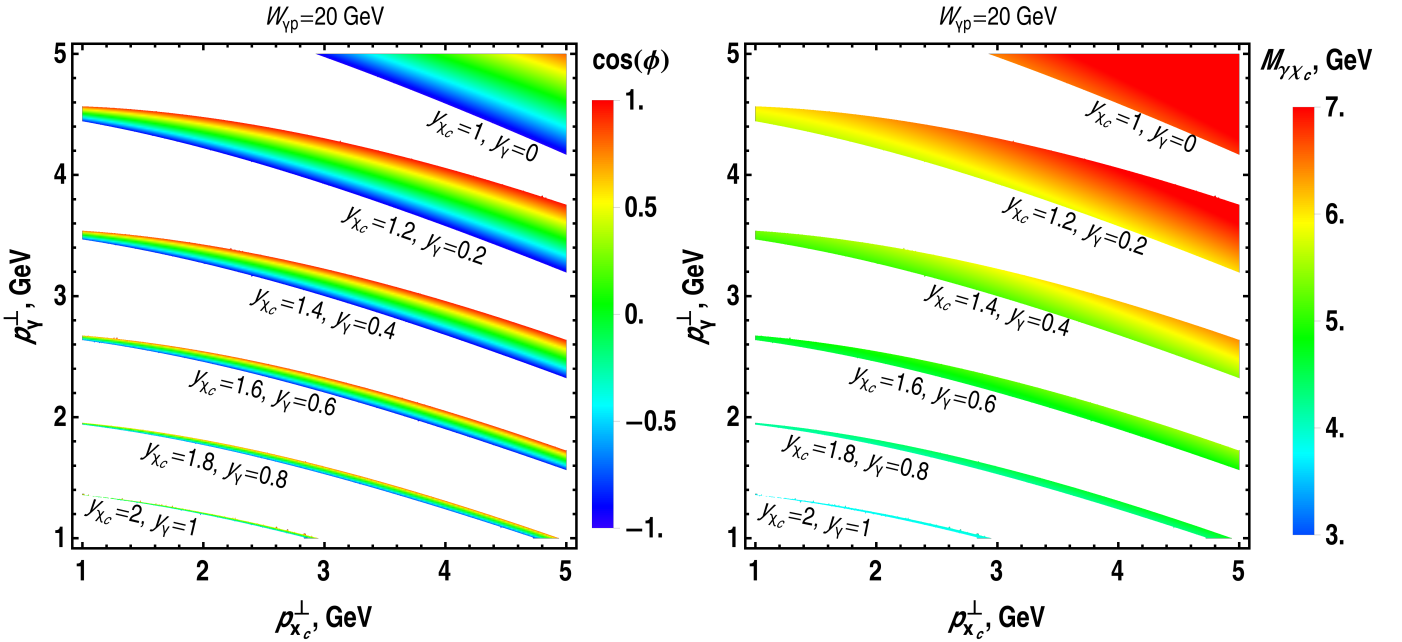


Figure 1. (Color online) Colored bands represent kinematically allowed region for $\chi_c\gamma$ pair production at fixed invariant energy W and fixed rapidities y_{χ_c}, y_γ . For both particles we chose positive sign of rapidity in direction of the photon. Since photon moves in “minus” direction in (4), this corresponds to nonstandard definition of rapidity $y_a = \frac{1}{2} \ln(k_a^-/k_a^+)$, $a = \chi_c, \gamma$. The increase of rapidities implies increase of the longitudinal momenta, and thus in view of energy conservation corresponds to smaller transverse momenta. In the left plot the color of each pixel reflects the azimuthal angle ϕ between the transverse momenta $\mathbf{p}_{\chi_c}^\perp = -\mathbf{p}_\perp - \Delta_\perp/2$ and $\mathbf{p}_\gamma^\perp = \mathbf{p}_\perp - \Delta_\perp/2$. Similarly, in the right plot the color reflects the value of invariant mass $M_{\gamma\chi_c}$ in the chosen kinematics.

together with constraint $\mathbf{p}_\perp^2 \geq 0$ implies that the variable α_{χ_c} is bound by

$$M_{\chi_c}^2/M_{\gamma\chi_c}^2 \leq \alpha_{\chi_c} \leq 1, \quad (20)$$

so for the Mandelstam variable u' we get

$$0 \leq -u' \leq (-u')_{\max} = M_{\gamma\chi_c}^2 - M_{\chi_c}^2 - t. \quad (21)$$

The produced χ_c and emitted photon are kinematically well-separated from the recoil proton, if the corresponding invariant masses satisfy

$$(P_{\text{out}} + p_{\chi_c})^2 \approx M_{\chi_c}^2 + s\alpha_{\chi_c}(1-\xi) \gg (m_N + M_{\chi_c})^2, \quad (P_{\text{out}} + k)^2 \approx s(1-\alpha_{\chi_c})(1-\xi) \gg m_N^2 \quad (22)$$

These conditions are satisfied everywhere except a border region $\alpha_{\chi_c} \approx 1$, or equivalently $u' \approx 0$. The invariant cross-section of the process $\gamma p \rightarrow \chi_c \gamma p$ can be rewritten in terms of these variables as

$$\frac{d\sigma_{\gamma p \rightarrow \chi_c \gamma p}^{(\lambda, \sigma, H)}}{dt dt' dM_{\gamma\chi_c}} \approx \frac{\left| \mathcal{A}_{\gamma p \rightarrow \chi_c \gamma p}^{(\lambda, \sigma, H)} \right|^2}{128\pi^3 W^4 M_{\gamma\chi_c}} \quad (23)$$

where $\mathcal{A}_{\gamma p \rightarrow \chi_c \gamma p}^{(\lambda, \sigma, H)}$ is the invariant amplitude, λ, σ are the helicities of the incoming and outgoing photons, and H is the helicity of χ_c meson. Similarly, the *electroproduction* cross-section is given by a convolution of the leptonic tensor $L_{\mu\nu}$ with the corresponding amplitudes, which in the helicity basis can be rewritten as

$$\frac{d\sigma_{ep \rightarrow e\chi_c \gamma p}^{(\sigma, H)}}{d\Omega} \approx \frac{1}{Q^4} \sum_{\lambda, \bar{\lambda}} L_{\lambda, \bar{\lambda}} \frac{\left(\mathcal{A}_{\gamma p \rightarrow \chi_c \gamma p}^{(\lambda, \sigma, H)} \right)^* \mathcal{A}_{\gamma p \rightarrow \chi_c \gamma p}^{(\bar{\lambda}, \sigma, H)}}{128\pi^3 W^4 M_{\gamma\chi_c}}, \quad (24)$$

the shorthand notation $d\Omega$ stands for the phase volume $d\Omega \equiv d\ln W^2 dQ^2 dt dt' dM_{\gamma\chi_c} d\varphi$, the angle φ is the angle between the leptonic and hadronic scattering planes (see Figure 3 for more accurate definition), and $\lambda, \bar{\lambda}$ are the

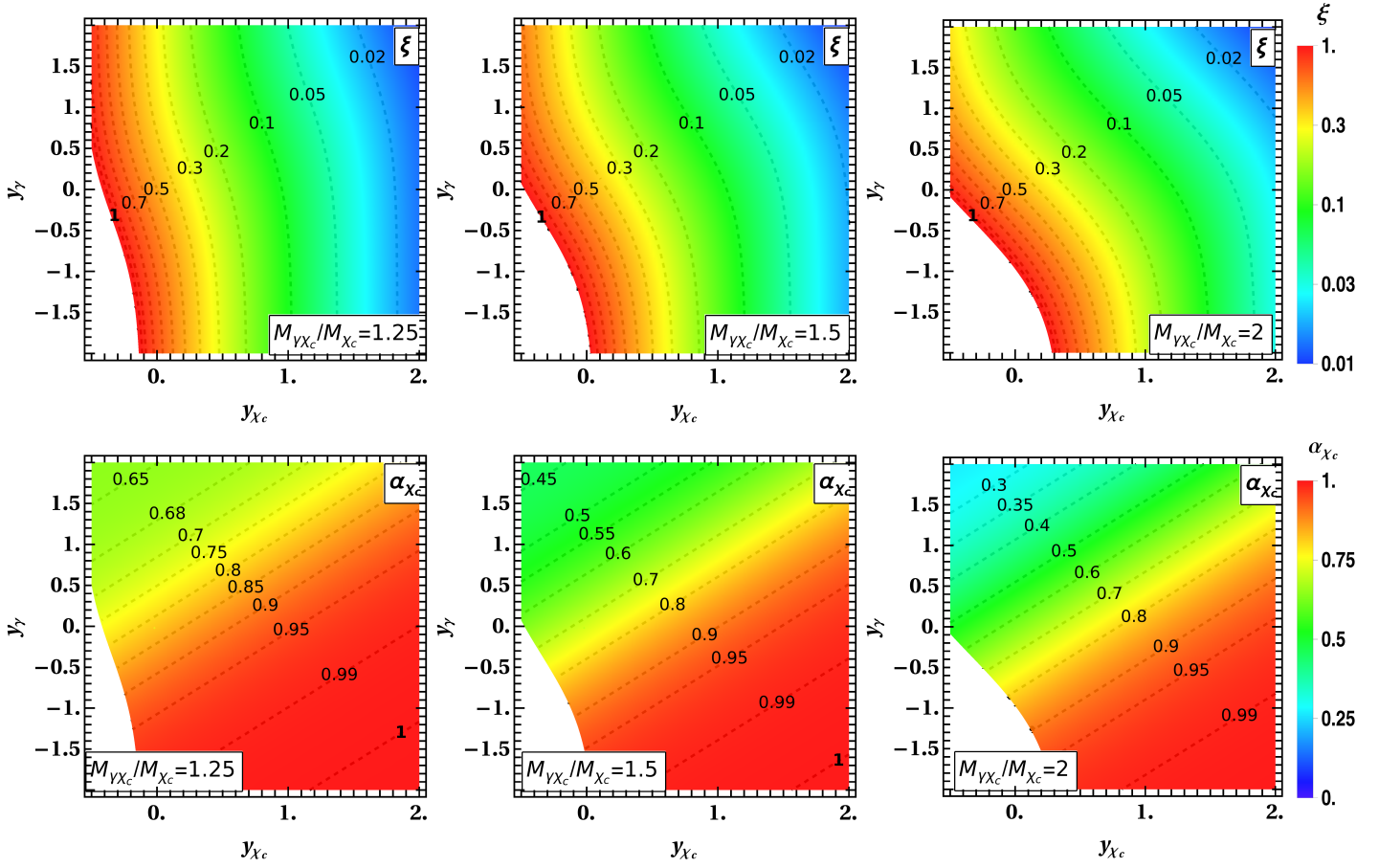


Figure 2. (Color online) The contour plot shows the dependence of the skewedness ξ (upper row) and the variable α_{χ_c} (lower row) on the rapidities of the final state particles y_{χ_c} , y_γ at different fixed values of the invariant mass $M_{\chi\gamma c}$. The labels near the contour lines (and corresponding color shading) show the values of ξ , α_{χ_c} . For both particles positive sign of rapidity corresponds to motion in the direction of the incoming photon. For the sake of simplicity we consider the kinematics with zero transverse momentum Δ_\perp , which gives the dominant contribution in the total cross-section.

helicities of the incoming photon in the amplitude and its conjugate. As was discussed in [45, 46], the leptonic tensor $L_{\lambda,\bar{\lambda}}$ has nondiagonal components in helicity basis. Due to these interference contribution, the cross-section of the electroproduction may have a nontrivial dependence on the angle φ , namely

$$\begin{aligned} \frac{d\sigma_{ep \rightarrow e\gamma\chi_c p}}{d\Omega} = & \epsilon \frac{d\sigma^{(L)}}{d\Omega} + \frac{d\sigma^{(T)}}{d\Omega} + \sqrt{\epsilon(1+\epsilon)} \cos \varphi \frac{d\sigma^{(LT)}}{d\Omega} + \sqrt{\epsilon(1+\epsilon)} \sin \varphi \frac{d\sigma^{(LT')}}{d\Omega} + \\ & + \epsilon \cos 2\varphi \frac{d\sigma^{(TT)}}{d\Omega} + \epsilon \sin 2\varphi \frac{d\sigma^{(T'T')}}{d\Omega}, \end{aligned} \quad (25)$$

where we introduced the superscript letters L, T, T' in the right-hand side of (25) to show the contributions of the longitudinal and transverse polarizations $\lambda, \bar{\lambda}$ (as well as their possible interference). The shorthand notation ϵ in (25) is the usual ratio of the longitudinal and transverse photon fluxes,

$$\epsilon \approx \frac{1-y}{1-y+y^2/2}, \quad (26)$$

and y is the fraction of the electron energy which passes to the virtual photon (the so-called inelasticity). This variable may be related to the invariant energy $\sqrt{s_{ep}}$ of the electron-proton collision as

$$y = \frac{W^2 + Q^2 - m_N^2}{s_{ep} - m_N^2}. \quad (27)$$

Since we are mostly interested in the small- Q kinematics, which gives the dominant contribution, we may disregard the contributions of the longitudinal polarization and rewrite the cross-section (25) as

$$\frac{d\sigma_{ep \rightarrow e\gamma\chi_c p}}{d\Omega} \approx \frac{d\sigma^{(T)}}{d\Omega} + \epsilon \cos 2\varphi \frac{d\sigma^{(TT)}}{d\Omega} + \epsilon \sin 2\varphi \frac{d\sigma^{(T'T)}}{d\Omega} \approx \frac{d\sigma^{(T)}}{d\Omega} (1 + c_2 \cos 2\varphi + s_2 \sin 2\varphi) \quad (28)$$

where the leading (angular independent) contribution may be related to the photoproduction cross-section (23) in the equivalent photon approximation [48–50] as

$$\frac{d\sigma^{(T)}}{\ln W^2 dQ^2 dt dt' dM_{\gamma\chi_c} d\varphi} \approx \frac{\alpha_{\text{em}}}{2\pi^2 Q^2} \left(1 - y + \frac{y^2}{2} - (1-y) \frac{Q_{\min}^2}{Q^2} \right) \frac{d\sigma_{\gamma p \rightarrow \gamma\chi_c p}}{dt dt' dM_{\gamma\chi_c}}, \quad (29)$$

the variable $Q_{\min}^2 = m_e^2 y^2 / (1-y)$, m_e is the mass of the electron. The coefficients (angular harmonics) c_2 , s_2 in (28) may be related to different components of the amplitude $\mathcal{A}_{\gamma p \rightarrow \chi_c \gamma p}^{(\lambda, \sigma, H)}$ as

$$c_2 = \frac{2\epsilon \operatorname{Re} \left(\mathcal{A}_{\gamma p \rightarrow \chi_c \gamma p}^{(-,+H)*} \mathcal{A}_{\gamma p \rightarrow \chi_c \gamma p}^{(+,+H)} \right)}{\left| \mathcal{A}_{\gamma p \rightarrow \chi_c \gamma p}^{(+,+H)} \right|^2 + \left| \mathcal{A}_{\gamma p \rightarrow \chi_c \gamma p}^{(-,+H)} \right|^2}, \quad s_2 = \frac{2\epsilon \operatorname{Im} \left(\mathcal{A}_{\gamma p \rightarrow \chi_c \gamma p}^{(-,+H)*} \mathcal{A}_{\gamma p \rightarrow \chi_c \gamma p}^{(+,+H)} \right)}{\left| \mathcal{A}_{\gamma p \rightarrow \chi_c \gamma p}^{(+,+H)} \right|^2 + \left| \mathcal{A}_{\gamma p \rightarrow \chi_c \gamma p}^{(-,+H)} \right|^2}, \quad (30)$$

and for derivation of (30) we used explicit expressions for the components of the leptonic tensor $L_{\lambda, \bar{\lambda}}$ in helicity basis [46]

$$L_{\pm, \pm} = e^2 \frac{Q^2 (2 - 2y + y^2)}{y^2}, \quad L_{\pm, \mp} = e^2 e^{\pm 2i\varphi} \frac{2Q^2 (1-y)}{y^2}. \quad (31)$$

The ratio of c_2 and s_2 gives us access to the relative phase of $\mathcal{A}_{\gamma p \rightarrow \chi_c \gamma p}^{(+,+H)}$ and $\mathcal{A}_{\gamma p \rightarrow \chi_c \gamma p}^{(-,+H)}$ amplitudes, namely

$$\frac{s_2}{c_2} = \tan \left[\arg \left(\mathcal{A}_{\gamma p \rightarrow \chi_c \gamma p}^{(+,+H)} \right) - \arg \left(\mathcal{A}_{\gamma p \rightarrow \chi_c \gamma p}^{(-,+H)} \right) \right] \quad (32)$$

which presents a new observable.

B. The amplitude of the $\chi_c \gamma$ pair production

The evaluation of the amplitude $\mathcal{A}_{\gamma p \rightarrow \chi_c \gamma p}$ follows the standard rules of the collinear factorization framework, and allows to express it in terms of the GPDs of the target [1, 3–5, 7] convoluted with process-dependent partonic amplitudes (coefficient functions). As discussed earlier, in the heavy quark mass limit we may disregard the proton mass of the proton m_N and all components of the momentum transfer Δ^μ . We will consider that the invariant mass $M_{\gamma\chi_c}$ is large enough to get rid of the feed-down contributions from radiative decays of higher state charmonia. In our evaluations we may disregard the fact that the frame (4–9) differs from the symmetric frame where the GPDs conventionally are introduced, because the transverse Lorentz boost which relates the two frames is given by

$$\ell^+ \rightarrow \ell^+, \quad \ell^- \rightarrow \ell^- + \ell^+ \beta_\perp^2 + \boldsymbol{\ell}_\perp \cdot \boldsymbol{\beta}_\perp, \quad \boldsymbol{\ell}_\perp \rightarrow \boldsymbol{\ell}_\perp + \ell^+ \boldsymbol{\beta}_\perp, \quad \text{where } \boldsymbol{\beta}_\perp = -\boldsymbol{\Delta}_\perp / (2\bar{P}_{\text{SRF}}^+), \quad (33)$$

and the momentum $\boldsymbol{\Delta}_\perp$ is eventually disregarded in coefficient function. For this reason, the momenta of the active parton (gluon) before and after interaction can be approximated as

$$k_i = ((x + \xi)\bar{P}^+, 0, 0), \quad k_f = ((x - \xi)\bar{P}^+, 0, \boldsymbol{\Delta}_\perp), \quad (34)$$

where $\bar{P}^+ = (P_{\text{in}}^+ + P_{\text{out}}^+)/2$ and the variable x is the light-cone fraction of the average parton momentum defined as $x = (k_i^+ + k_f^+) / (2\bar{P}^+)$. For unpolarized proton the straightforward spinor algebra yields for the square of the amplitude [51]

$$\sum_{\text{spins}} \left| \mathcal{A}_{\gamma p \rightarrow M_1 M_2 p}^{(\lambda, \sigma, H)} \right|^2 = \left[4(1 - \xi^2) \left(\left| \mathcal{H}_{\gamma\chi_c}^{(\lambda, \sigma, H)} \right|^2 + \left| \tilde{\mathcal{H}}_{\gamma\chi_c}^{(\lambda, \sigma, H)} \right|^2 \right) - 2\xi^2 \operatorname{Re} \left(\mathcal{H}_{\gamma\chi_c}^{(\lambda, \sigma, H)} \mathcal{E}_{\gamma\chi_c}^{(\lambda, \sigma, H)*} + \tilde{\mathcal{H}}_{\gamma\chi_c}^{(\lambda, \sigma, H)} \tilde{\mathcal{E}}_{\gamma\chi_c}^{(\lambda, \sigma, H)*} \right) \right] \quad (35)$$

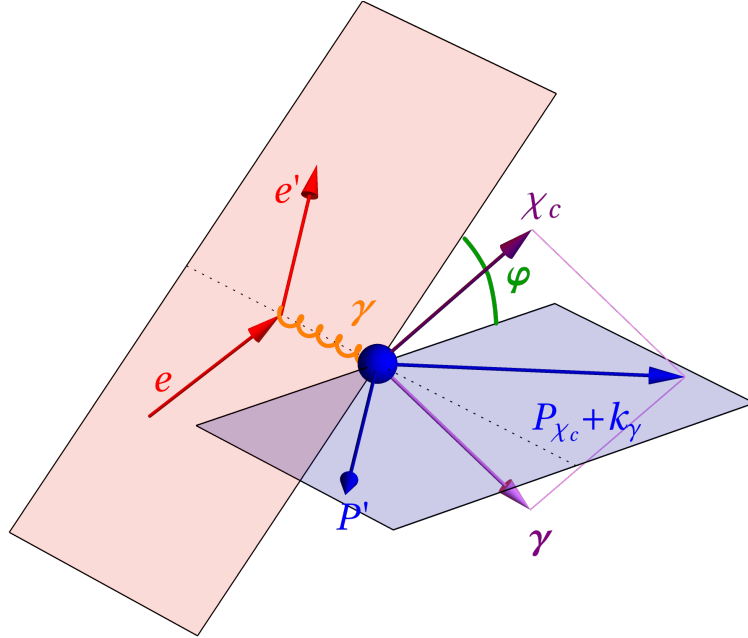


Figure 3. (Color online) Definition of the angle φ between the lepton and hadron scattering planes for electroproduction of $\chi_c\gamma$ pairs. The target is shown as a colored sphere, which rests in its reference frame or moves along a dotted line towards the collision point with photon γ^* . The lepton plane is formed by the momenta of the electron before and after the scattering (marked with labels e, e') and also include the momentum of the photon γ^* due to momentum conservation. The hadron plane by definition is formed by the momenta of incoming photon γ^* and the recoiled proton P_{out} . The momenta of quarkonium and emitted photon in general do not collinear to the hadronic plane, however their sum $p_{\chi_c} + k_\gamma$ in view of the momentum conservation also belongs to the hadron scattering plane.

$$-\left(\xi^2 + \frac{t}{4m_N^2}\right) \left| \mathcal{E}_{\gamma\chi_c}^{(\lambda, \sigma, H)} \right|^2 - \xi^2 \frac{t}{4m_N^2} \left| \tilde{\mathcal{E}}_{\gamma\chi_c}^{(\lambda, \sigma, H)} \right|^2 \Bigg],$$

where, inspired by previous studies of Compton scattering and single-meson production [51, 52], we introduced shorthand notations for the convolutions of the partonic amplitudes with GPDs

$$\mathcal{H}_{\gamma\chi_c}^{(\lambda, \sigma, H)}(\xi, t) = \int dx C_{\gamma\chi_c}^{(\lambda, \sigma, H)}(x, \xi) H_g(x, \xi, t), \quad \mathcal{E}_{\gamma\chi_c}^{(\lambda, \sigma, H)}(y_1, y_2, t) = \int dx C_{\gamma\chi_c}^{(\lambda, \sigma, H)}(x, \xi) E_g(x, \xi, t), \quad (36)$$

$$\tilde{\mathcal{H}}_{\gamma\chi_c}^{(\lambda, \sigma, H)}(\xi, t) = \int dx \tilde{C}_{\gamma\chi_c}^{(\lambda, \sigma, H)}(x, \xi) \tilde{H}_g(x, \xi, t), \quad \tilde{\mathcal{E}}_{\gamma\chi_c}^{(\lambda, \sigma, H)}(y_1, y_2, t) = \int dx \tilde{C}_{\gamma\chi_c}^{(\lambda, \sigma, H)}(x, \xi) \tilde{E}_g(x, \xi, t). \quad (37)$$

The partonic amplitudes $C_{\gamma\chi_c}^{(\lambda, \sigma, H)}$, $\tilde{C}_{\gamma\chi_c}^{(\lambda, \sigma, H)}$ can be evaluated perturbatively, taking into account the diagrams shown in the Figure 4. For evaluation of these amplitudes we assume that the quarkonium is described by the wave function $\Phi_{\chi_c}(z, \mathbf{k}_\perp)$, and use explicit expressions for different helicity components of the latter from [43]. Since the quarkonium moves with nonzero transverse momentum in chosen frame, the relative momentum between the quark and antiquark can be expressed in terms of z, \mathbf{k}_\perp as

$$k_Q^\mu - k_{\bar{Q}}^\mu = k^\mu = \left(\frac{(1-2z)(M_{\chi_c}^2 + \mathbf{p}_{\perp\chi_c}^2) - 2\mathbf{k}_\perp \cdot \mathbf{p}_{\perp\chi_c}}{\sqrt{2}p_{\chi_c}^-}, \quad \sqrt{2}p_{\chi_c}^-(2z-1), \quad \mathbf{k}_\perp \right) \quad (38)$$

and is orthogonal to the vector $p_{\chi_c}^\mu$. In the heavy quark mass limit the internal motion of the quarks becomes slow, so the the wave function $\Phi_{\chi_c}(z, \mathbf{k}_\perp)$ becomes very narrow in the momentum space. For this reason, we can make expansion of the partonic amplitudes over the small components \mathbf{k}_\perp , $(1-2z)$ up to the first nonvanishing order. Due

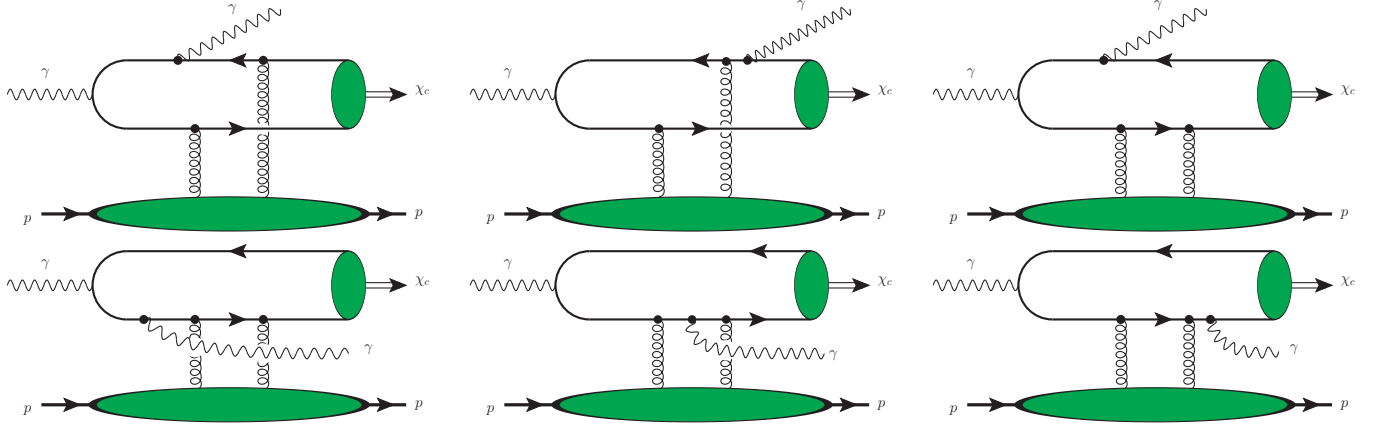


Figure 4. The diagrams which contribute to $\chi_c \gamma$ photoproduction. It is implied that each diagram should be supplemented with a charge conjugate diagram (with inverted heavy quark lines) and additional contribution with permuted gluon vertices in t -channel (24 diagrams in total, see Appendix B for more details). We assume that the electromagnetic field is given in axial gauge $\epsilon \cdot p_{\chi_c} = 0$ and thus do not take into account contributions with coupling of the electromagnetic field to the Wilson line inside χ_c .

to C -parity all the odd powers of $(1 - 2z)$, \mathbf{k}_\perp eventually cancel and the expansion starts from the second order terms in \mathbf{k}_\perp^2 , $(2z - 1)^2$. Matching of this procedure with NRQCD framework in the heavy quark mass limit is discussed in Appendix A (we remind that for P -wave the NRQCD projector is more complicated than for the S -wave and includes differential operators). Using the relations (A14, A15) for light-cone amplitudes and explicit parametrization (A16) provided in Appendix, we may express the averages

$$\left\langle \left(z - \frac{1}{2} \right)^2 \right\rangle = \int \frac{dz d^2 \mathbf{k}}{z(1-z)8\pi^2} \phi(z, \mathbf{k}_\perp) \left(z - \frac{1}{2} \right)^2, \quad \langle \mathbf{k}_\perp^2 \rangle = \int \frac{dz d^2 \mathbf{k}}{z(1-z)8\pi^2} \phi(z, \mathbf{k}_\perp) \mathbf{k}_\perp^2 \quad (39)$$

in terms of the NRQCD LDME $\left\langle \mathcal{O}_{\chi_c}^{[1]} \left({}^3P_J^{[1]} \right) \right\rangle$. The remaining steps of evaluation of these amplitudes are straightforward and are discussed in more detail in Appendix B. The final expressions for the coefficient functions conveniently can be represented as

$$C_{\gamma\chi_c}^{(\lambda, \sigma, H)} = \frac{m_c^2}{M_{\chi_c}^2} c_{\gamma\chi_c}^{(\lambda, \sigma, H)} + d_{\gamma\chi_c}^{(\lambda, \sigma, H)} \approx \frac{1}{4} c_{\gamma\chi_c}^{(\lambda, \sigma, H)} + d_{\gamma\chi_c}^{(\lambda, \sigma, H)} \quad (40)$$

$$\tilde{C}_{\gamma\chi_c}^{(\lambda, \sigma, H)} = \frac{m_c^2}{M_{\chi_c}^2} \tilde{c}_{\gamma\chi_c}^{(\lambda, \sigma, H)} + \tilde{d}_{\gamma\chi_c}^{(\lambda, \sigma, H)} \approx \frac{1}{4} \tilde{c}_{\gamma\chi_c}^{(\lambda, \sigma, H)} + \tilde{d}_{\gamma\chi_c}^{(\lambda, \sigma, H)} \quad (41)$$

where the terms $c_{\gamma\chi_c}^{(\lambda, \sigma, H)}$, $d_{\gamma\chi_c}^{(\lambda, \sigma, H)}$ correspond to contributions which stem from expansion over $(z - \frac{1}{2})$ and \mathbf{k}_\perp , respectively. The explicit expressions for the $c_{\gamma\chi_c}^{(\lambda, \sigma, H)}$, $d_{\gamma\chi_c}^{(\lambda, \sigma, H)}$, $\tilde{c}_{\gamma\chi_c}^{(\lambda, \sigma, H)}$ and $\tilde{d}_{\gamma\chi_c}^{(\lambda, \sigma, H)}$ are given in Appendix B in view of their extensive size. In general the coefficient functions are rational functions of the variable $\zeta = x/\xi$ with isolated poles at $\zeta = \pm 1 \mp i0$ and $\zeta = \pm \kappa \mp i0$ ($x = \pm \xi \mp i0$ and $x = \pm \kappa \xi \mp i0$ in conventional notations), where

$$\kappa = 1 - \frac{1 - 1/r^2}{1 - \alpha/2} = \frac{1}{r^2} \frac{2 - \alpha r^2}{2 - \alpha}, \quad r = M_{\gamma\chi_c}/M_{\chi_c} = \frac{W}{M_{\chi_c}} \sqrt{\frac{2\xi}{1 + \xi} \left(1 - \frac{m_N^2}{W^2} \right)} \approx \frac{W}{M_{\chi_c}} \sqrt{\frac{2\xi}{1 + \xi}}. \quad (42)$$

The values of κ are limited by $|\kappa| < 1$ in the physically relevant kinematics ($r > 1$, $\alpha \in (1/r^2, 1)$). In contrast to our previous results for $\eta_c \gamma$ production [33], the poles are of the second order. This happens because for S -wave quarkonia we just disregarded the relative motion of the quarks in the heavy quark mass limit, whereas for the P -wave quarkonia we expand individual diagrams over the relative momentum (velocity) and pick up higher order terms, thus increasing the order of the poles when such expansion comes from denominator. Fortunately, the standard $m^2 \rightarrow m^2 - i0$ prescription in Feynman propagators provides contour deformation prescription near these poles, and allows to avoid the potential ambiguities in the integration. Afterwards the integration in the vicinity of these poles formally can be

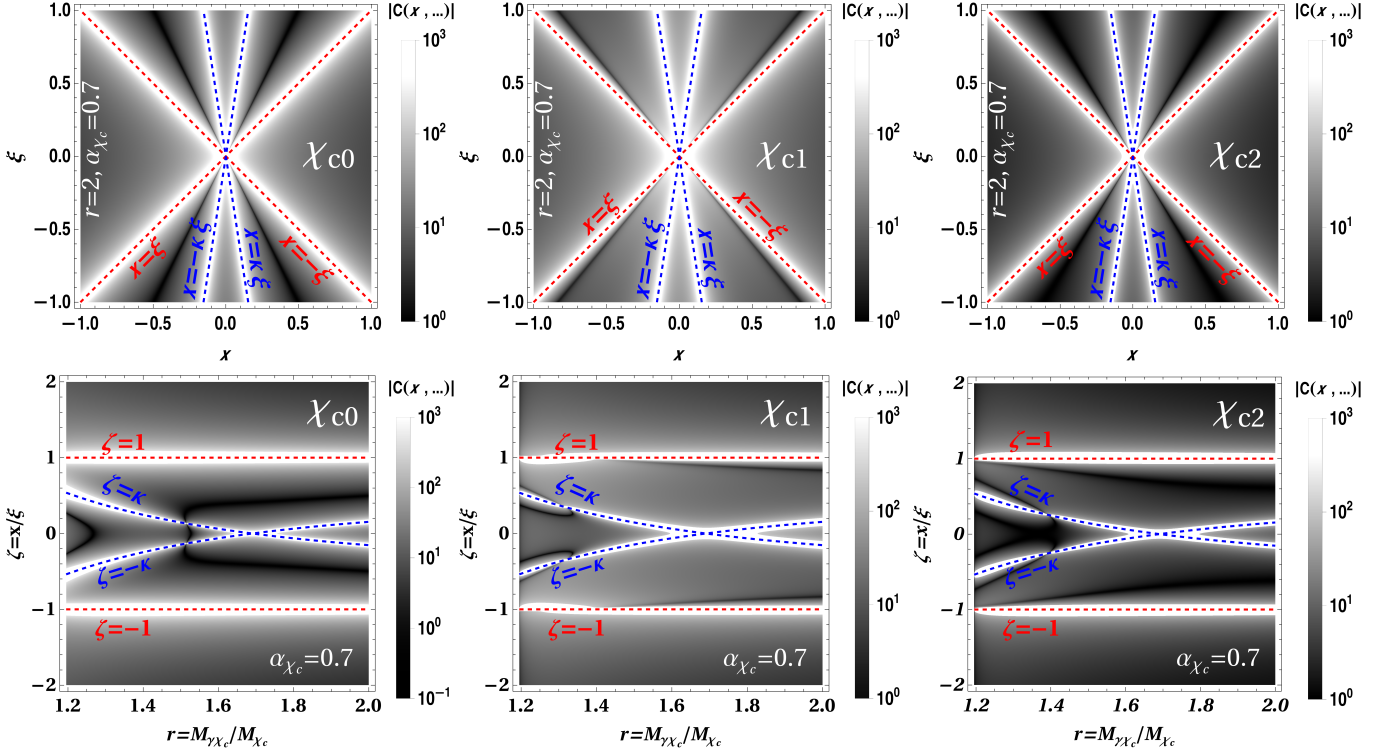


Figure 5. The density plot which illustrates the coefficient function $C_{\gamma\chi_c}^{(++)}$ (in relative units). Upper row: dependence on variables x , ξ at fixed $r = M_{\gamma\chi_c}/M_{\chi_c}$, $\alpha_{\chi_c} = (-u')/M_{\gamma\chi_c}$. Lower row: Dependence on the ratio $\zeta = x/\xi$ and r at fixed α_{χ_c} . In both rows for χ_{c1} and χ_{c2} mesons we have shown the coefficient function of the dominant component with helicity $H_{\chi_c} = +1$ (same as for the incoming photon). White strips with colored dashed lines effectively demonstrate the position of the double poles $x = \pm\xi$, $x = \pm\kappa\xi$ ($\zeta = \pm 1, \pm\kappa$) in the coefficient function (40). The parameter κ depends on the kinematics of the process and is given in (42); it is always bound by the constraint $|\kappa| < 1$ in the physically relevant kinematics.

carried out using a set of well-known identities

$$\int_{-1}^1 dx \frac{F(x, \xi, t)}{(x - x_0 \pm i0)^2} = - \int_{-1}^1 dx F(x, \xi, t) \frac{d}{dx} \frac{1}{(x - x_0 \pm i0)} = - \frac{F(x, \xi, t)}{(x - x_0 \pm i0)} \Big|_{x=-1}^{x=+1} + \int_{-1}^1 dx \frac{\partial_x F(x, \xi, t)}{(x - x_0 \pm i0)}. \quad (43)$$

$$\int_{-1}^1 dx \frac{H(x, \xi, t)}{(x - x_0 \pm i0)} = \text{P.V.} \int_{-1}^1 dx \frac{H(x, \xi, t)}{(x - x_0)} \mp i\pi H(x_0, \xi, t) \quad (44)$$

where x_0 is some constant which may depend parametrically on α , r , ξ . At special point $\alpha = 2/r^2$ the value of κ vanishes and the poles $x = \pm\kappa\xi \mp i0$ apparently start pinching the integration contour. However, this does not lead to a physical singularity in the amplitude because each individual term which contributes additively to $C_{\gamma\chi_c}^{(\lambda, \sigma, H)}$ has an isolated pole either at $x = \kappa\xi - i0$ or $x = -\kappa\xi + i0$.

In the Figure 5 we have shown dependence of $C_{\gamma\chi_c}^{(+, +, H)}$ on its arguments for different mesons. Due to space limitations, for χ_{c1} and χ_{c2} mesons we have shown only the results for the component with helicity $H_{\chi_c} = +1$, which are expected to give the largest contribution. While in general the coefficient functions depend significantly on the spin and helicity state of the produced quarkonia, the position of the poles (white strips with dashed lines inside) remains largely the same because it stems from denominators of the Feynman diagrams. We can see that the functions $C_{\gamma\chi_c}^{(\lambda, \sigma, H)}$ have pronounced peaks in the vicinity of their poles, and decrease rapidly when we move away from them. This implies that position of the poles determines the region which gives the dominant contribution in convolution integrals (36-37). Varying the invariant mass $M_{\gamma\chi_c}$ and the value of α_{χ_c} , it is possible to change the parameter κ in the region $|\kappa| < 1$ and in this way probe the behavior of the gluon GPDs H_g in the whole ERBL domain.

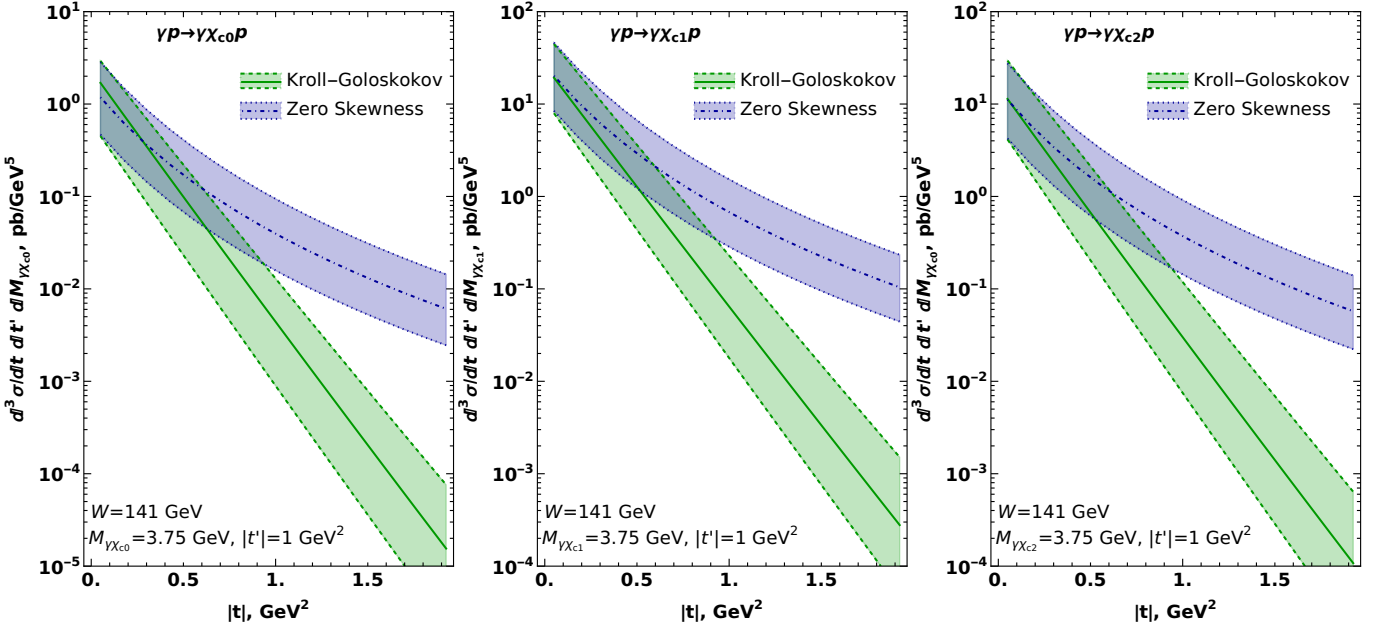


Figure 6. Dependence of the unpolarized photoproduction cross-section (23) on the invariant momentum transfer t to the target at fixed invariant mass $M_{\gamma\chi_c}$. For χ_{c1} and χ_{c2} summation over all helicities is implied. The upper and lower colored bands correspond to Zero Skewness and Kroll-Goloskokov parametrizations of the gluon GPD. The width of each band reflects uncertainty due to the omitted higher order corrections and was obtained varying the factorization scale μ in the range $\mu \in (0.5 \dots 2) M_{\gamma\chi_c}$.

III. NUMERICAL ESTIMATES

A. Differential cross-sections

At present, the largest uncertainty for our predictions stems from the choice of the Generalized Parton Distributions. In order to illustrate the magnitude of this choice, in the Figure 6 we have shown the differential cross-section (23) evaluated with different parametrizations of GPD and plotted as a function of the invariant momentum transfer t to the target. The dependence on this variable is the simplest for interpretation because the latter is disregarded in coefficient function in the collinear kinematics, and thus the observed dependence on $|t|$ is entirely due to the implemented parametrization of the GPD. For comparison, we considered the Kroll-Goloskokov parametrization from [45, 53–56] and the so-called Zero Skewness parametrization, which disregards the dependence on the variable ξ altogether and models the GPD of each flavor as a product of the nucleon form factor and forward Parton Distribution Function. We can see that the difference between the predictions of the two parametrizations grows as a function t , when the off-forward effects become more pronounced. Though the cross-section (23,35) obtains contributions of GPDs with different helicity states, for unpolarized target the contribution of the GPD $H^g(x, \xi, t)$ is clearly the dominant. The width of the band in these plots illustrates the uncertainty due to omitted higher order corrections and was found varying the factorization scale μ in the range $\mu \in (0.5 - 2) M_{\gamma\chi_c}$. In the Figure 7 we show that the shape of the t -dependence almost does not depend on the total spin state of χ_c , the energy of collision and invariant mass $M_{\gamma\chi_c}$. We also found that the slope of the t -dependence does not depend on the choice of the variable t' , and on helicity of χ_{c1}, χ_{c2} . Such sharply decreasing t -dependence is common to many exclusive processes, and, as was explained in [57], stems from the fact that the (large) transverse momentum in exclusive process should be shared equally between all partons inside the target in order to avoid its destruction, and each such exchange is suppressed by the (perturbative) propagators at large t . The t -dependence implemented in phenomenological parametrizations of the GPDs is fitted to the DVCS and DVMP data, which confirm such pronounced decrease. Technically, this implies that the $\gamma\chi_c$ pairs predominantly are produced in the kinematics where the variables Δ_\perp^2, t are negligibly small, so the transverse momenta $\mathbf{p}_\perp^{\chi_c}, \mathbf{k}_\perp^\gamma$ are oppositely directed and have comparable magnitudes. Due to simplicity of t -dependence, in our further presentation we will tacitly assume that $|t| = |t_{\min}|$, or consider the observables in which the dependence on t is integrated out.

In the Figure 8 we show the dependence of the cross-section (23) on the variable $|t'|$ for unpolarized case, and in the Figure 9 we also show the t' dependence for the cross-sections with definite (fixed) helicity H_{χ_c} at fixed helicity +1 of

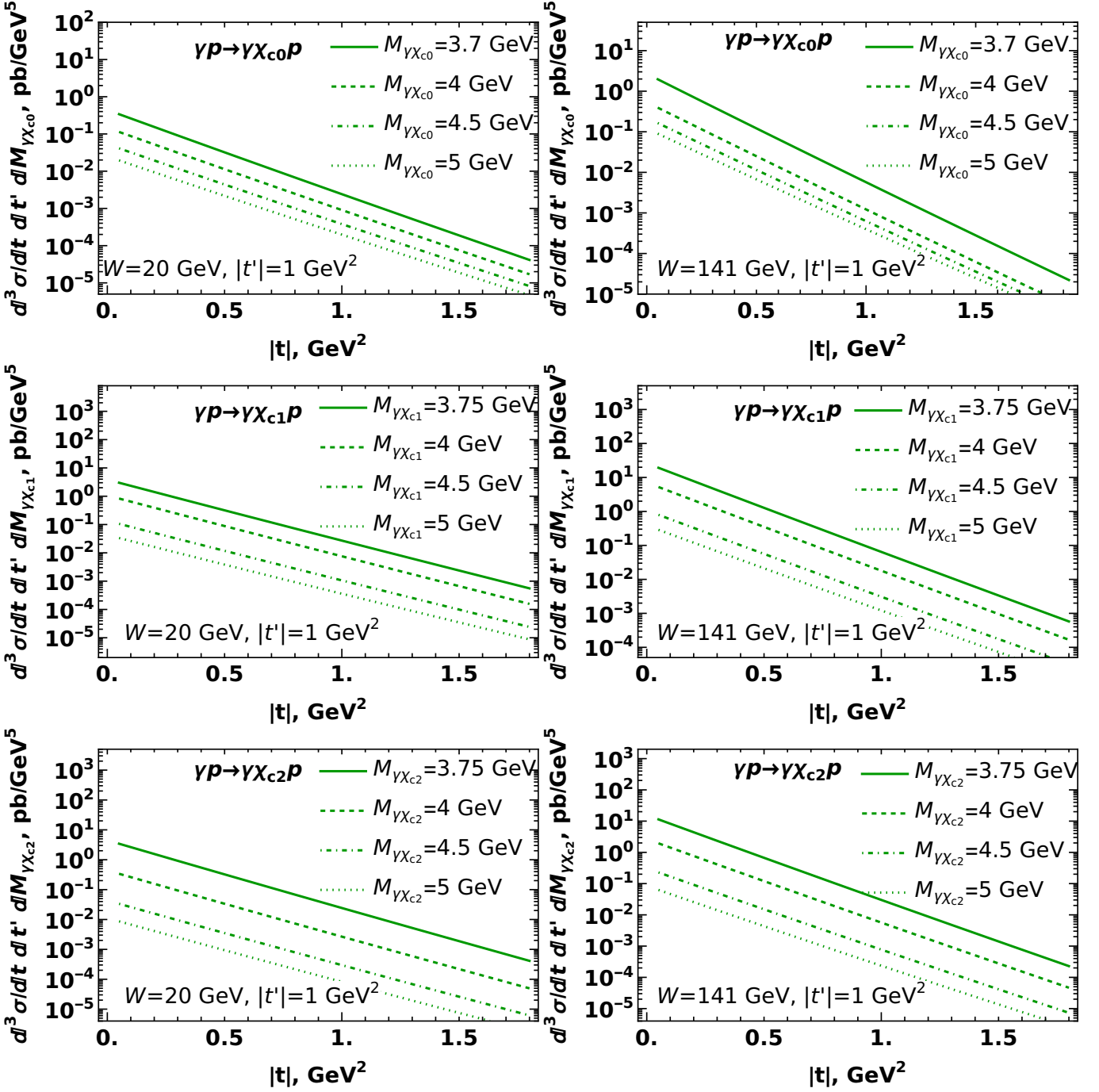


Figure 7. The differential cross-section (23) as a function of the invariant momentum transfer t for different fixed invariant mass M_{χ_c} . The upper, central and lower rows correspond to χ_{c0} , χ_{c1} and χ_{c2} mesons. The left and right columns differ by the value of collision energy W . We also checked that the shape of the t -dependence has negligible dependence on the energy W .

the incoming photon. The observed behavior could be partially understood from conservation of angular momentum. In general χ_{cJ} meson and the photon move with nonzero (and parametrically large) transverse momenta $\sim |\mathbf{p}_\perp|$. However, we may observe from (17, 18) that $|\mathbf{p}_\perp|$ may vanish at points $\alpha_{\chi_c} \approx \alpha_{\min} = 1/r^2$, and $\alpha_{\chi_c} \approx \alpha_{\max} = 1$ which correspond to $t' \approx 0$ and $t' \approx |t'|_{\max} = M_{\gamma\chi_c}^2 - M_{\chi_c}^2$, respectively. At the point $\alpha_{\chi_c} \approx \alpha_{\min}$ the final-state χ_c and γ move along the collision axis in nearly the same direction, and for this reason a conservation of total angular momentum (its projection on collision axis) requires a conservation of a sum of helicities. Similarly, at the point $\alpha_{\chi_c} \approx \alpha_{\max}$ the χ_c and γ move along the collision axis in opposite directions, so the conservation of angular

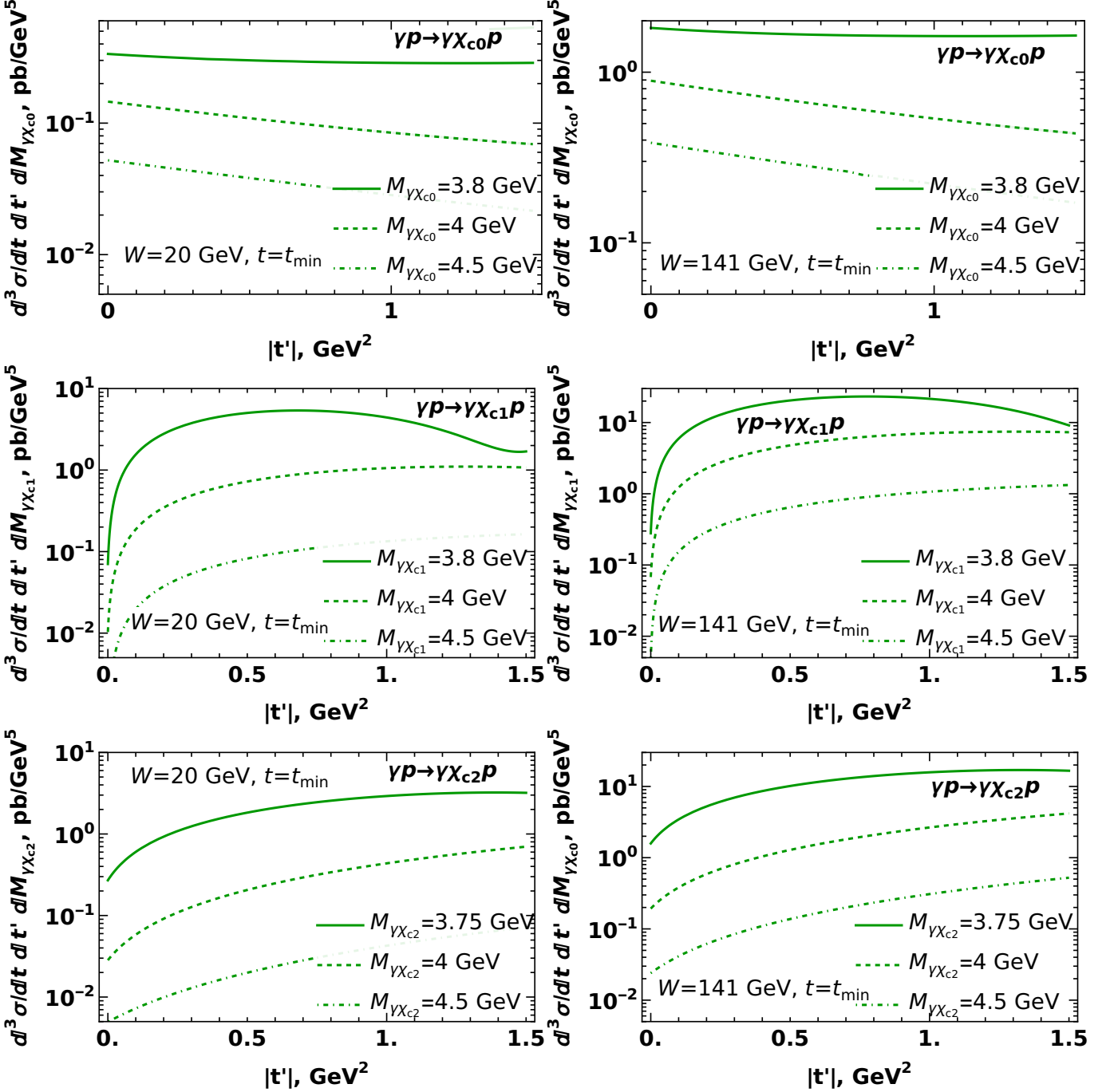


Figure 8. The unpolarized photoproduction cross-section (23) as a function of the the variable $|t'|$ defined in (23). The upper, central and lower rows correspond to χ_{c0} , χ_{c1} and χ_{c2} mesons; the left and right columns correspond to different values of the collision energy W . See the next Figure 9 for t' -dependence of the individual helicity components in χ_{c1}, χ_{c2} .

momentum leads to conservation of difference of helicities. This consideration allows to understand the observed suppression of the dominant components with $H_{\chi_c} = +1$ at small- t' , and suppression at $|t'| \gtrsim 1.5$ GeV² for the curve $M_{\gamma\chi_c} = 3.8$ GeV. Such suppression also occurs for larger values of $M_{\gamma\chi_c}$, though starts later and is not seen in the plot. Technically, this suppression happens due to explicit factors $\sim |\mathbf{p}_\perp|$ and $(1 - \alpha_{\chi_c} r^2)$ in the coefficient function.

In the Figure 10 we have shown the dependence of the cross-section on the invariant energy W . The nearly linear growth in double logarithmic coordinates suggests that the cross-section has a power law dependence on energy, $d\sigma(W) \sim W^\lambda$, where the parameter λ has a mild dependence on other kinematic variables. This behavior may be understood if we take into account that the amplitude gets the dominant contribution from the gluon GPD

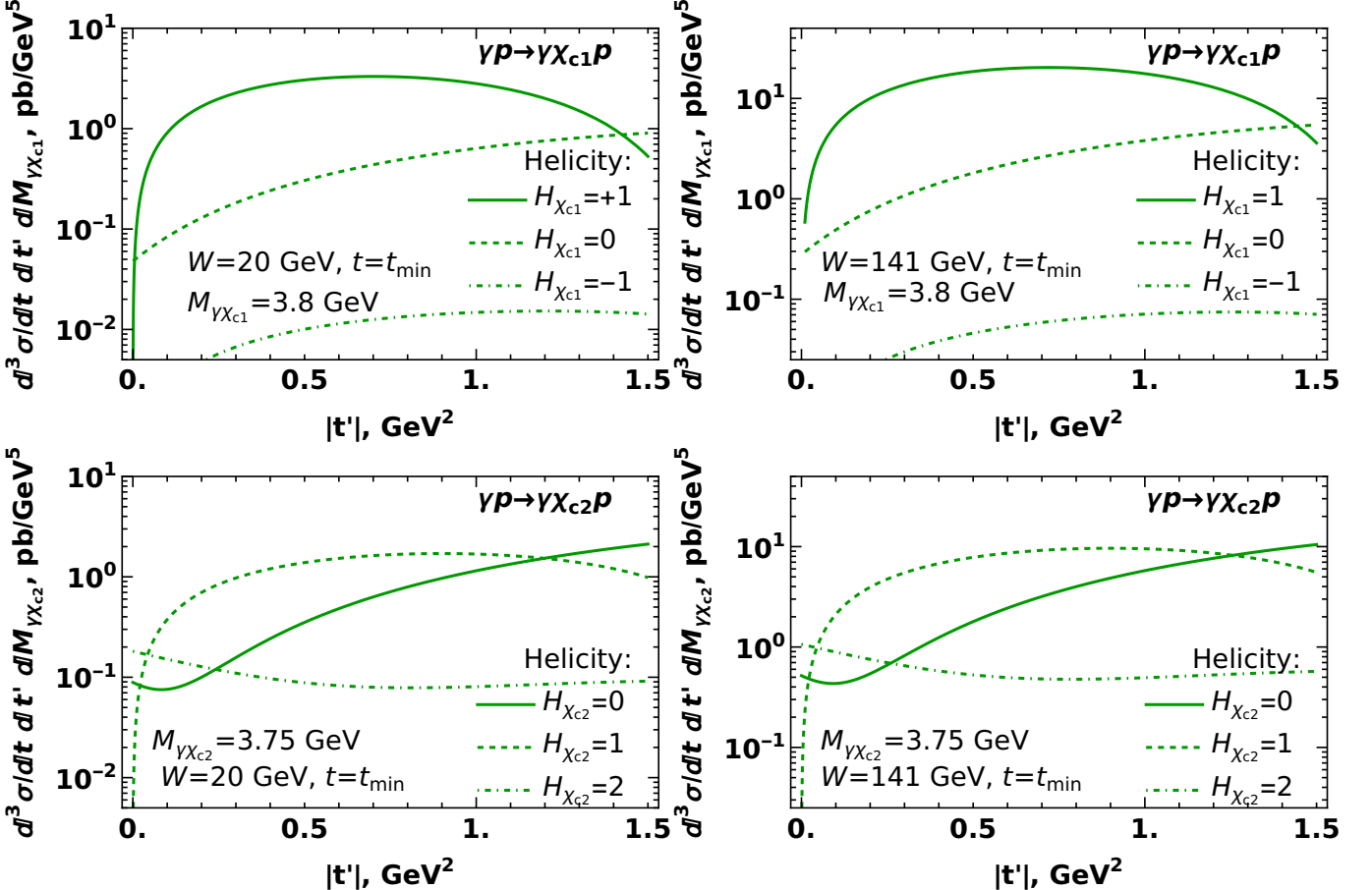


Figure 9. The photoproduction cross-sections of χ_{c1} and χ_{c2} with different helicity projections H_{χ_c} . We assume that the incoming photon has helicity +1 (for helicity -1 should invert the sign of all helicities). For χ_{c2} , the cross-sections of states with helicities $H_{\chi_{c2}} = -1$ and $H_{\chi_{c2}} = -2$ are negligible, and were omitted for the sake of legibility. The left and right columns correspond to different collision energy W . See the text for discussion of the observed t' -dependence.

near $|x| \sim \xi \sim 1/W^2$, and the fact that the gluon GPDs grows as a function of the light-cone fraction x . In the implemented phenomenological parametrization, the small- x behavior of the GPD roughly may be approximated as $H_g(x, \xi, t) \sim x^{-\delta_g}$ [53]. After convolution with coefficient functions (40-41), this translates into a power law behavior for the cross-section,

$$\frac{d\sigma(W)}{dt dt' dM_{\chi_c}} \sim \xi^{-2\delta_g} \sim W^{4\delta_g}, \quad \lambda = 4\delta_g, \quad (45)$$

in agreement with results of numerical evaluation. The typical values of the parameter λ are $\lambda \approx 0.8 - 1.1$.

In the Figure 11 we show the dependence of the cross-section on the invariant mass $M_{\gamma\chi_c}$. This dependence largely stems from the prefactor $\sim 1/(r^2 - 1) = M_{\chi_c}^2 / (M_{\gamma\chi_c}^2 - M_{\chi_c}^2)$ in the coefficient functions and additional factor $\sim 1/M_{\gamma\chi_c}$ in the cross-section (23), which together lead to a strong suppression of the cross-section. On the other hand, the dependence on $M_{\gamma\chi_c}$ in the kinematical constraint (20) implies that the phase volume increases as a function of $M_{\gamma\chi_c}$ and partially attenuates the pronounced suppression of the cross-section discussed earlier, however it is not sufficient to change the observed decrease of the cross-section. The observed strong suppression of the cross-section as a function of the invariant mass agrees with findings of [14, 16] for other photon-meson channels. In the Figure 12 we have shown the contributions of different helicity components for χ_{c1} and χ_{c2} mesons. The increase of $M_{\gamma\chi_c}$ at fixed values of other kinematic variables decreases the variable $\alpha_{\chi_c} = (M_{\chi_c}^2 + |t'|) / M_{\gamma\chi_c}^2$ and increases the transverse momentum $|\mathbf{p}_\perp|$, as could be seen from (17). At very small values of $|\mathbf{p}_\perp|$, the final-state meson and photon move almost in the same direction as incoming photon. A production of χ_c with negative helicity in this kinematics is suppressed, since it would require to change the helicities of both quarks, leading to a strong suppression. At larger masses $M_{\gamma\chi_c}$, the angle between the oncoming photon and the produced quarkonia increases and may achieve large

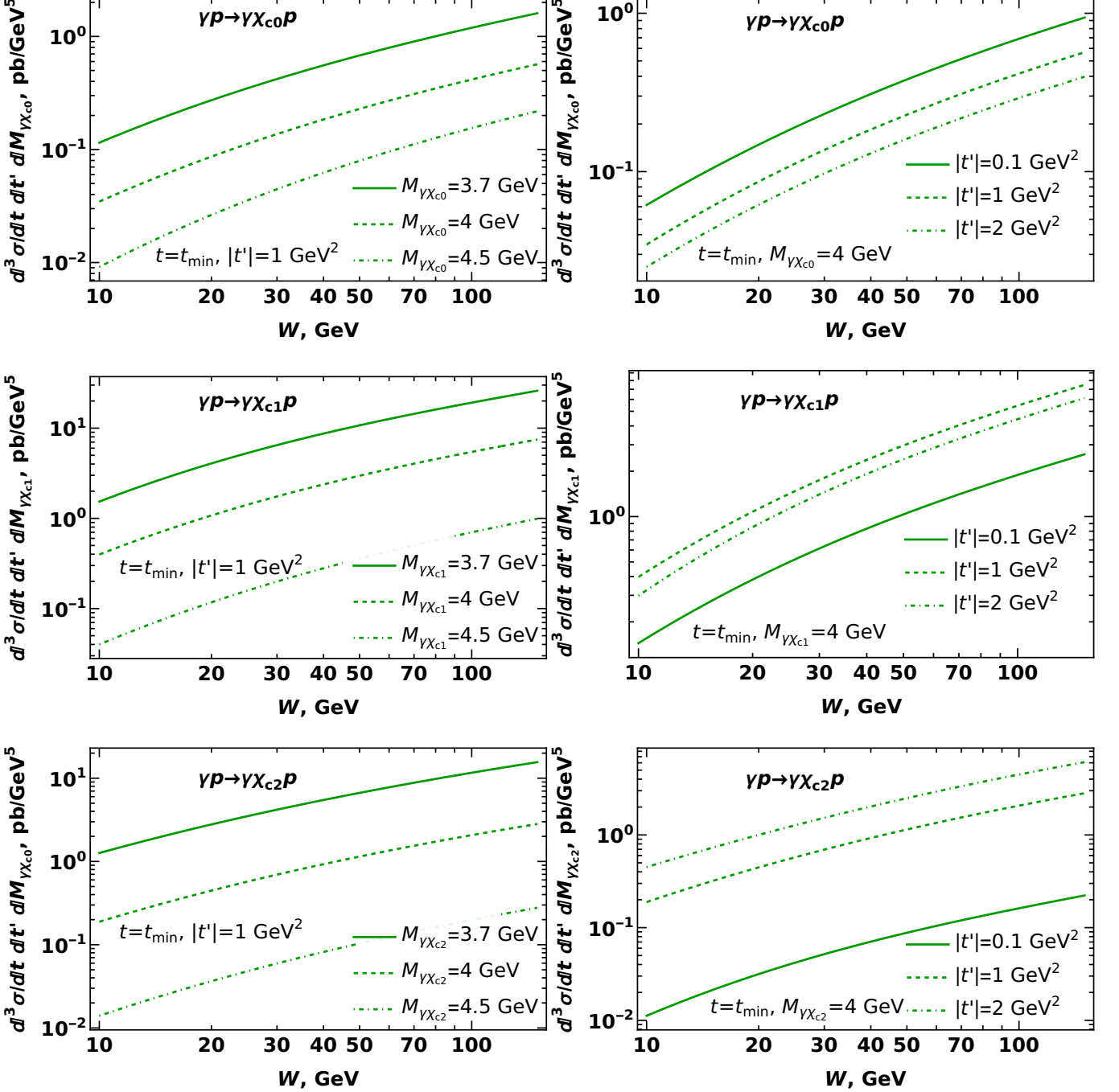


Figure 10. The cross-section of χ_{cJ} production as a function of the invariant collision energy W at different values of the invariant mass $M_{\chi_{cJ}}$ (left row) and variable $|t'|$ (right row). The almost linear dependence (in double logarithmic coordinates) with approximately the same slope indicates that the dependence of the cross-section on W largely factorizes and can be approximated as $d\sigma(W)/dt dt' dM_{\chi_{cJ}} \sim W^\lambda$, where the slope parameter $\lambda \approx 0.8 - 1.1$ depends mildly on other variables.

values (up to $\pi/2$), to the direction of the incoming photon, for this reason the cross-sections with opposite helicities start approaching each other.

Finally, we would like to discuss the relative contribution of different polarizations of the final state photon to the total cross-section. In the Figure 13 we plotted the fraction of the contribution with photon helicity flip in the total

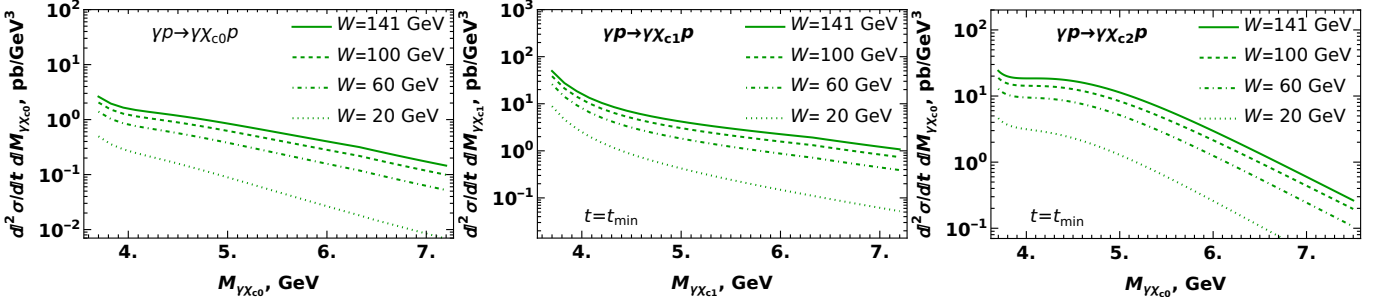


Figure 11. Dependence of the cross-section on the invariant masses of produced $\gamma\chi_c$ pair, for several proton energies W .

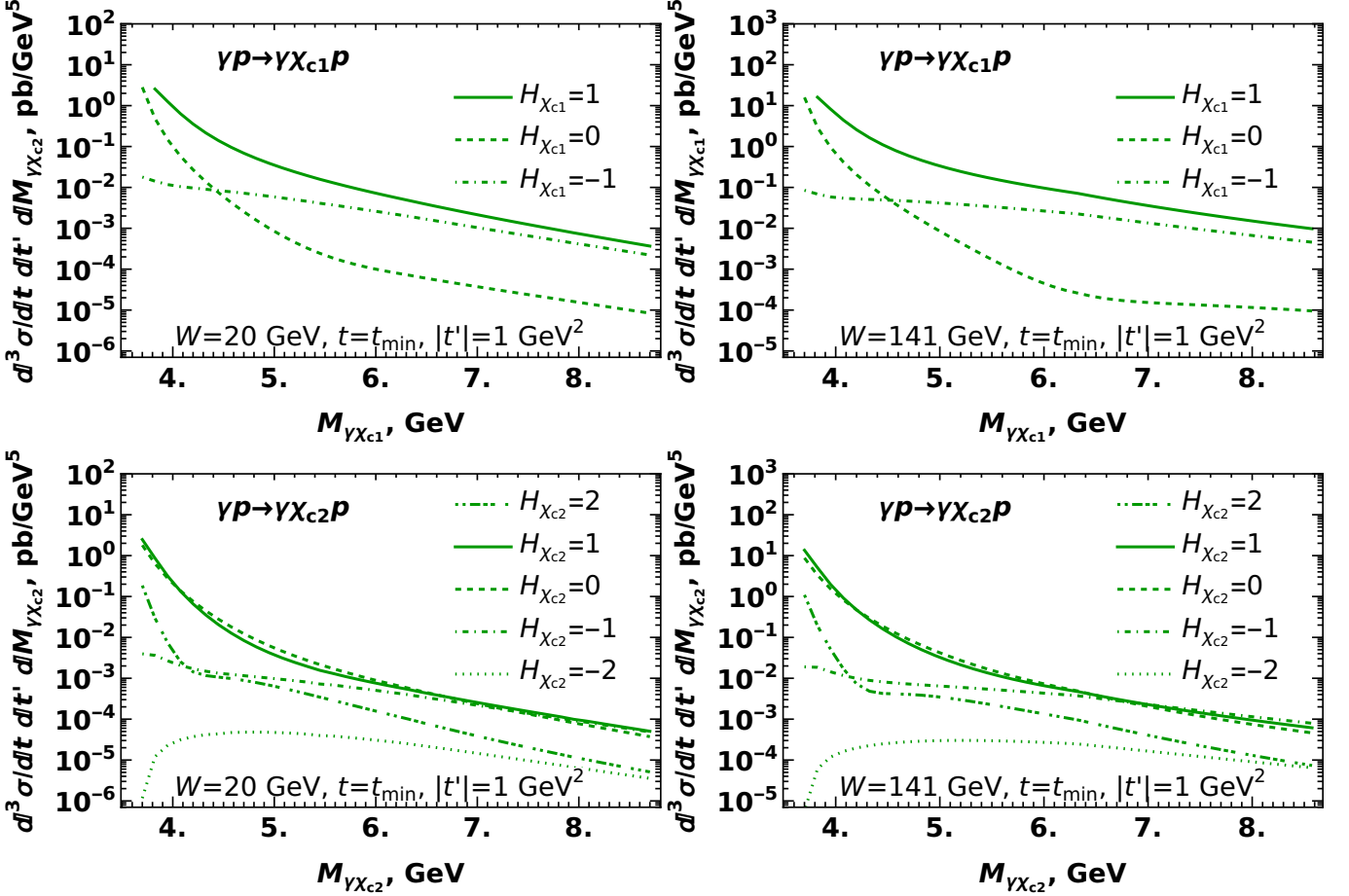


Figure 12. The dependence of different helicity components in the cross-sections of χ_{c1} and χ_{c2} production on the invariant masses of produced $\gamma\chi_c$ pair. Left and right columns differ by value of the collision energy W . The sign of helicity of the hadron is positive, if it coincides with helicity of the incoming photon.

cross-section

$$\frac{\Delta\sigma}{\sigma} \equiv \frac{d\sigma_{\gamma p \rightarrow \chi_c \gamma p}^{(+,-,H)}}{d\sigma_{\gamma p \rightarrow \chi_c \gamma p}^{(+,-,H)} + d\sigma_{\gamma p \rightarrow \chi_c \gamma p}^{(+,+H)}} = \frac{\left| \mathcal{A}_{\gamma p \rightarrow \chi_c \gamma p}^{(+,-,H)} \right|^2}{\left| \mathcal{A}_{\gamma p \rightarrow \chi_c \gamma p}^{(+,-,H)} \right|^2 + \left| \mathcal{A}_{\gamma p \rightarrow \chi_c \gamma p}^{(+,+H)} \right|^2}. \quad (46)$$

As we explained earlier, in general the produced χ_c meson and photon have a relatively large transverse momentum $\pm \mathbf{p}_\perp$, as could be seen from (4-9), and thus move with nonzero angle w.r.t. direction of the incoming photon. However, for special points where $\mathbf{p}_\perp = 0$, the final state particle move collinear (or anticollinear) w.r.t. incoming photon, and for this reason the conservation of angular momentum requires suppression of certain modes in which a sum (or

a difference) of helicities does not conserve. Since the angle which forms the particle with collision axis decreases with energy W , we expect that at very high energies W or small \mathbf{p}_\perp (small t') the contributions which break the above-mentioned selection rule may be suppressed. In agreement with our expectations, the ratio (46) decreases as a function of energy W for all χ_c mesons. This selection rule also allows to understand the observed t' -dependence of different harmonics in χ_{c2} meson: the helicity conservation requires that state with helicity $H_{\chi_{c2}} = +2$ at small t' (small angles) should proceed only via the photon helicity flip, whereas for $H_{\chi_{c2}} = 0$ the helicity conservation requires that the photon's helicity is conserved. However, as we increase $|t'|$, the contributions of the “forbidden” (suppressed) modes become more and more important. For the mode with $H_{\chi_{c1}} = +1$, both helicity flip and non-flip contributions are suppressed at small t' , however this suppression is exactly the same for both modes, and the ratio (46) for this mode has a relatively mild dependence on t' , with comparable (within factor of 2) contributions of helicity flip and non-flip parts. The harmonics with helicities $H_{\chi_c} < 0$ are numerically negligible and thus do not present much interest.

As we discussed earlier, in *electroproduction* experiments it is impossible to fix the sign of the virtual (incoming) photon, for this reason the ratio (46) reveals itself via angular asymmetries c_2, s_2 defined in (30). In the Figure 14 we have shown these harmonics for the case when the detector does not distinguish (\approx sums over) the polarizations of the final state photon. In this setup, the cross-sections of χ_c production do not distinguish the sign of helicity H_{χ_c} . In the Figure 15 we have shown the results for χ_{c1} and χ_{c2} when the detector picks up only events with definite polarization of the final state photon (+1 for definiteness). As we can infer from (30), a sizable asymmetry is possible only if the amplitudes $|\mathcal{A}_{++,H}|$ and $|\mathcal{A}_{-+,H}| = |\mathcal{A}_{+-,-H}|$ are comparable by magnitude. Apparently this condition is satisfied only for χ_{c2} meson with $H_{\chi_{c2}} = 0$ in the kinematics of small t' .

B. Integrated cross-sections & counting rates

So far we considered the differential cross-sections, which are best suited for theoretical studies. Unfortunately, it is difficult to measure such small cross-sections because of insufficient statistics, and for this reason now we will provide predictions for the yields integrated over some or all kinematic variables. In the left panel of the Figure 16 we have shown the cross-section $d\sigma/dM_{\gamma\chi_c}$ for different energies. The observed dependence on $M_{\gamma\chi_c}$ largely repeats the $M_{\gamma\chi_c}$ -dependence of the differential cross-section shown in the Figure 16. This is a consequence of our earlier observations that dependence on different variables in the differential cross-section largely factorize, i.e. the *shape* of dependence on any of the variables $t, t', M_{\gamma\chi_c}$ depends very weakly on the other variables.

In the left panel of the Figure 17 we show the energy dependence of the total (fully integrated) cross-section $\sigma_{\text{tot}}(W)$ for the photoproduction of $\chi_c\gamma$. As we discussed earlier, the suggested approach cannot be applied when the emitted photon is soft, for this reason we consider only the kinematics where the invariant mass $M_{\gamma\chi_c}$ of the photon-meson pair is sufficiently large. The choice of the minimal value $(M_{\gamma\chi_c})_{\min}$ is somewhat arbitrary, for this reason we have shown the result for several possible cutoffs. This dependence is stronger at small energies due to phase space contraction for production of $\chi_c\gamma$ pair with large invariant mass. At large W , for all cutoffs the W -dependence may be approximated as

$$\sigma_{\text{tot}}(W, M_{\gamma\chi_{c0}} \geq 3.7 \text{ GeV}) \approx 0.48 \text{ pb} \left(\frac{W}{100 \text{ GeV}} \right)^{0.97}, \quad (47)$$

$$\sigma_{\text{tot}}(W, M_{\gamma\chi_{c1}} \geq 3.7 \text{ GeV}) \approx 3.7 \text{ pb} \left(\frac{W}{100 \text{ GeV}} \right)^{1.14}, \quad (48)$$

$$\sigma_{\text{tot}}(W, M_{\gamma\chi_{c2}} \geq 3.7 \text{ GeV}) \approx 4.2 \text{ pb} \left(\frac{W}{100 \text{ GeV}} \right)^{0.9}, \quad (49)$$

in agreement with our earlier findings (45) for the energy dependence of the differential cross-sections. In the right panel of the same Figure 17 we have shown our estimates for the fully integrated cross-section¹ of the electroproduction $e p \rightarrow e \gamma \chi_c p$ as a function of the invariant electron-proton collision energy $\sqrt{s_{ep}}$.

For the sake of reference in the Table I we provided the estimates of the cross-section for the upper EIC energy $\sqrt{s_{ep}} \approx 141 \text{ GeV}$, together with corresponding production and detection rates. The small values of the electroproduction cross-sections $\sigma_{\text{tot}}^{(ep)}$ are a consequence of $\sim \alpha_{\text{em}}$ in the leptonic prefactor (see (29)) and a very rapid decrease of the t -dependence in the exclusive process. For estimates of the detection rates we assumed that the χ_c meson is

¹ The evaluation of the total electroproduction cross-section requires to integrate over all possible virtualities Q of the incoming photons. In our evaluations we disregarded this Q -dependence for simplicity, since the flux of equivalent photons falls off rapidly as a function of Q , and the Q -dependence of the *photoproduction* part is controlled by the scale M_{χ_c} (namely is very mild for $Q < M_{\chi_c}$ and drops sharply for $Q > M_{\chi_c}$). For our numerical estimate we assumed that the Q -dependence of the *photoproduction* cross-section is given by $d\sigma(Q) = \Theta(M_{\chi_c} - Q) d\sigma(Q = 0)$, where Θ is a Heaviside step function.

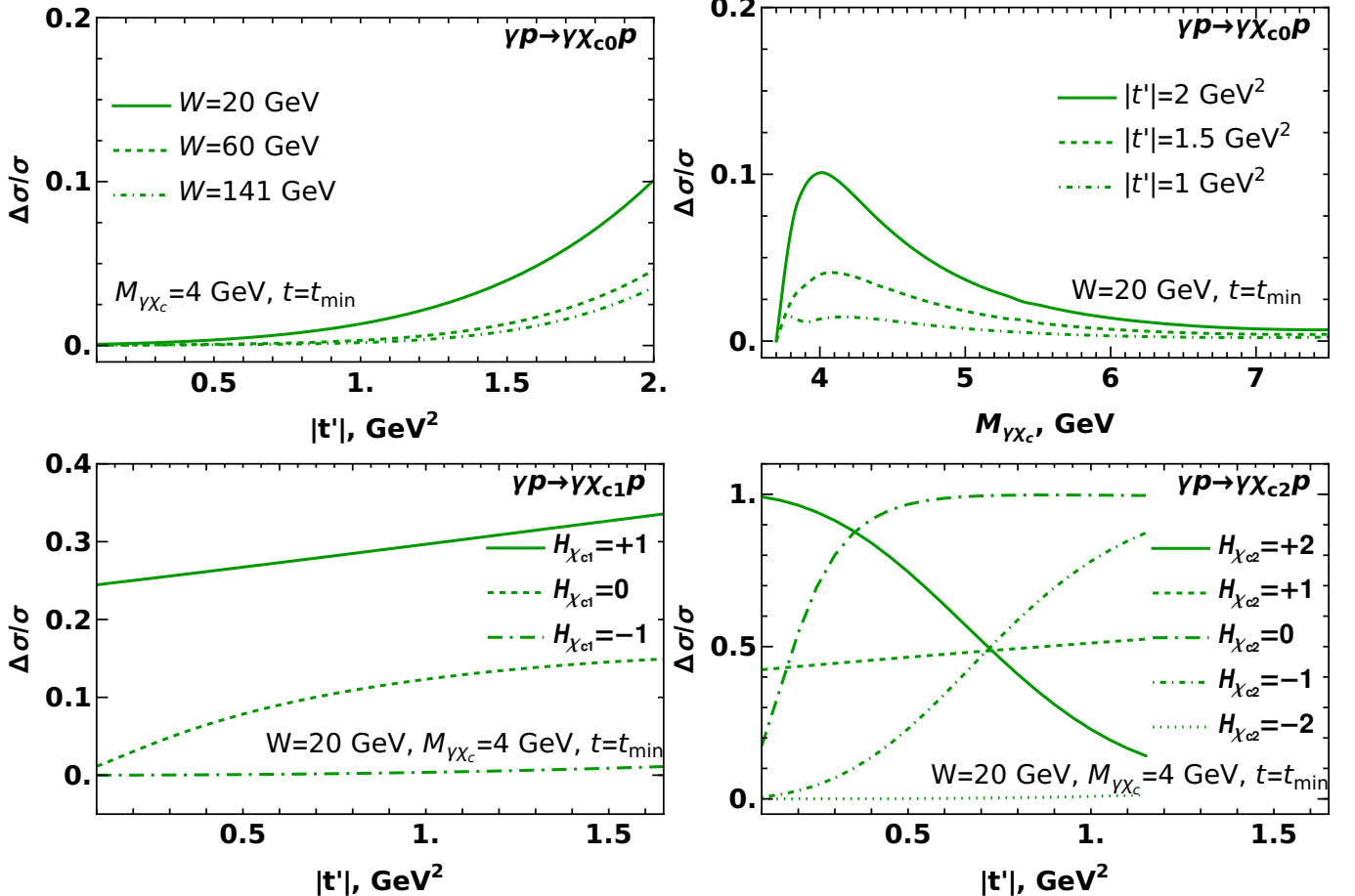


Figure 13. The fraction of the contribution with photon helicity flip $\Delta\sigma$ in the total cross-section. The upper row shows this fraction for χ_{c0} . In the left plot we show dependence on the variable t' , which controls the angles between the final state χ_c, γ and the direction of the incoming photon at fixed energies. Similarly, the helicity flip components are suppressed at higher energies for χ_{c0} due to decreasing scattering (production) angles; similar dependence was also observed for χ_{c1}, χ_{c2} . The plots in the bottom row show the dependence of the above-mentioned fraction on t' for χ_{c1}, χ_{c2} (in different harmonics). The harmonics with helicities $H_{\chi_c} < 0$ are numerically negligible. The ratio remains small (below 10%) for χ_{c0} , in the whole range analyzed in this paper, yet may be sizable for χ_{c1}, χ_{c2} production with certain helicity projections

reconstructed from its radiative decays into J/ψ , and the latter is reconstructed from its decays into $\mu^+\mu^-$ or e^+e^- . For χ_{c0} mesons due to small value of $\text{Br}(\chi_{c0}(1P) \rightarrow J/\psi\gamma)$ we got very small values of the counting rates. However, χ_{c0} has a number of other 2-, 3- and 4-body decay channels with larger branchings, e.g. $\text{Br}(\chi_c(1P) \rightarrow \pi^+\pi^-\pi^0\pi^0) = 3.3\%$, $\text{Br}(\chi_c(1P) \rightarrow \rho^+\pi^-\pi^0) = 2.9\%$, $\text{Br}(\chi_c(1P) \rightarrow \pi^+\pi^-K^+K^-) = 1.8\%$, $\text{Br}(\chi_c(1P) \rightarrow \rho^+K^-K^0) = 1.21\%$. If these channels will be used for reconstruction of χ_{c0} , the expected counting rates will be at least a factor of 20 larger than what is shown in the Table I.

A significantly larger counting rates could be achieved in the ultraperipheral kinematics at LHC, due to enhancement of the gluonic densities in small- x kinematics. However, the collinear factorization approach is not reliable in that kinematics due to onset of saturation effects, for this reason we do not make predictions for LHC energies.

C. Comparison with χ_c photoproduction

The exclusive photoproduction of C -even quarkonia, such as $\gamma p \rightarrow \eta_c p$ and $\gamma p \rightarrow \chi_c p$ are considered in the literature as possible tools for analysis of the 3-gluon exchanges in t -channel (the so-called odderons) [60–62]. While the odderons have been predicted many years ago [63–65], for a long time the magnitude of the odderon-mediated processes remained largely unknown because it is controlled by a completely new nonperturbative amplitude (see [62, 66] for a short overview). A recent comparison of pp and $p\bar{p}$ elastic cross-sections measured at LHC and Tevatron [67, 68]

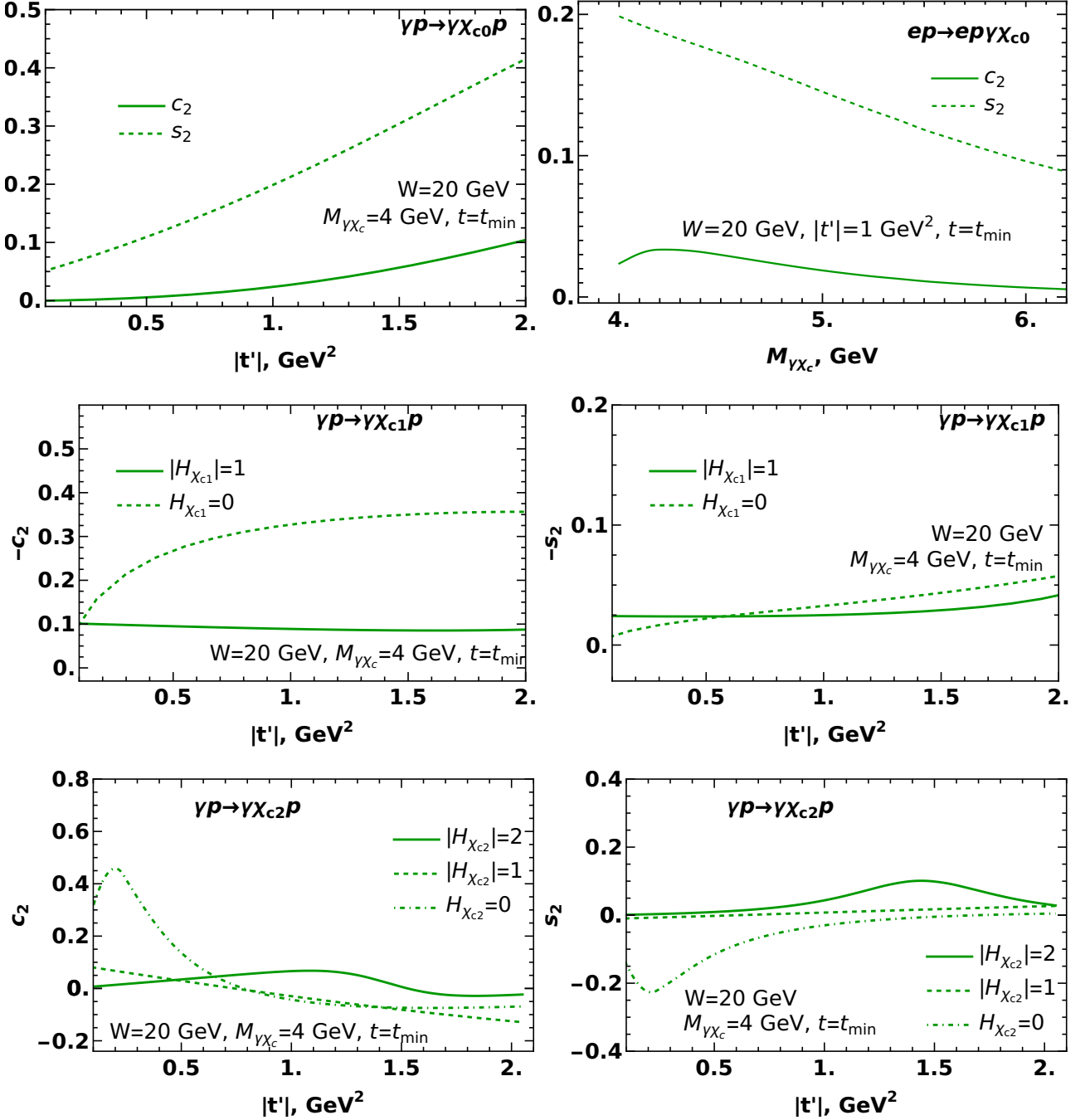


Figure 14. The angular harmonics c_2, s_2 defined in (25-30). In this Figure we assume that the detector sums different polarizations of the final-state photons. For χ_{c1}, χ_{c2} in view of P -parity the cross-sections with different signs of helicity $H_{\chi_{c}}$ are equal. Top, central and bottom rows correspond to χ_{c0}, χ_{c1} and χ_{c2} respectively. For the sake of definiteness we assumed that the parameter ϵ defined in (26) equals $\epsilon = 0.5$.

apparently corroborates the existence of odderons, though includes sizable uncertainties introduced by the extrapolation procedure, and does not allow to study them in detail using perturbative methods due to lack of a hard scale. For this reason, at present the searches of odderons mostly focus on production channels which proceed via the C -odd exchanges in t -channels. The photoproduction $\gamma p \rightarrow \chi_{cp}$ is a rather clean channel for study of odderons which has been suggested in [43] as alternative to η_c photoproduction. The cross-section of the odderon-mediated χ_c photoproduction is on par with that of η_c , yet it is preferable for experimental studies due to smaller contamination by the photon-photon fusion (the so-called Primakoff mechanism).

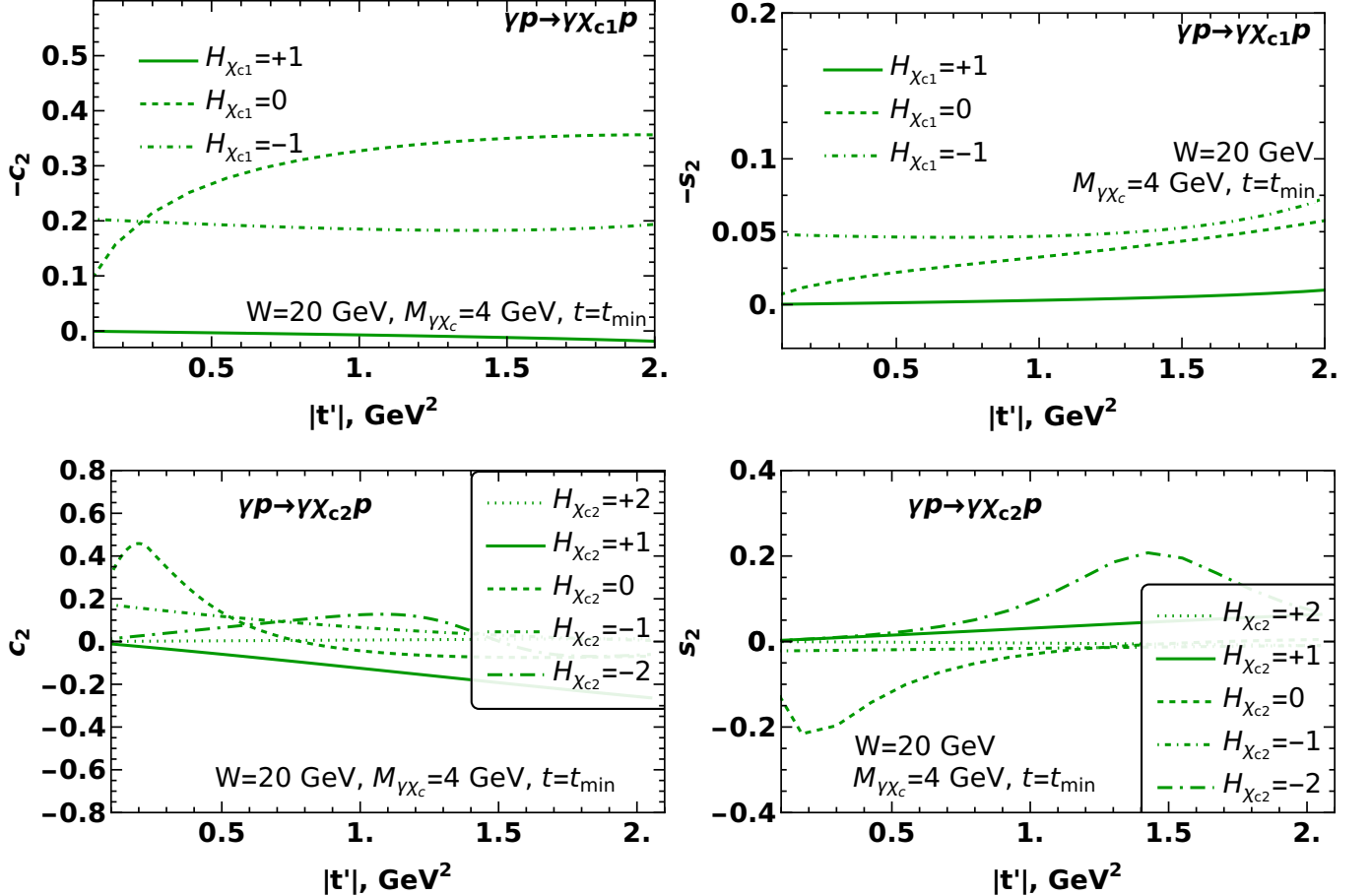


Figure 15. Sensitivity of the angular harmonics c_2, s_2 defined in (25-30) to the polarization of the final-state photon (for the sake of definiteness we consider polarization “+1”). The notation H_{χ_c} is the helicity of the produced χ_c meson. Top and bottom rows correspond to χ_{c1} and χ_{c2} respectively (for spinless χ_{c0} , the cross-section is not sensitive to the sign of the final-state helicity). For the sake of definiteness we assumed that the parameter ϵ defined in (26) equals $\epsilon = 0.5$.

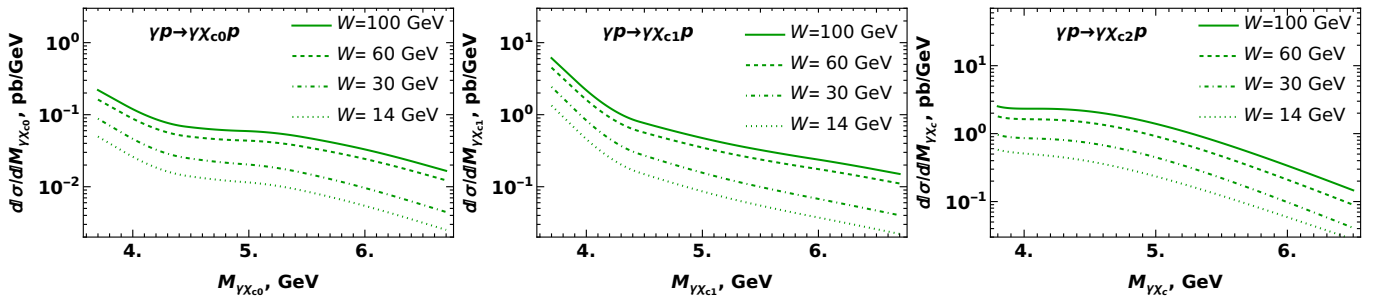


Figure 16. The single-differential cross-section $d\sigma/dM_{\gamma \chi_c}$ as a function of the invariant mass of $\chi_c \gamma$ pair at different collision energies.

The $\chi_c \gamma$ photoproduction proposed in this manuscript deserves a lot of interest as a potential background to χ_c photoproduction. Indeed, since the acceptance for photons at modern detectors is below unity, there is a sizable probability that the final photon is not observed, and so the $\chi_c \gamma$ photoproduction could be misinterpreted as exclusive χ_c production. Formally the cross-section of $\chi_c \gamma$ is suppressed by factor $\mathcal{O}(\alpha_{\text{em}})$, however this suppression can be partially compensated by lack of the small C -odd exchanges in t -channel, thus leading to a comparable sizable contribution. In general the accurate estimate of this background requires detailed knowledge of the detector’s geometry and acceptance. In what follows we will assume for simplicity that *all* photons remain undetected, and will

	$\sigma_{\text{tot}}^{(\text{ep})}$	dN/dt	N	$\text{Br}(\chi_c(1P) \rightarrow J/\psi\gamma)$	$\text{Br}(J/\psi \rightarrow \mu^+\mu^-)$	dN_d/dt	N_d
χ_{c0}	31 fb.	27/day	3.1×10^3	1.4 %	5.9 %	0.65/month	2.5
χ_{c1}	230 fb	199/day	2.3×10^4	34.3 %		120/month	460
χ_{c2}	250 fb	216/day	2.5×10^4	19 %		73/month	280

Table I. Estimates of the cross-section, production and counting rates in the kinematics of the future EIC collider. Values of the cross-section $\sigma_{\text{tot}}^{(\text{ep})}$ are evaluated at $\sqrt{s_{\text{ep}}} = 141$ GeV with cutoff on the invariant mass $M_{\gamma\chi_{c0}} \geq 3.7$ GeV. For estimates of the production rate dN/dt we used the instantaneous luminosity $\mathcal{L} = 10^{34} \text{ cm}^{-2}\text{s}^{-1} = 10^{-5} \text{ fb}^{-1}\text{s}^{-1}$, and the total number of produced events N was estimated using integrated luminosity $\int dt \mathcal{L} = 100 \text{ fb}^{-1}$ [8, 9, 58]. The detection rate N_d and the total number of events was obtained multiplying these numbers by a product of branchings $\text{Br}(\chi_c(1P) \rightarrow J/\psi\gamma) \text{Br}(J/\psi \rightarrow \mu^+\mu^-)$, whose values were taken from [58, 59].

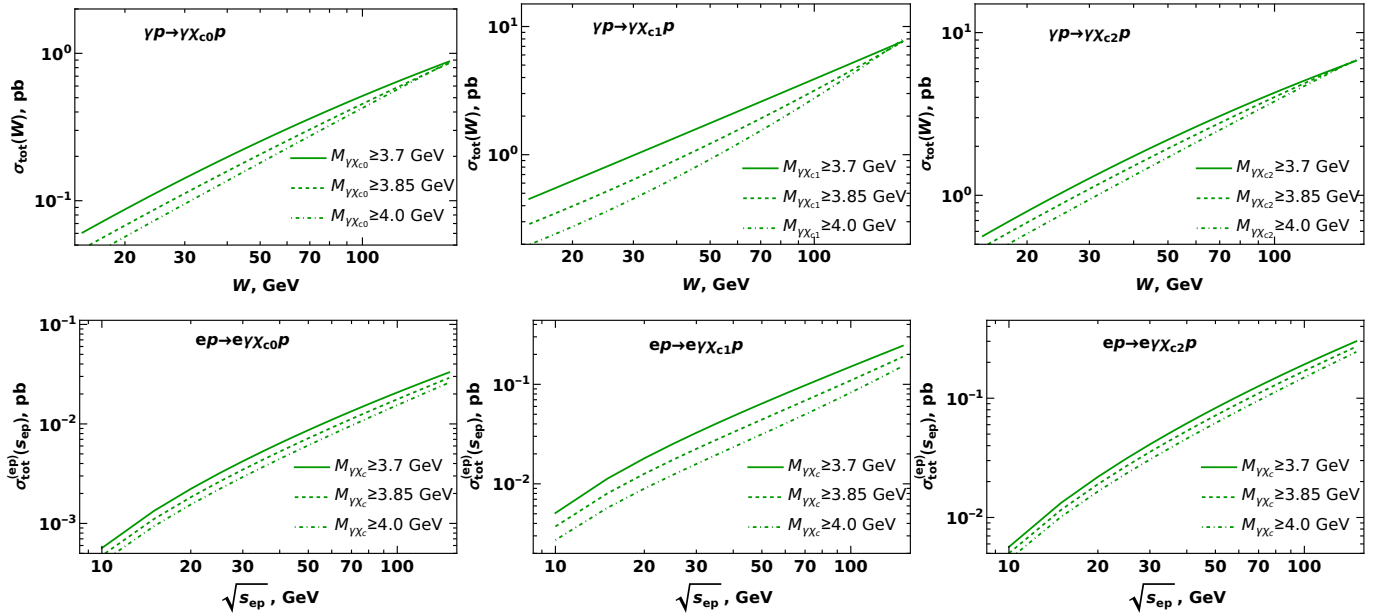


Figure 17. Predictions for the total (“fiducial”) cross-section of photoproduction (upper row) and electroproduction (lower row) as a function of energy W for different cutoffs on the invariant mass of $\chi_c\gamma$ pairs.

integrate over the momentum of the produced photon. Such approach gives an upper estimate for the $\chi_c\gamma$ background.

In the Figure (18) we have shown the cross-sections of the χ_c and $\chi_c\gamma$ with unobserved photon in the final state. For χ_{c1} and χ_{c2} the cross-section of the process $\chi_c\gamma$ exceeds the cross-section of the χ_c photoproduction in the small- t kinematics ($|t| \lesssim 1 \text{ GeV}^2$), though is exponentially suppressed at large t due to implemented GPD model [45, 53–56]. The fact that odderon contribution in the small- t kinematics can be smaller than contributions of other mechanisms is known from the literature, and the Primakoff mechanism has been considered as a major background to odderon-mediated production [43, 66]. Our findings indicate that for χ_{c1} and χ_{c2} , the production via $\gamma p \rightarrow \chi_c\gamma p$ mechanism gives a comparable background. Furthermore, in contrast to Primakoff contribution, this mechanism gives the same contribution for proton and neutron targets, and thus cannot be eliminated using neutron-rich target.

IV. CONCLUSIONS

In this paper we analyzed the exclusive $\chi_c\gamma$ photoproduction in the collinear factorization approach and calculated separately contributions of different helicity components. We provide the analytic expressions for the coefficient function of all helicity components, which are the rational functions of their arguments. They have a pair of “classical” poles at $x = \pm\xi$, and a pair of supplementary poles at $x = \pm\kappa\xi$, where the parameter κ is a function of kinematics and is restricted by $|\kappa| < 1$ in the physically allowed region. The complex structure of the coefficient function does not permit direct deconvolution (inversion of the integrals in 36–37 for extraction of GPDs). Nonetheless, it has been observed that the coefficient functions are mostly sensitive to the behavior of the GPDs in the vicinity of its poles,

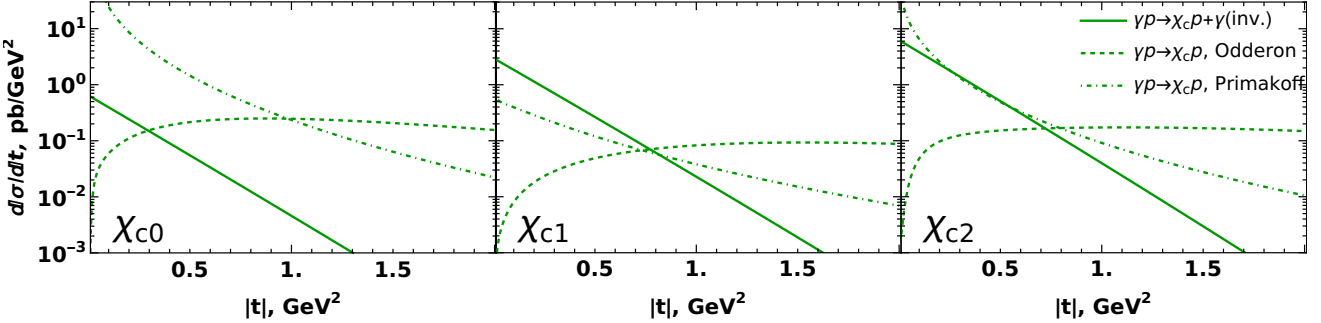


Figure 18. The cross-section of the process $\gamma p \rightarrow \chi_c \gamma p$ with invisible photon is compared with the cross-sections of the $\gamma p \rightarrow \chi_c p$ production via odderon exchange and Primakoff mechanism. The cross-sections of $\gamma p \rightarrow \chi_c p$ with different spins are taken from [43] (Fig 3 for $x = 10^{-2}$); the cross-section of $\gamma p \rightarrow \chi_c \gamma p$ is evaluated at the same invariant energy $W = \sqrt{M_{\chi_c}^2/x} \approx 35$ GeV.

and by varying the kinematics and thereby altering the position of the poles, the proposed process can be utilized to constrain existing phenomenological parametrizations of GPDs across the entire ERBL region. We also demonstrated that in electroproduction for some helicity components there are sizable angular asymmetries which can be used as complementary observables for experimental study.

Numerically, the cross-sections for all spins on unpolarized target get the dominant contribution from the unpolarized gluon GPD H_g . We found that the χ_{c1} and χ_{c2} mesons have sufficiently large cross-sections for experimental study, and that predominantly these mesons are produced with the same sign of helicity as the incoming photon. The typical cross-sections for these mesons are of order a few picobarns in the kinematics of low-energy EIC experiments, comparable by magnitude to cross-sections of $\gamma^* p \rightarrow \gamma M p$, $M = \eta_c, \pi, \rho$ processes evaluated for the same (large) values of invariant masses of meson-photon pair. We believe that this process is within the reach of experimental studies: for instance, for ep collisions at EIC we expect the production rate of a few thousand $\chi_c \gamma$ pairs per each 100 fb^{-1} of integrated luminosity. For χ_{c0} meson, the production cross-section and the expected detection rates are significantly smaller and apparently insufficient for reliable experimental study.

We believe that the suggested process can be studied experimentally in the ultraperipheral kinematics at LHC, in electron-proton collisions at the future Electron Ion Collider (EIC) [7–9] and possibly at JLAB after future 22 GeV upgrade [69].

ACKNOWLEDGEMENTS

We thank our colleagues at UTSFSM university for encouraging discussions. This research was partially supported by ANID PIA/APOYO AFB230003 (Chile) and Fondecyt (Chile) grants 1220242 and 1251975. I. Z. also acknowledges support of the fellowship “ANID Beca de Doctorado Nacional”, and expresses his gratitude to the Institute of Physics of PUCV. “Powered@NLHPC: This research was partially supported by the supercomputing infrastructure of the NLHPC (ECM-02)”.

Appendix A: Wave function of the χ_c meson

In the literature there are several complementary descriptions of heavy quarkonia dynamics, in terms of the light cone wave functions (LCWFs), and in terms of the NRQCD matrix elements, which may be obtained from the LCWFs in the heavy quark mass limit [70–72]. We will start our discussion with the former in view of its simplicity and will discuss its matching with NRQCD at the end of this section.

Following the historical tradition, in this section we will temporarily choose the frame in which the χ_c meson moves with infinitely large momentum in “ $-$ ” direction and zero transverse momentum,

$$p_{\chi_c}^\mu = \left(\frac{M_{\chi_c}^2}{2p_{\chi_c}^-}, p_{\chi_c}^-, \mathbf{0}_\perp \right). \quad (\text{A1})$$

This frame is related to any other frame in which the quarkonium has nonzero transverse momentum \mathbf{p}_\perp by a

transverse boost which keeps the " - " component of the arbitrary vector v ,

$$v^- \rightarrow v^-, \quad v^+ \rightarrow v^+ + \beta_\perp \cdot v_\perp + v^- \beta_\perp^2/2, \quad v_\perp \rightarrow v_\perp + v^- \beta_\perp. \quad (\text{A2})$$

with $\beta_\perp = -\mathbf{p}_\perp/p^-$. The leading twist quarkonia wave functions may be defined in momentum space

$$\Phi_{\chi_{cJ}}(z, \mathbf{k}_\perp) = \int d^2 \mathbf{r}_\perp e^{-i\mathbf{k}_\perp \cdot \mathbf{r}_\perp} \int \frac{d\lambda}{2\pi} e^{izp_{\chi_c}^\perp \lambda} \times \quad (\text{A3})$$

$$\times \left\langle 0 \left| \bar{\Psi} \left(-\frac{\lambda}{2} n_+ - \frac{\mathbf{r}_\perp}{2} \right) \Gamma_{\chi_{cJ}} \mathcal{L} \left(-\frac{\lambda}{2} n_+ - \frac{\mathbf{r}_\perp}{2}, \frac{\lambda}{2} n_+ + \frac{\mathbf{r}_\perp}{2} \right) \Psi \left(\frac{\lambda}{2} n_+ + \frac{\mathbf{r}_\perp}{2} \right) \right| \chi_c(p) \right\rangle, \\ \mathcal{L}(xy) \equiv \mathcal{P}\exp \left(ig \int_y^x d\zeta A_a^-(\zeta) t^a + ie \int_y^x d\zeta A^-(\zeta) \right). \quad (\text{A4})$$

where z is the fraction of its momentum carried by the c -quark, $\mathbf{k}_\perp = \mathbf{k}_Q^\perp - \mathbf{k}_{\bar{Q}}^\perp$ is the transverse component of the relative momentum, and \mathcal{L} is the usual Wilson link introduced to guarantee the gauge invariance of the result. In presence of the electromagnetic field, in order to guarantee the local gauge invariance of the defined wave function, the Wilson link must also include the second term $ie \int_y^x d\zeta A_{(\text{em})}^-(\zeta)$ in the argument of the exponent. In diagrammatic language, as explained in [47], this Wilson link implies additional contributions with coupling of the gauge boson, as shown in the Figure 19. After integration over \mathbf{k}_\perp (which corresponds to the limit $\mathbf{r}_\perp = 0$ in the configuration space), these objects reduce to the light-cone distribution amplitudes (LCDAs) discussed in detail in [73–77]. The matrix Γ_{χ_c} which appears in (A3) depends on the spin J of the χ_c meson and its helicity H , and is given explicitly by

$$\Gamma_{\chi_{cJ}} = \begin{cases} 1, & J = 0 \\ i\gamma_5 \gamma_\mu E^\mu, & J = 1 \\ \frac{1}{2} (\gamma_\mu k_\nu + \gamma_\nu k_\mu) E^{\mu\nu}, & J = 2 \end{cases} \quad (\text{A5})$$

where the vector E^μ and tensor $E^{\mu\nu}$ are defined in arbitrary frame as

$$E_{H=\pm 1}^\mu = \left(\frac{e_H^\perp \cdot \mathbf{p}_\perp^{\chi_c}}{p_{\chi_c}^-}, 0, e_H^\perp \right), \quad e_H^\perp = \frac{1}{\sqrt{2}} \begin{pmatrix} 1 \\ iH \end{pmatrix}, \quad (\text{A6})$$

$$E_{H=0}^\mu = \frac{p_{\chi_c}^\mu}{M_{\chi_c}} - \frac{M_{\chi_c}}{p_{\chi_c}^-} n_-^\mu = \frac{1}{M_{\chi_c}} \left(\frac{(\mathbf{p}_\perp^{\chi_c})^2 - M_{\chi_c}^2}{2p_{\chi_c}^-}, p_{\chi_c}^-, \mathbf{p}_\perp^{\chi_c} \right), \quad (\text{A7})$$

$$E^{\mu\nu} = \begin{cases} E_{\pm 1}^\mu E_{\pm 1}^\nu, & H = \pm 2 \\ \frac{1}{\sqrt{2}} (E_{\pm 1}^\mu E_0^\nu + E_{\pm 1}^\nu E_0^\mu), & H = \pm 1 \\ \frac{1}{\sqrt{6}} (E_{+1}^\mu E_{-1}^\nu + E_{-1}^\mu E_{+1}^\nu + 2E_0^\mu E_0^\nu), & H = 0 \end{cases} \quad (\text{A8})$$

and $k^\mu \equiv k_Q^\mu - k_{\bar{Q}}^\mu \approx p_{\chi_c}^- (2z - 1) n_-^\mu + \mathbf{k}_\perp^\mu$ is the relative momentum of the quark-antiquark motion. Note that the vector k^μ always remains orthogonal to p_{χ_c} , namely $k \cdot p_{\chi_c} = 0$. From (A5) we may observe that in the limit $k^\mu \rightarrow 0$ the corresponding vertex with $J = 2$ vanishes, as expected for the P -wave. It is straightforward to show that a similar property is valid for the states $J = 0$ and $J = 1$, if we take into account that $\Gamma_{\chi_{cJ}}$ is plugged between the spinors \bar{u}, v of the quark and antiquark (hidden in $\bar{\psi}, \psi$) and use the Dirac equation together with orthogonality of polarization vector $E_H \cdot p_{\chi_c} = 0$, namely

$$\bar{u}(k_0) \Gamma_{\chi_{cJ}} v(k_1) = \frac{1}{2m} \bar{u}(k_0) (m \Gamma_{\chi_{cJ}} + \Gamma_{\chi_{cJ}} m) v(k_1) = \frac{1}{2m} \bar{u}(k_0) (\hat{k}_0 \Gamma_{\chi_{cJ}} - \Gamma_{\chi_{cJ}} \hat{k}_1) v(k_1) \quad (\text{A9})$$

$$= \frac{1}{4m} \bar{u}(k_0) (\hat{p}_{\chi_c} \Gamma_{\chi_{cJ}} - \Gamma_{\chi_{cJ}} \hat{p}_{\chi_c}) v(k_1) + \frac{1}{4m} \bar{u}(k_0) (\hat{k} \Gamma_{\chi_{cJ}} + \Gamma_{\chi_{cJ}} \hat{k}) v(k_1) = \frac{k^\mu}{4m} \bar{u}(k_0) (\gamma^\mu \Gamma_{\chi_{cJ}} + \Gamma_{\chi_{cJ}} \gamma^\mu) v(k_1)$$

In view of this, we can replace the matrix $\Gamma_{\chi_{cJ}}$ with an equivalent $\Gamma_{\chi_{cJ}}^{(\text{eff})} = (\gamma^\mu \Gamma_{\chi_{cJ}} + \Gamma_{\chi_{cJ}} \gamma^\mu)/4m = \gamma_{\chi_{cJ}}^\mu k_\mu$, where $\gamma_{\chi_{c0}}^\mu \equiv \gamma^\mu/2m$, $\gamma_{\chi_{c1}}^\mu \equiv [\gamma^\mu, \hat{E}_H] \gamma^5/4m$ and $\gamma_{\chi_{c2}}^\mu = E^{\mu\nu} \gamma_\nu$. In the configuration space, the corresponding relative momentum k_μ can be replaced with $i \overleftrightarrow{\partial}_\mu$. In the hard processes, whose scale significantly exceeds the inverse

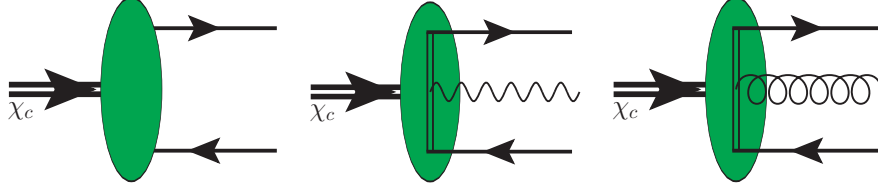


Figure 19. The diagrammatic representation of the leading twist Fock components of the χ_c meson, in notations of [47]. The last two diagrams explicitly show contributions of the photons and gluons connected to Wilson line (a double line connecting two quarks). In NRQCD picture these diagrams schematically illustrate the contributions of operators which include gauge field in the covariant derivatives D_μ .

charmonium radius, it is possible to disregard completely the dependence on z, \mathbf{k}_\perp in the partonic-level amplitude, so the final result will depend only the wave function integrated over z, \mathbf{k}_\perp , namely

$$\begin{aligned} & \int dz \int \frac{d^2 \mathbf{k}_\perp}{(2\pi)^2} \Phi_{\chi_c}(z, \mathbf{k}_\perp) = \\ &= \lim_{\lambda, \mathbf{r}_\perp \rightarrow 0} \left\langle 0 \left| \bar{\Psi} \left(-\frac{\lambda}{2} n_+ - \frac{\mathbf{r}_\perp}{2} \right) \gamma_{\chi_{cJ}}^\mu i \overleftrightarrow{\partial}_\mu \mathcal{L} \left(-\frac{\lambda}{2} n_+ - \frac{\mathbf{r}_\perp}{2}, \frac{\lambda}{2} n_+ + \frac{\mathbf{r}_\perp}{2} \right) \Psi \left(\frac{\lambda}{2} n_+ + \frac{\mathbf{r}_\perp}{2} \right) \right| \chi_c(p) \right\rangle \\ &= \left\langle 0 \left| \bar{\Psi}(0) \gamma_{\chi_{cJ}}^\mu \frac{i}{2} \overleftrightarrow{D}_\mu \Psi(0) \right| \chi_c(p) \right\rangle \end{aligned} \quad (\text{A10})$$

where $\overleftrightarrow{D}_\mu = \overrightarrow{\partial}_\mu - \overleftarrow{\partial}_\mu + 2igA_\mu^a t_a + 2ieA_\mu$ is the covariant derivative. The square of the matrix element which appears in the last line of (A10) in the nonrelativistic limit reduces to NRQCD LDMEs. Indeed, using explicit form of $\gamma_{\chi_{cJ}}^\mu$ for $J = 0, 1, 2$, we may recover the familiar NRQCD operators from [70–72]

$$\left| \left\langle 0 \left| \bar{\psi}(0) \gamma_{\chi_{cJ}}^\mu i \overleftrightarrow{D}_\mu \psi(0) \right| \chi_c(p) \right\rangle \right|^2 = \frac{1}{4m^2} \times \begin{cases} \left| \left\langle 0 \left| \bar{\psi} \left(\frac{i}{2} \overleftrightarrow{D}_\top^\mu \gamma_\mu^\top \right) \chi \right| \chi_c(p) \right\rangle \right|^2 = \left\langle \mathcal{O}_{\chi_c}^{[1]} \left({}^3P_0^{[1]} \right) \right\rangle, & J = 0 \\ \left| \left\langle 0 \left| \psi^\dagger \left(-\frac{i}{4} \overleftrightarrow{D}_\top^\nu [\gamma_\top^\top, \gamma_\mu^\top] \right) \gamma_5 \chi \right| \chi_c(p) \right\rangle \right|^2 = \left\langle \mathcal{O}_{\chi_c}^{[1]} \left({}^3P_1^{[1]} \right) \right\rangle, & J = 1 \\ \left| \left\langle 0 \left| \psi^\dagger \left(-\frac{i}{2} \overleftrightarrow{D}_\top^{(\mu} \gamma_\top^{\nu)} \right) \chi \right| \chi_c(p) \right\rangle \right|^2 = \left\langle \mathcal{O}_{\chi_c}^{[1]} \left({}^3P_2^{[1]} \right) \right\rangle, & J = 2 \end{cases} \quad (\text{A11})$$

where \top implies a part of the vector which is transverse to $p_{\chi_c}^\mu$, namely $v_\top^\mu = (g^{\mu\nu} - p_{\chi_c}^\mu p_{\chi_c}^\nu / M_{\chi_c}^2) v^\nu$; $a_\top^{(\mu} b_\top^{\nu)} = (a_\top^\mu b_\top^\nu + a_\top^\nu b_\top^\mu) / 2 - a_\top \cdot b_\top (g^{\mu\nu} - p_{\chi_c}^\mu p_{\chi_c}^\nu / M_{\chi_c}^2) / 3$, the operators ψ^\dagger, χ are the Pauli spinor operators which create a quark and an antiquark, respectively. The presence of the gauge fields in covariant derivative $\overleftrightarrow{D}_\mu$ implies that we should consider the χ_c meson as a mixture of $|\bar{Q}Q\rangle$, $|\bar{Q}Qg\rangle$ and $|\bar{Q}Q\gamma\rangle$ Fock components, as shown in the Figure 19. Only in the special gauge $A^- = 0$, $A_a^- = 0$ we may disregard the contributions of $|\bar{Q}Qg\rangle$ and $|\bar{Q}Q\gamma\rangle$. This choice of the gauge condition remains invariant under transverse boosts (A2) and for this reason in what follows we will use it for the electromagnetic field. We also need to mention that in the leading order there is no diagrams with gluons connected directly to χ_c , so we do not impose any gauge conditions for the gluonic field.

The explicit expression for the NRQCD projectors of P -wave include differential operators which eventually require taking derivatives of the partonic amplitude of the whole process with respect to components of the momentum k^μ , and eventually lead to sophisticated expressions. For this reason, instead of applying NRQCD directly, we will assume that the nonperturbative wave function $\Phi_{\chi_{cJ}}(z, \mathbf{k}_\perp)$ is given by

$$\Phi_{\chi_{cJ}}(z, \mathbf{k}_\perp) = \bar{u} \left(\frac{p_{\chi_{cJ}}}{2} + \frac{\mathbf{k}}{2} \right) \Gamma_{\chi_{cJ}} v \left(\frac{p_{\chi_{cJ}}}{2} - \frac{\mathbf{k}}{2} \right) \phi(z, \mathbf{k}_\perp) \quad (\text{A12})$$

where the scalar light-cone wave function $\phi(z, \mathbf{k}_\perp)$ is related to the rest frame wave function of χ_c via [78]

$$\frac{dz d^2 \mathbf{k}}{z(1-z) 16\pi^3} \phi(z, \mathbf{k}_\perp) = \frac{1}{4\pi^2 \sqrt{M_{\chi_c}}} \frac{1}{2\sqrt{2}} d^3 k \frac{u(k)}{k^2}, \quad k_z \equiv M_{\chi_c} \left(z - \frac{1}{2} \right) \quad (\text{A13})$$

and $u(k)/k$ is the radial part of the rest frame wave function in the momentum space. Using the identity

$$\int_0^\infty dk k^2 dk u(k) = 3 \sqrt{\frac{\pi}{2}} R'(0) = \sqrt{2M_{\chi_c}} \int \frac{dz d^2 \mathbf{k}}{z(1-z) 8\pi^2} \phi(z, \mathbf{k}_\perp) \left[M_{\chi_c}^2 \left(z - \frac{1}{2} \right)^2 + \mathbf{k}_\perp^2 \right] \quad (\text{A14})$$

where $R'_{\chi_c}(0)$ is the slope of the radial wave function of χ_c , we may relate the light-cone wave function with NRQCD matrix elements

$$\left\langle \mathcal{O}_{\chi_c}^{[1]} \left({}^3P_J^{[1]} \right) \right\rangle = 6N_c (2J+1) |R'_{\chi_c}(0)|^2 / 4\pi \quad (\text{A15})$$

Using the explicit parametrization from [43] rewritten in momentum space,

$$\phi(z, \mathbf{k}_\perp) = \mathcal{N} \exp \left(-\frac{\mathcal{R}^2}{8} \left(\frac{\mathbf{k}_\perp^2 + m^2}{z(1-z)} - 4m^2 \right) \right) \quad (\text{A16})$$

where \mathcal{N}, \mathcal{R} are some numerical constants, we found that the results for $|R'(0)|$ agree within 10 per cent with value $|R'(0)|^2 = 0.075 \text{ GeV}^5$ calculated in potential models and widely used in the literature for numerical estimates.

Appendix B: Evaluation of the coefficient functions

The evaluation of the coefficient functions can be performed using the standard light-cone rules from [1, 3, 44, 57, 79, 80]. As discussed in Section II A, we disregard the proton mass m_N and the invariant momentum transfer to the proton $t = \Delta^2$, treating all the other variables as parametrically large quantities of order m_c . The evaluation of the partonic amplitudes shown in the Figure 4 is straightforward.

In general, the coefficient functions $C_{\gamma\chi_c}$, $\tilde{C}_{\gamma\chi_c}$ which appear in (36-37) should be understood as convolutions of partonic-level amplitudes with wave function Φ_{χ_c} , namely,

$$C_{\gamma\chi_c}^{(\lambda,\sigma,H)}(x, \xi) = \int \frac{dz d^2\mathbf{k}}{z(1-z)16\pi^3} c^{(\lambda,\sigma)}(x, \xi, z, \mathbf{k}_\perp) \Phi_{\chi_c}^{(H)}(z, \mathbf{k}_\perp), \quad (\text{B1})$$

$$\tilde{C}_{\gamma\chi_c}^{(\lambda,\sigma,H)}(x, \xi) = \int_0^1 \frac{dz d^2\mathbf{k}}{z(1-z)16\pi^3} \tilde{c}^{(\lambda,\sigma)}(x, \xi, z, \mathbf{k}_\perp) \Phi_{\chi_c}^{(H)}(z, \mathbf{k}_\perp). \quad (\text{B2})$$

The evaluation of the partonic amplitudes $c(x, \xi, z, \mathbf{k}_\perp)$, $\tilde{c}(x, \xi, z, \mathbf{k}_\perp)$ may be done perturbatively for all diagrams shown in the Figure 4. The (implicit) summation over helicities of the quark and antiquark in the wave function (A12) and the partonic amplitude using identities $\sum_h u_h(k)\bar{u}_h(k) = \hat{k} + m$, $\sum_{\bar{h}} v_{\bar{h}}(k)\bar{v}_{\bar{h}}(k) = \hat{k} - m$ yields an effective vertex (projector) [41, 42, 81],

$$\hat{P}_{\chi_{cJ}} = -\sqrt{\frac{\langle \mathcal{O}_{\chi_c} \rangle}{m_Q}} \frac{1}{8m_Q} \left(\frac{\hat{p}_{\chi_c}}{2} - \frac{\hat{k}}{2} - m_c \right) \Gamma_{\chi_{cJ}} \left(\frac{\hat{p}_{\chi_c}}{2} + \frac{\hat{k}}{2} + m_c \right) \otimes \frac{\delta_{ij}}{\sqrt{N_c}}, \quad (\text{B3})$$

where the vector of relative momentum $k = k_Q - k_{\bar{Q}}$ was defined in (38), the helicity-dependent matrix $\Gamma_{\chi_{cJ}}$ was defined in (A5). $\langle \mathcal{O}_{\chi_c} \rangle \equiv \left\langle \mathcal{O}_{\chi_c} \left({}^3P_J^{[1]} \right) \right\rangle$ is the corresponding color singlet LDME of χ_c meson [82]. We need to mention that in the heavy quark mass limit the internal motion is negligible, so the wave function $\Phi_{\chi_c}^{(H)}(z, \mathbf{k}_\perp)$ is strongly peaked near the point $z = 1/2$, $\mathbf{k}_\perp = 0$. For this reason, making expansion near this point and using the relations (A14,A15), we obtain a result which includes an LDME multiplied by the functions of variables x, ξ which do not depend on z, \mathbf{k}_\perp . We need to mention that C -conjugate diagrams (with inverted direction of quark lines) mutually cancel odd terms in the series expansion over $(z - 1/2)$, \mathbf{k}_\perp and double the coefficients in front of even powers.

The interaction of the heavy quarks with the target proceeds via exchange of gluons in t -channel. At high energies this interaction is parametrized by the leading twist gluon GPDs, which are defined as [3, 81]

$$\begin{aligned} F^g(x, \xi, t) &= \frac{1}{P^+} \int \frac{dz}{2\pi} e^{ix\bar{P}^+} \left\langle P' \left| G^{+\mu a} \left(-\frac{z}{2} n \right) \mathcal{L} \left(-\frac{z}{2}, \frac{z}{2} \right) G_\mu^{+a} \left(\frac{z}{2} n \right) \right| P \right\rangle = \\ &= \left(\bar{U}(P') \gamma_+ U(P) H^g(x, \xi, t) + \bar{U}(P') \frac{i\sigma^{+\alpha} \Delta_\alpha}{2m_N} U(P) E^g(x, \xi, t) \right), \end{aligned} \quad (\text{B4})$$

$$\begin{aligned} \tilde{F}^g(x, \xi, t) &= \frac{-i}{P^+} \int \frac{dz}{2\pi} e^{ix\bar{P}^+} \left\langle P' \left| G^{+\mu a} \left(-\frac{z}{2} n \right) \mathcal{L} \left(-\frac{z}{2}, \frac{z}{2} \right) \tilde{G}_\mu^{+a} \left(\frac{z}{2} n \right) \right| P \right\rangle = \\ &= \left(\bar{U}(P') \gamma_+ \gamma_5 U(P) \tilde{H}^g(x, \xi, t) + \bar{U}(P') \frac{\Delta^+ \gamma_5}{2m_N} U(P) \tilde{E}^g(x, \xi, t) \right). \end{aligned} \quad (\text{B5})$$

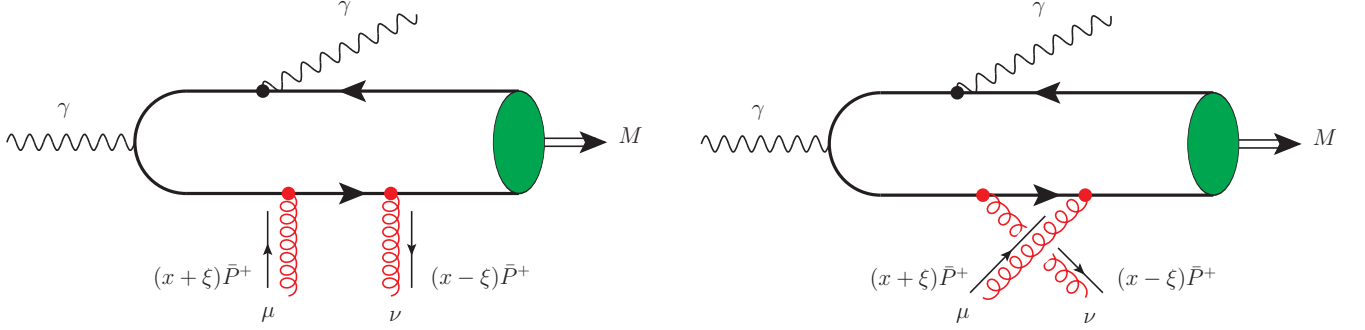


Figure 20. Example of the diagrams with direct and permuted t -channel gluons, which are related to each other by inversion of sign in front of light-cone fraction $x \leftrightarrow -x$, and permutation of the Lorentz indices $\mu \leftrightarrow \nu$.

$$\tilde{G}^{\mu\nu,a} \equiv \frac{1}{2} \varepsilon^{\mu\nu\alpha\beta} G_{\alpha\beta}^a, \quad \mathcal{L}\left(-\frac{z}{2}, \frac{z}{2}\right) \equiv \mathcal{P}\exp\left(i \int_{-z/2}^{z/2} d\zeta A^+(\zeta)\right). \quad (\text{B6})$$

where we introduced notations U, \bar{U} for the spinors of the incoming and outgoing proton. In the light-cone gauge $A^+ = 0$ the Wilson link \mathcal{L} can be disregarded, so the gluon operators in (B4, B5) can be rewritten as

$$G^{+\mu_\perp a}(z_1) G_{\mu_\perp}^{+a}(z_2) = g_{\mu\nu}^\perp (\partial^+ A^{\mu_\perp, a}(z_1)) (\partial^+ A^{\nu_\perp, a}(z_2)), \quad (\text{B7})$$

$$\begin{aligned} G^{+\mu_\perp a}(z_1) \tilde{G}_{\mu_\perp}^{+a}(z_2) &= G^{+\mu_\perp a}(z_1) \tilde{G}_{-\mu_\perp}^a(z_2) = \frac{1}{2} \varepsilon_{-\mu_\perp\alpha\nu} G^{+\mu_\perp a}(z_1) G^{\alpha\nu, a}(z_2) = \\ &= \varepsilon_{-\mu_\perp+\nu_\perp} G^{+\mu_\perp a}(z_1) G^{+\nu_\perp, a}(z_2) = \varepsilon_{\mu\nu}^\perp G^{+\mu_\perp a}(z_1) G^{+\nu_\perp, a}(z_2) = \varepsilon_{\mu\nu}^\perp (\partial^+ A^{\mu, a}(z_1)) (\partial^+ A^{\nu, a}(z_2)). \end{aligned} \quad (\text{B8})$$

The integration over the light-cone separation z in (B4, B5) effectively corresponds to Fourier transformation to the momentum space, where the derivatives $\partial_{z_1}^+, \partial_{z_2}^+$ turn into the multiplicative factors $k_{1,2}^+ \sim (x \pm \xi) \bar{P}^+$. This allows to rewrite the Eqs. (B4, B5) as [81]

$$\frac{1}{\bar{P}^+} \int \frac{dz}{2\pi} e^{ix\bar{P}^+} \left\langle P' \left| A_\mu^a \left(-\frac{z}{2} n\right) A_\nu^b \left(\frac{z}{2} n\right) \right| P \right\rangle \Big|_{A^+=0 \text{ gauge}} = \frac{\delta^{ab}}{N_c^2 - 1} \left(\frac{-g_{\mu\nu}^\perp F^g(x, \xi, t) - \varepsilon_{\mu\nu}^\perp \tilde{F}^g(x, \xi, t)}{2(x - \xi + i0)(x + \xi - i0)} \right). \quad (\text{B9})$$

The Eq. (B9) suggests that the coefficient functions $C_{\gamma\chi_c}$ and $\tilde{C}_{\gamma\chi_c}$ can be obtained making convolutions of the Lorentz indices of t -channel gluons in diagrams of Figure 4 with $g_{\mu\nu}^\perp$ and $\varepsilon_{\mu\nu}^\perp$ respectively. The remaining steps in evaluation of the diagrams shown in Figure 4 were performed using Mathematica and yield

$$c(x, \xi) = 2 [\mathcal{C}(x, \xi) + \mathcal{C}(-x, \xi)], \quad (\text{B10})$$

$$\tilde{c}(x, \xi) = 2 [\tilde{\mathcal{C}}(x, \xi) - \tilde{\mathcal{C}}(-x, \xi)], \quad (\text{B11})$$

where the terms $\mathcal{C}(x, \xi)$ and $\tilde{\mathcal{C}}(x, \xi)$ in the right-hand sides of (B10, B11) correspond to the contributions of the six diagrams shown explicitly in the Figure 4, the last two terms (with $x \rightarrow -x$ substitution) are the contributions of diagrams with permuted gluons in the t -channel, as shown in the Figure 20, and the prefactor 2 in parenthesis in the right-hand side takes into account that C -conjugate diagrams (with inverted direction of quark lines) eventually give exactly the same contribution. From the right-hand side of (B10, B11) we may infer that c and \tilde{c} are even and odd functions of their first argument x . Explicitly, the components $\mathcal{C}^{(\lambda, \sigma, H)}(x, \xi, z)$ and $\tilde{\mathcal{C}}^{(\lambda, \sigma, H)}(x, \xi, z)$ are given in Appendix B.

Appendix C: Final results for the coefficient functions

In this Appendix we provide explicit expressions for the coefficient functions (partonic amplitudes) of the $\chi_c J\gamma$ production in helicity basis. Due to the P -parity the cross-sections which differ by global inversion of the sign of all helicities should coincide, $\mathcal{A}_{\gamma p \rightarrow \chi_c \gamma p}^{(-\lambda, -\sigma, -H)} = \mathcal{A}_{\gamma p \rightarrow \chi_c \gamma p}^{(\lambda, \sigma, H)}$, which implies that only half of all possible combinations are independent. For the sake of definiteness we will assume that for each helicity H , the incoming photon always has

helicity “+”, the emitted photon may have helicity +” or “-” (we’ll refer to them as helicity non-flip and helicity flip components, $C_{\gamma\chi_c}^{(+,+H)}$ and $C_{\gamma\chi_c}^{(+,-H)}$ respectively). We’ll assume that the remaining components can be recovered changing the sign of all helicities. For the sake of definiteness, we’ll choose the direction of the axis \hat{x} in direction of the vector \mathbf{p}_\perp . In any other frame, which differs by azimuthal rotation in transverse plane Oxy , the amplitudes in helicity basis are multiplied by a trivial phase factors $\sim e^{i\Lambda\alpha}$, where Λ is a linear combination of helicities of the incoming and outgoing bosons. In the cross-section, all such phase factors eventually cancel.

1. Coefficient functions for χ_{c0}

$$\begin{aligned}
 c_{\gamma\chi_{c0}}^{(++)}(r, \alpha, \zeta = x/\xi) = & -\frac{4\mathfrak{C}_{\chi_c}}{\alpha^2 (1+\bar{\alpha})^2 (\bar{\alpha}+1/r^2) (r^2-1)^2 (\zeta+1-i0) (\zeta-1+i0) (\zeta-\kappa+i0)^2} \times \\
 & \times \left\{ \begin{aligned}
 & (\alpha^6 - 3\alpha^5 - 13\alpha^4 + 68\alpha^3 - 68\alpha^2 + 16\alpha) \zeta^4 + \alpha^7 + 10\alpha^6 + 84\alpha^5 - 227\alpha^4 + 122\alpha^3 + 120\alpha^2 \\
 & + (43\alpha^7 - 273\alpha^6 + 665\alpha^5 - 834\alpha^4 + 754\alpha^3 - 584\alpha^2 + 328\alpha - 96) \zeta^3 - 144\alpha + 32 \\
 & + (-149\alpha^7 + 713\alpha^6 - 1473\alpha^5 + 1844\alpha^4 - 1474\alpha^3 + 628\alpha^2 + 8\alpha - 96) \zeta^2 \\
 & + (105\alpha^7 - 323\alpha^6 + 487\alpha^5 - 290\alpha^4 - 286\alpha^3 + 560\alpha^2 - 256\alpha) \zeta \\
 & + \frac{1}{r^2} [(4\alpha^5 - 14\alpha^4 + 2\alpha^3 + 16\alpha^2 - 8\alpha) \zeta^4 + (-48\alpha^6 + 252\alpha^5 - 468\alpha^4 + 306\alpha^3 - 56\alpha^2 + 40\alpha - 32) \zeta^3 + \\
 & + (264\alpha^6 - 1044\alpha^5 + 1624\alpha^4 - 1602\alpha^3 + 1256\alpha^2 - 664\alpha + 160) \zeta^2 - 8\alpha^6 - 52\alpha^5 - 150\alpha^4 \\
 & - (272\alpha^6 - 696\alpha^5 + 960\alpha^4 - 782\alpha^3 + 48\alpha^2 + 384\alpha - 192) \zeta + 640\alpha^3 - 624\alpha^2 + 168\alpha + 32] \\
 & + \frac{1}{r^4} [(-5\alpha^4 + 24\alpha^3 - 36\alpha^2 + 16\alpha) \zeta^4 + (31\alpha^5 - 134\alpha^4 + 222\alpha^3 - 144\alpha^2 - 8\alpha + 32) \zeta^3 \\
 & + (-249\alpha^5 + 780\alpha^4 - 710\alpha^3 + 192\alpha^2 - 104\alpha + 96) \zeta^2 + 25\alpha^5 + 125\alpha^4 - 18\alpha^3 \\
 & + (369\alpha^5 - 670\alpha^4 + 642\alpha^3 - 656\alpha^2 + 344\alpha - 32) \zeta - 524\alpha^2 + 552\alpha - 160] \\
 & + \frac{1}{r^6} [(-10\alpha^4 + 38\alpha^3 - 64\alpha^2 + 72\alpha - 32) \zeta^3 + (142\alpha^4 - 410\alpha^3 + 320\alpha^2 + 48\alpha - 96) \zeta^2 + \\
 & + (-302\alpha^4 + 338\alpha^3 + 40\alpha^2 + 24\alpha - 96) \zeta - 38\alpha^4 - 126\alpha^3 + 216\alpha^2 + 32\alpha - 96] \\
 & + \frac{4(7\alpha^3 + 9\alpha^2 - (10\alpha^3 - 33\alpha^2 + 40\alpha - 16) \zeta^2 + (39\alpha^3 - 42\alpha^2 - 22\alpha + 24) \zeta - 30\alpha + 16)}{r^8} + \frac{8\bar{\alpha}((5\alpha - 4)\zeta + \alpha)}{r^{10}} \Big\} \\
 & + \left(\zeta \rightarrow -\zeta \right)
 \end{aligned} \tag{C1}$$

where we introduced shorthand notations $\alpha \equiv \alpha_{\chi_c} = (-u')/M_{\gamma\chi_c}$, $\zeta = x/\xi$, the constant \mathfrak{C}_{χ_c} in the prefactor is given explicitly by

$$\mathfrak{C}_{\chi_c} = \frac{4}{9N_c} \pi^2 \alpha_{\text{em}} \alpha_s(\mu) \pi \sqrt{\frac{3 \langle \mathcal{O}_{\chi_c}^{[1]} [{}^3P_J^{[1]}] \rangle}{2m_c^5 N_c (2J+1)}}, \tag{C2}$$

$\langle \mathcal{O}_{\chi_c} \rangle \equiv \langle \mathcal{O}_{\chi_c} [{}^3P_J^{[1]}] \rangle$ is the color singlet long-distance matrix element (LDME) of χ_c [82], and the notations κ, r were defined in (42). Similarly, we may obtain for the constants $c_{\gamma\chi_{c0}}^{(\lambda,\sigma)}, d_{\gamma\chi_{c0}}^{(\lambda,\sigma)}$ of other helicity states

$$\begin{aligned}
 d_{\gamma\chi_{c0}}^{(++)}(r, \alpha, \zeta = x/\xi) = & \frac{4\mathfrak{C}_{\chi_c}}{\alpha^4 (1+\bar{\alpha})^2 (\bar{\alpha}+1/r^2)^2 (r^2-1)^2 (\zeta+1-i0) (\zeta-1+i0) (\zeta-\kappa+i0)^2} \times \\
 & \times \left\{ \begin{aligned}
 & \frac{\bar{\alpha}\alpha^2}{8} [-5(1+\bar{\alpha})^2 (\alpha^2 + 2\bar{\alpha}) \zeta^4 + (1+\bar{\alpha}) (8\alpha^5 - 45\alpha^4 + 100\alpha^3 - 126\alpha^2 + 92\alpha - 40) \zeta^3 \\
 & + (16\alpha^6 - 91\alpha^5 + 212\alpha^4 - 254\alpha^3 + 156\alpha^2 - 24\alpha - 24) \zeta^2 - \alpha (8\alpha^5 - 31\alpha^4 + 42\alpha^3 + 2\alpha^2 - 56\alpha + 40) \zeta \\
 & - (\alpha^5 + 7\alpha^4 - 12\alpha^3 - 26\alpha^2 + 64\alpha - 32)] +
 \end{aligned} \right. \tag{C3}
 \end{aligned}$$

$$\begin{aligned}
& + \frac{1}{8r^2} [(-\alpha^7 - \alpha^6 + 29\alpha^5 - 88\alpha^4 + 124\alpha^3 - 96\alpha^2 + 32\alpha) \zeta^4 + \\
& \quad + (-19\alpha^8 + 157\alpha^7 - 513\alpha^6 + 914\alpha^5 - 1054\alpha^4 + 872\alpha^3 - 520\alpha^2 + 160\alpha) \zeta^3 \\
& \quad + (69\alpha^8 - 449\alpha^7 + 1209\alpha^6 - 1772\alpha^5 + 1514\alpha^4 - 628\alpha^3 - 72\alpha^2 + 128\alpha) \zeta^2 \\
& \quad + (-49\alpha^8 + 239\alpha^7 - 463\alpha^6 + 370\alpha^5 + 82\alpha^4 - 352\alpha^3 + 176\alpha^2) \zeta \\
& \quad - \alpha^8 - 10\alpha^7 - 24\alpha^6 + 187\alpha^5 - 182\alpha^4 - 160\alpha^3 + 288\alpha^2 - 96\alpha] \\
& + \frac{1}{4r^4} [(3\alpha^5 - 15\alpha^4 + 24\alpha^3 - 12\alpha^2) \zeta^4 + (8\alpha^7 - 70\alpha^6 + 214\alpha^5 - 317\alpha^4 + 276\alpha^3 - 172\alpha^2 + 96\alpha - 32) \zeta^3 + \\
& \quad + (-52\alpha^7 + 338\alpha^6 - 840\alpha^5 + 1105\alpha^4 - 928\alpha^3 + 508\alpha^2 - 96\alpha - 32) \zeta^2 \\
& \quad + (56\alpha^7 - 276\alpha^6 + 508\alpha^5 - 419\alpha^4 + 8\alpha^3 + 280\alpha^2 - 160\alpha) \zeta \\
& \quad + 4\alpha^7 + 16\alpha^6 - 5\alpha^5 - 242\alpha^4 + 404\alpha^3 - 116\alpha^2 - 96\alpha + 32] \\
& + \frac{1}{8r^6} [(\alpha^5 - 12\alpha^4 + 44\alpha^3 - 64\alpha^2 + 32\alpha) \zeta^4 + (-7\alpha^6 + 74\alpha^5 - 242\alpha^4 + 360\alpha^3 - 280\alpha^2 + 96\alpha) \zeta^3 + \\
& \quad + (73\alpha^6 - 532\alpha^5 + 1238\alpha^4 - 1256\alpha^3 + 696\alpha^2 - 352\alpha + 128) \zeta^2 \\
& \quad + (-121\alpha^6 + 642\alpha^5 - 1030\alpha^4 + 760\alpha^3 - 280\alpha^2 - 96\alpha + 128) \zeta \\
& \quad - 25\alpha^6 - 41\alpha^5 + 142\alpha^4 + 444\alpha^3 - 1032\alpha^2 + 512\alpha] \\
& + \frac{1}{4r^8} [(\alpha^5 - 11\alpha^4 + 36\alpha^3 - 60\alpha^2 + 64\alpha - 32) \zeta^3 + (-15\alpha^5 + 141\alpha^4 - 352\alpha^3 + 320\alpha^2 - 64\alpha - 32) \zeta^2 + \\
& \quad + (35\alpha^5 - 233\alpha^4 + 296\alpha^3 - 68\alpha^2 - 32) \zeta + 19\alpha^5 + 7\alpha^4 - 108\alpha^3 - 8\alpha^2 + 192\alpha - 96] \\
& + \frac{(2\alpha^4 - 21\alpha^3 + 60\alpha^2 - 72\alpha + 32) \zeta^2 + (-7\alpha^4 + 62\alpha^3 - 78\alpha^2 - 8\alpha + 32) \zeta - 7\alpha^4 + 3\alpha^3 + 26\alpha^2 - 24\alpha}{2r^{10}} \\
& - \bar{\alpha} \frac{(\alpha^2 + 8\bar{\alpha}) \zeta + \alpha^2}{r^{12}} \Big\} + \left(\zeta \rightarrow -\zeta \right)
\end{aligned}$$

$$\begin{aligned}
c_{\gamma\chi_{c0}}^{(+)}(r, \alpha, \zeta = x/\xi) &= \frac{4\mathfrak{C}_{\chi_c}(1 - \alpha r^2)}{\alpha (1 + \bar{\alpha})^2 (\bar{\alpha} + 1/r^2) (r^2 - 1)^2 (\zeta + 1 - i0) (\zeta - 1 + i0) (\zeta - \kappa + i0)^2} \times \tag{C4} \\
&\times \left\{ -\bar{\alpha} \left[8\alpha(2 - \alpha)^2 \zeta^4 + (16\alpha^5 - 87\alpha^4 + 174\alpha^3 - 192\alpha^2 + 112\alpha) \zeta^3 - \alpha^2 (32\alpha^3 - 109\alpha^2 + 142\alpha) \zeta^2 \right. \right. \\
&\quad \left. + 92\alpha^2 \zeta^2 + (16\alpha^5 - 21\alpha^4 + 18\alpha^3 + 12\alpha^2 + 8\alpha - 16) \zeta - \alpha^4 + 6\alpha^3 + 24\alpha^2 - 24\alpha \right] + \\
&+ \frac{1}{r^2} \left[(4\alpha^3 - 16\alpha^2 + 16\alpha) \zeta^4 + (-25\alpha^5 + 130\alpha^4 - 208\alpha^3 + 128\alpha^2 - 56\alpha + 32) \zeta^3 + \right. \\
&\quad \left. + (115\alpha^5 - 446\alpha^4 + 672\alpha^3 - 560\alpha^2 + 184\alpha + 32) \zeta^2 + (-91\alpha^5 + 182\alpha^4 - 172\alpha^3 + 16\alpha^2 + 72\alpha) \zeta + \right. \\
&\quad \left. + \alpha^5 + 6\alpha^4 - 72\alpha^3 + 48\alpha^2 + 56\alpha - 32 \right] \\
&+ \frac{1}{r^4} \left[(-4\alpha^3 + 16\alpha^2 - 16\alpha) \zeta^4 + (17\alpha^4 - 66\alpha^3 + 72\alpha^2 - 8\alpha - 32) \zeta^3 + \right. \\
&\quad \left. + (-135\alpha^4 + 386\alpha^3 - 308\alpha^2 + 152\alpha - 96) \zeta^2 \right. \\
&\quad \left. + (187\alpha^4 - 290\alpha^3 + 248\alpha^2 - 56\alpha - 96) \zeta - 5\alpha^4 + 6\alpha^3 + 132\alpha^2 - 152\alpha \right] \\
&+ \frac{4}{r^6} \left[(-2\alpha^3 + 6\alpha^2 - 8\alpha + 8) \zeta^3 + (21\alpha^3 - 44\alpha^2 + 4\alpha + 24) \zeta^2 + (-45\alpha^3 + 34\alpha^2 - 12\alpha + 24) \zeta + \right. \\
&\quad \left. + 2\alpha^3 - 12\alpha^2 - 12\alpha + 24 \right] \\
&- \frac{4((8\alpha^2 - 20\alpha + 16)\zeta^2 + (6 - 25\alpha)\alpha\zeta + (\alpha - 10)\alpha + 20\zeta + 8)}{r^8} + \frac{32\bar{\alpha}\zeta}{r^{10}} \Big\} + \left(\zeta \rightarrow -\zeta \right)
\end{aligned}$$

$$\begin{aligned}
d_{\gamma\chi_{c0}}^{(+)}(r, \alpha, \zeta = x/\xi) &= -\frac{4\mathfrak{C}_{\chi_c}(1/r^2 - \alpha)}{\alpha^2 r^2 (1 + \bar{\alpha})^2 (\bar{\alpha} + 1/r^2)^2 (r^2 - 1)^2 (\zeta + 1 - i0) (\zeta - 1 + i0) (\zeta - \kappa + i0)^2} \times \tag{C5} \\
&\times \left\{ \frac{\bar{\alpha}}{8} \left[4(\alpha - 2)^2 \alpha \zeta^4 + (8\alpha^5 - 47\alpha^4 + 106\alpha^3 - 132\alpha^2 + 96\alpha - 16) \zeta^3 + \alpha^2 (-16\alpha^3 + 61\alpha^2 - 94\alpha) \zeta^2 \right. \right. \\
&\quad \left. \left. + 4(\alpha - 2)^2 \alpha \zeta^2 + (8\alpha^5 - 47\alpha^4 + 106\alpha^3 - 132\alpha^2 + 96\alpha - 16) \zeta + 4(\alpha - 2)^2 \alpha \right] \right\} + \left(\zeta \rightarrow -\zeta \right)
\end{aligned}$$

$$\begin{aligned}
& + 68\alpha^2\zeta^2 + (8\alpha^5 - 13\alpha^4 + 14\alpha^3 - 8\alpha^2 + 24\alpha - 16)\zeta - \alpha(\alpha^3 - 2\alpha^2 - 24\alpha + 24) \Big] + \\
& + \frac{1}{8r^2} \left[(17\alpha^5 - 94\alpha^4 + 180\alpha^3 - 160\alpha^2 + 96\alpha - 32)\zeta^3 - \alpha^5 - 6\alpha^4 + 60\alpha^3 - 24\alpha^2 - 64\alpha + 32 \right. \\
& \quad \left. + (-67\alpha^5 + 278\alpha^4 - 480\alpha^3 + 488\alpha^2 - 240\alpha + 32)\zeta^2 + \alpha(51\alpha^4 - 114\alpha^3 + 112\alpha^2 - 48)\zeta \right] \\
& + \frac{1}{8r^4} \left[4(\alpha - 2)^2\alpha\zeta^4 - (17\alpha^4 - 78\alpha^3 + 124\alpha^2 - 80\alpha + 16)\zeta^3 + (103\alpha^4 - 330\alpha^3 + 348\alpha^2 - 208\alpha)\zeta^2 + \right. \\
& \quad \left. + 64\zeta^2 + (-123\alpha^4 + 222\alpha^3 - 220\alpha^2 + 80 + 16)\zeta + \alpha(5\alpha^3 - 6\alpha^2 - 132\alpha + 128) \right] \\
& + \frac{1}{2r^6} \left[2(2 - \alpha)(\alpha^2 - \alpha + 2)\zeta^3 - \alpha(21\alpha^2 - 56\alpha + 36)\zeta^2 + (37\alpha^3 - 42\alpha^2 + 20\alpha - 8)\zeta + \right. \\
& \quad \left. - (2\alpha^3 - 12\alpha^2 - 16\alpha + 16) \right] \\
& \left. - \frac{4(2\alpha^2 - 5\alpha + 4)\zeta^2 - (25\alpha^2 - 18\alpha + 8)\zeta + (\alpha^2 - 10\alpha)}{2r^8} - \frac{4\bar{\alpha}\zeta}{r^{10}} \right\} + \left(\zeta \rightarrow -\zeta \right)
\end{aligned}$$

$$\begin{aligned}
\tilde{c}_{\gamma\chi_{c0}}^{(++)}(r, \alpha, \zeta = x/\xi) = & -\frac{4\mathfrak{C}_{\chi_c}}{\alpha^2(1 + \bar{\alpha})^2(\bar{\alpha} + 1/r^2)(r^2 - 1)^2(\zeta + 1 - i0)(\zeta - 1 + i0)(\zeta - \kappa + i0)^2} \times \quad (C6) \\
& \times \left\{ \begin{aligned}
& -\alpha(\alpha^5 - 29\alpha^4 + 137\alpha^3 - 262\alpha^2 + 212\alpha - 56)\zeta^4 - \alpha(3\alpha^6 - 33\alpha^5 + 141\alpha^4 - 256\alpha^3 + 116\alpha^2 + 24\alpha)\zeta^3 \\
& - \alpha(3\alpha^6 + 5\alpha^5 - 5\alpha^4 - 178\alpha^3 + 280\alpha^2 - 236\alpha + 120)\zeta^2 + \\
& + \alpha(15\alpha^6 - 117\alpha^5 + 421\alpha^4 - 876\alpha^3 + 1088\alpha^2 - 648\alpha + 112)\zeta \\
& - \alpha(9\alpha^6 - 90\alpha^5 + 330\alpha^4 - 435\alpha^3 + 186\alpha^2 + 24\alpha - 16) \\
& + \frac{1}{r^2} \left[(-4\alpha^5 + 12\alpha^4 + 4\alpha^3 - 40\alpha^2 + 32\alpha)\zeta^4 + (6\alpha^6 - 60\alpha^5 + 296\alpha^4 - 712\alpha^3 + 792\alpha^2 - 448\alpha + 128)\zeta^3 + \right. \\
& \quad \left. + (6\alpha^6 + 24\alpha^5 - 140\alpha^4 - 20\alpha^3 + 176\alpha^2 - 208\alpha + 128)\zeta^2 \right. \\
& \quad \left. + (-78\alpha^6 + 320\alpha^5 - 508\alpha^4 + 488\alpha^3 - 600\alpha^2 + 368\alpha)\zeta \right. \\
& \quad \left. + 66\alpha^6 - 200\alpha^5 + 484\alpha^4 - 704\alpha^3 + 408\alpha^2 - 32\alpha \right] \\
& + \frac{1}{r^4} \left[(5\alpha^4 - 26\alpha^3 + 44\alpha^2 - 24\alpha)\zeta^4 + (-3\alpha^5 - 20\alpha^3 + 144\alpha^2 - 192\alpha + 64)\zeta^3 \right. \\
& \quad \left. - (3\alpha^5 + 30\alpha^4 - 320\alpha^3 + 616\alpha^2 - 560\alpha + 192)\zeta^2 \right. \\
& \quad \left. + (147\alpha^5 - 524\alpha^4 + 564\alpha^3 - 240\alpha^2 + 384\alpha - 256)\zeta - 189\alpha^5 + 309\alpha^4 - 246\alpha^3 + 428\alpha^2 - 280\alpha \right] \\
& - \frac{4}{r^6} \left[8(2 - \alpha)\bar{\alpha}^2\zeta^3 + (13\alpha^3 - 2\alpha^2 - 52\alpha + 48)\zeta^2 + (30\alpha^4 - 102\alpha^3 + 56\alpha^2 + 48\alpha)\zeta + \right. \\
& \quad \left. - 66\alpha^4 + 93\alpha^3 - 18\alpha^2 + 56\alpha - 32 \right] \\
& \left. + \frac{4[(17\alpha^2 - 46\alpha + 32)\zeta^2 + (9\alpha^3 - 40\alpha^2 + 4\alpha + 48)\zeta - 45\alpha^3 + 59\alpha^2 + 10\alpha + 16]}{r^8} + 16\frac{3\alpha^2 + (1 + 3\bar{\alpha})\bar{\zeta}}{r^{10}} \right\} \\
& + \left(\zeta \rightarrow -\zeta \right)
\end{aligned}
\right.$$

$$\begin{aligned}
\tilde{d}_{\gamma\chi_{c0}}^{(++)}(r, \alpha, \zeta = x/\xi) = & \frac{4\mathfrak{C}_{\chi_c}}{\alpha^4(1 + \bar{\alpha})^2(\bar{\alpha} + 1/r^2)^2(r^2 - 1)^2(\zeta + 1 - i0)(\zeta - 1 + i0)(\zeta - \kappa + i0)^2} \times \quad (C7) \\
& \times \left\{ \begin{aligned}
& \frac{\bar{\alpha}\alpha^2}{8} \left[(\alpha - 2)^2\alpha(5\alpha - 4)\zeta^4 + (3\alpha^5 - 28\alpha^4 + 72\alpha^3 - 72\alpha^2 + 32\alpha)\zeta^3 \right. \\
& \quad \left. + (3\alpha^5 - 34\alpha^4 + 132\alpha^3 - 184\alpha^2 + 112\alpha - 16)\zeta^2 + (-15\alpha^5 + 84\alpha^4 - 188\alpha^3 + 224\alpha^2 - 96\alpha)\zeta \right. \\
& \quad \left. + 9\alpha^5 - 27\alpha^4 + 24\alpha^3 - 4\alpha^2 + 32\alpha - 32 \right] + \\
& + \frac{1}{8r^2} \left[(\alpha - 2)^2\alpha^2(\alpha^3 - 23\alpha^2 + 45\alpha - 22)\zeta^4 + (\alpha^8 - 19\alpha^7 + 127\alpha^6 - 284\alpha^5 + 164\alpha^4 + 120\alpha^3 - 112\alpha^2)\zeta^3 \right. \\
& \quad \left. + (\alpha^8 - 19\alpha^7 + 127\alpha^6 - 284\alpha^5 + 164\alpha^4 + 120\alpha^3 - 112\alpha^2)\zeta^3 \right]
\end{aligned}
\right.$$

$$\begin{aligned}
& + (\alpha^8 + 15\alpha^7 - 47\alpha^6 - 150\alpha^5 + 444\alpha^4 - 356\alpha^3 + 88\alpha^2) \zeta^2 \\
& + (-5\alpha^8 + 55\alpha^7 - 263\alpha^6 + 592\alpha^5 - 816\alpha^4 + 568\alpha^3 - 128\alpha^2) \zeta \\
& + 3\alpha^8 - 52\alpha^7 + 194\alpha^6 - 299\alpha^5 + 86\alpha^4 + 104\alpha^3 - 32\alpha] \\
& + \frac{1}{4r^4} [(\alpha - 2)^2 \alpha (\alpha^3 + 5\alpha^2 - 16\alpha + 8) \zeta^4 + \\
& - (\alpha^7 - 20\alpha^6 + 150\alpha^5 - 430\alpha^4 + 520\alpha^3 - 248\alpha^2 + 32\alpha) \zeta^3 \\
& + (-5\alpha^7 - 8\alpha^6 + 82\alpha^5 + 72\alpha^4 - 424\alpha^3 + 384\alpha^2 - 96\alpha) \zeta^2 + \\
& + (21\alpha^7 - 90\alpha^6 + 228\alpha^5 - 342\alpha^4 + 376\alpha^3 - 184\alpha^2) \zeta \\
& + -15\alpha^7 + 69\alpha^6 - 177\alpha^5 + 328\alpha^4 - 140\alpha^3 - 96\alpha^2 + 32\alpha] \\
& + \frac{1}{8r^6} [3\alpha^2 (2 - \alpha)^3 \zeta^4 + (\alpha^6 - 4\alpha^5 + 92\alpha^4 - 440\alpha^3 + 752\alpha^2 - 512\alpha + 128) \zeta^3 + \\
& + (17\alpha^6 + 10\alpha^5 - 404\alpha^4 + 784\alpha^3 - 400\alpha^2 - 128\alpha + 128) \zeta^2 \\
& + (-113\alpha^6 + 416\alpha^5 - 804\alpha^4 + 1080\alpha^3 - 1168\alpha^2 + 512\alpha) \zeta \\
& + 111\alpha^6 - 291\alpha^5 + 378\alpha^4 - 876\alpha^3 + 504\alpha^2 + 64\alpha] \\
& + \frac{1}{2r^8} [(-5\alpha^4 + 24\alpha^3 - 36\alpha^2 + 16\alpha) \zeta^3 + (-2\alpha^5 + 8\alpha^4 + 32\alpha^3 - 148\alpha^2 + 176\alpha - 64) \zeta^2 + \\
& (30\alpha^5 - 97\alpha^4 + 112\alpha^3 - 68\alpha^2 + 112\alpha - 64) \zeta - 48\alpha^5 + 106\alpha^4 - 76\alpha^3 + 200\alpha^2 - 112\alpha] \\
& + \frac{(-11\alpha^3 + 38\alpha^2 - 32\alpha) \zeta^2 + (-11\alpha^4 + 36\alpha^3 - 12\alpha^2 - 64\alpha + 32) \zeta + 39\alpha^4 - 73\alpha^3 + 10\alpha^2 - 72\alpha + 32}{2r^{10}} \\
& + \frac{-6\alpha^3 + 8\alpha^2 + 8\alpha + (8\alpha - 4\alpha^2) \zeta}{r^{12}} \Big\} + (\zeta \rightarrow -\zeta)
\end{aligned} \tag{C8}$$

$$\begin{aligned}
\tilde{c}_{\gamma\chi_{c0}}^{(+)}(r, \alpha, \zeta = x/\xi) &= -\frac{4\mathfrak{C}_{\chi_c}(1 - \alpha r^2)}{\alpha(1 + \bar{\alpha})^2(\bar{\alpha} + 1/r^2)(r^2 - 1)^2(\zeta + 1 - i0)(\zeta - 1 + i0)(\zeta - \kappa + i0)^2} \times \\
&\times \left\{ \bar{\alpha} [\alpha(2\alpha^2 - 16)\zeta^4 + \alpha(5\alpha^3 - 34\alpha^2 + 52\alpha - 48)\zeta^3 + \alpha(5\alpha^3 - 46\alpha^2 + 104\alpha - 72)\zeta^2 \right. \\
&+ \alpha(-25\alpha^3 + 106\alpha^2 - 88\alpha + 8)\zeta + (15\alpha^4 - 28\alpha^3 + 76\alpha^2 - 112\alpha + 48)] + \\
&+ \frac{1}{r^2} [(-2\alpha^4 + 14\alpha^3 - 40\alpha^2 + 32\alpha)\zeta^4 + (-3\alpha^5 + 30\alpha^4 - 148\alpha^3 + 268\alpha^2 - 248\alpha + 112)\zeta^3 + \\
&+ (-3\alpha^5 - 14\alpha^4 + 76\alpha^3 - 44\alpha^2 - 112\alpha + 112)\zeta^2 + (15\alpha^5 - 86\alpha^4 + 360\alpha^3 - 524\alpha^2 + 248\alpha)\zeta + \\
&+ -9\alpha^5 + 72\alpha^4 - 62\alpha^3 + 20\alpha^2 + \zeta^2 + \zeta - 80\alpha + 64] \\
&+ \frac{1}{r^4} [-4\alpha(1 + \bar{\alpha})^2\zeta^4 + (3\alpha^4 - 6\alpha^3 + 36\alpha^2 - 56\alpha)\zeta^3 + (3\alpha^4 + 42\alpha^3 - 272\alpha^2 + 416\alpha - 224)\zeta^2 \\
&+ (-63\alpha^4 + 98\alpha^3 - 212\alpha^2 + 360\alpha - 224)\zeta + 57\alpha^4 - 178\alpha^3 + 16\alpha^2 + 176\alpha - 96] \\
&+ \frac{4[(-5\alpha^2 + 12\alpha - 4)\zeta^3 + (7\alpha^2 + 2\alpha - 4)\zeta^2 + (21\alpha^3 - 7\alpha^2 - 36\alpha + 28)\zeta - 33\alpha^3 + 69\alpha^2 - 22\alpha - 4]}{r^6} \\
&+ \frac{4(8\bar{\alpha}\zeta^2 + (-9\alpha^2 + 6\alpha + 8)\zeta + (33\alpha^2 - 50\alpha + 12))}{r^8} - \frac{16(\zeta + 3\bar{\alpha})}{r^{10}} \Big\} + (\zeta \rightarrow -\zeta)
\end{aligned} \tag{C9}$$

$$\begin{aligned}
\tilde{d}_{\gamma\chi_{c0}}^{(+)}(r, \alpha, \zeta = x/\xi) &= -\frac{4\mathfrak{C}_{\chi_c}(1/r^2 - \alpha)}{\alpha^3(1 + \bar{\alpha})^2(\bar{\alpha} + 1/r^2)^2(r^2 - 1)^2(\zeta + 1 - i0)(\zeta - 1 + i0)(\zeta - \kappa + i0)^2} \times \\
&\times \left\{ -\frac{\alpha\bar{\alpha}}{8} [(6\alpha^3 - 16\alpha^2 + 8\alpha)\zeta^4 + (3\alpha^4 - 30\alpha^3 + 52\alpha^2 - 32\alpha)\zeta^3 + (3\alpha^4 - 30\alpha^3 + 76\alpha^2 - 40\alpha - 16)\zeta^2 \right. \\
&+ (-15\alpha^4 + 78\alpha^3 - 88\alpha^2 + 24\alpha)\zeta + (9\alpha^4 - 24\alpha^3 + 56\alpha^2 - 88\alpha + 48)] + \\
&+ \frac{1}{8r^2} [16\alpha\bar{\alpha}^2(2 - \alpha)\zeta^4 + (\alpha^6 - 14\alpha^5 + 128\alpha^4 - 304\alpha^3 + 288\alpha^2 - 96\alpha)\zeta^3
\end{aligned} \tag{C10}$$

$$\begin{aligned}
& + (\alpha^6 + 22\alpha^5 - 88\alpha^4 + 192\alpha^2 - 128\alpha) \zeta^2 + (-5\alpha^6 + 30\alpha^5 - 228\alpha^4 + 416\alpha^3 - 192\alpha^2 - 32\alpha) \zeta \\
& + 3\alpha^6 - 38\alpha^5 + 60\alpha^4 + 64\alpha^2 - 160\alpha + 64] \\
& + \frac{1}{8r^4} [2\alpha^2 (2-\alpha)^2 \zeta^4 + (-\alpha^5 + 2\alpha^4 - 84\alpha^3 + 240\alpha^2 - 224\alpha + 64) \zeta^3 + (-9\alpha^5 - 22\alpha^4 + 284\alpha^3 - 432\alpha^2 + 112\alpha + 64) \zeta^2 + \\
& + (37\alpha^5 - 30\alpha^4 + 140\alpha^3 - 464\alpha^2 + 320\alpha) \zeta - 27\alpha^5 + 96\alpha^4 - 124\alpha^3 - 184\alpha^2 + 240\alpha] \\
& + \frac{1}{2r^6} [4\alpha\bar{\alpha}(2-\alpha)\zeta^3 + (2\alpha^4 - 8\alpha^3 - 28\alpha^2 + 72\alpha - 32) \zeta^2 (-19\alpha^4 + 16\alpha^3 + 28\alpha^2 + 16\alpha - 32) \zeta \\
& + (21\alpha^4 - 40\alpha^3 + 76\alpha^2 - 32)] \\
& + \frac{(10\alpha^2 - 16\alpha) \zeta^2 + (11\alpha^3 - 18\alpha^2 - 24\alpha + 16) \zeta - 27\alpha^3 + 32\alpha^2 - 64\alpha + 16}{2r^8} + \frac{2(3\alpha^2 - 2\alpha + 4) + 4\alpha\zeta}{r^{10}} \Big\} + (\zeta \rightarrow -\zeta)
\end{aligned}$$

2. Coefficient functions for χ_{c1}

$$\begin{aligned}
c_{\gamma\chi_{c1}}^{(++, -1)}(r, \alpha, \zeta = x/\xi) &= \frac{4i\mathfrak{C}_{\chi_c}\sqrt{(1-\alpha)(\alpha r^2 - 1)}}{\alpha(1+\bar{\alpha})^2(\bar{\alpha} + 1/r^2)(r^2 - 1)^2(\zeta + 1 - i0)(\zeta - 1 + i0)(\zeta - \kappa + i0)^2} \times \quad (C11) \\
&\times \left\{ -4\alpha^7\bar{\zeta}^2\zeta + \alpha^6(25\zeta^3 - 23\zeta^2 + 3\zeta - 5) - \alpha^5(67\zeta^3 - 9\zeta^2 - 7\zeta - 3) + \alpha^4(15\zeta^4 + 49\zeta^3 + 103\zeta^2 - 17\zeta - 22) \right. \\
&+ \alpha^3(-90\zeta^4 + 16\zeta^3 - 208\zeta^2 + 4\zeta + 54) + 4\alpha^2(33\zeta^4 - 21\zeta^3 + 20\zeta^2 + 12\zeta + 4) \\
&- 8\alpha(7\zeta^4 - 20\zeta^3 - 15\zeta^2 + 6\zeta + 10) - 32(3\zeta^3 + 3\zeta^2 - 1) \\
&- \alpha\bar{\alpha}r^2(4\alpha^5\bar{\zeta}^2\zeta + \alpha^4(-23\zeta^3 + 33\zeta^2 - 13\zeta + 3) + \alpha^3(\zeta^4 + 58\zeta^3 - 68\zeta^2 + 30\zeta - 5) \\
&- 2\alpha^2(7\zeta^4 + 31\zeta^3 - 35\zeta^2 + 23\zeta - 10) + 4\alpha(13\zeta^4 + 12\zeta^3 - 9\zeta^2 + 8\zeta - 8) - 8(5\zeta^4 + 3\zeta^3 - 2\zeta^2 - 2)) \\
&+ \frac{1}{r^2}[2\alpha^6(5\zeta^3 - 17\zeta^2 + 11\zeta + 1) - \alpha^5(\zeta^4 + 54\zeta^3 - 136\zeta^2 + 50\zeta - 17) - \alpha^4(\zeta^4 - 138\zeta^3 + 248\zeta^2 - 74\zeta + 27) \\
&+ 2\alpha^3(15\zeta^4 - 50\zeta^3 + 72\zeta^2 - 44\zeta + 47) - 4\alpha^2(13\zeta^4 + 11\zeta^3 - 41\zeta^2 - 31\zeta + 64) \\
&+ 8\alpha(3\zeta^4 - 48\zeta^2 - 31\zeta + 22) + 48\zeta(\zeta^2 + 5\zeta + 4)] \\
&+ \frac{1}{r^4}[-4\alpha^5(2\zeta^3 - 13\zeta^2 + 12\zeta + 3) + \alpha^4(\zeta^4 + 35\zeta^3 - 167\zeta^2 + 69\zeta - 2) - 2\alpha^3(3\zeta^4 + 40\zeta^3 - 112\zeta^2 + 34\zeta - 5) \\
&+ 4\alpha^2(3\zeta^4 + 21\zeta^3 - 27\zeta^2 + 15\zeta - 8) - 8\alpha(\zeta^4 - 14\zeta^2 - 18\zeta - 25) - 32(\zeta^3 + 4\zeta^2 + 6\zeta + 5)] \\
&+ \frac{2}{r^6}[\alpha^4(\zeta^3 - 17\zeta^2 + 27\zeta + 13) - \alpha^3(5\zeta^3 - 49\zeta^2 + 11\zeta + 25) + 2\alpha^2(5\zeta^3 - 22\zeta^2 - 17\zeta + 6) \\
&- 12\alpha(\zeta^3 + 2\zeta^2 + 2\zeta + 3) + 8(\zeta + 1)^2(\zeta + 3)] \\
&+ \frac{4(2\alpha^3(\zeta^2 - 4\zeta - 3) + \alpha^2(-9\zeta^2 + 5\zeta + 16) + 2\alpha(7\zeta^2 + 8\zeta - 3) - 8\zeta(\zeta + 2))}{r^8} + \frac{8(\alpha^2 - 3\alpha + 2)(\zeta + 1)}{r^{10}} \Big\} \\
&+ (\zeta \rightarrow -\zeta)
\end{aligned}$$

$$\begin{aligned}
d_{\gamma\chi_{c1}}^{(++, -1)}(r, \alpha, \zeta = x/\xi) &= \frac{4i\mathfrak{C}_{\chi_c}\sqrt{(1-\alpha)(\alpha r^2 - 1)}}{\alpha^4(1+\bar{\alpha})^2(\bar{\alpha} + 1/r^2)^2(r^2 - 1)^2(\zeta + 1 - i0)(\zeta - 1 + i0)(\zeta - \kappa + i0)^2} \times \quad (C12) \\
&\times \left\{ \frac{\bar{\alpha}\alpha^2}{8}[4\alpha^5\bar{\zeta}^2\zeta + \alpha^4\bar{\zeta}(27\zeta^2 - 14\zeta + 3) + \alpha^3(\zeta^4 + 82\zeta^3 - 100\zeta^2 + 38\zeta - 5) + \right. \\
&- 2\alpha^2(7\zeta^4 + 59\zeta^3 - 59\zeta^2 + 27\zeta - 10) + 4\alpha(9\zeta^4 + 24\zeta^3 - 13\zeta^2 + 12\zeta - 8) - 8(3\zeta^4 + 5\zeta^3 + 2\zeta - 2)] + \\
&+ \frac{\alpha}{8r^2}[-4\alpha^7\bar{\zeta}^2\zeta - \alpha^6\bar{\zeta}(3\zeta + 1)(3\zeta + 5) + \alpha^5(37\zeta^3 - 151\zeta^2 + 63\zeta + 3) + \alpha^4(7\zeta^4 - 215\zeta^3 + 439\zeta^2 - 105\zeta - 30) \\
&+ \alpha^3(-10\zeta^4 + 404\zeta^3 - 632\zeta^2 + 72\zeta + 6) - 4\alpha^2(9\zeta^4 + 113\zeta^3 - 96\zeta^2 + 4\zeta - 38) \\
&+ 8\alpha(9\zeta^4 + 44\zeta^3 + 5\zeta^2 + 4\zeta - 24) - 32((\zeta + 1)(\zeta + 3)\zeta^2 + \zeta - 2)] \Big\}
\end{aligned}$$

$$\begin{aligned}
& + \frac{1}{8r^4} [-2\alpha^7\bar{\zeta}(5\zeta^2 - 12\zeta - 1) - \alpha^6(\zeta + 1)(\zeta^3 + 21\zeta^2 - 29\zeta - 17) - \alpha^5(\zeta^4 + 46\zeta^3 - 280\zeta^2 + 158\zeta + 27) + \\
& \quad + 2\alpha^4(7\zeta^4 + 118\zeta^3 - 336\zeta^2 + 68\zeta + 111) - 4\alpha^3(5\zeta^4 + 71\zeta^3 - 233\zeta^2 - 31\zeta + 100) + \\
& \quad + 8\alpha^2(\zeta^4 + 22\zeta^3 - 96\zeta^2 - 53\zeta + 8) + 16\alpha(-9\zeta^3 + 11\zeta^2 + 16\zeta + 12) + 64(\zeta^3 + \zeta^2 - 1)] \\
& + \frac{1}{8r^6} [-4\alpha^6(2\zeta^3 - 13\zeta^2 + 12\zeta + 3) + \alpha^5(\zeta^4 + 3\zeta^3 + 25\zeta^2 - 155\zeta - 2) + 2\alpha^4(\zeta^4 + 42\zeta^3 - 228\zeta^2 + 192\zeta - 15) + \\
& \quad - 4\alpha^3(7\zeta^4 + 55\zeta^3 - 153\zeta^2 + 73\zeta + 70) + 8\alpha^2(7\zeta^4 + 26\zeta^3 - 46\zeta^2 + 20\zeta + 93) \\
& \quad - 32\alpha(\zeta^4 + 2\zeta^3 - 9\zeta^2 - 3\zeta + 13) - 128\zeta(\zeta + 1)] \\
& + \frac{1}{4r^8} [\alpha^5(\zeta^3 - 17\zeta^2 + 27\zeta + 13) + \alpha^4(3\zeta^3 - 31\zeta^2 + 125\zeta - 25) + \alpha^3(76 - 2\zeta(11(\zeta - 10)\zeta + 125)) + \\
& \quad + 4\alpha^2(11\zeta^3 - 62\zeta^2 + 16\zeta - 1) - 8\alpha(7\zeta^3 - 5\zeta^2 + \zeta + 21) + 32(\zeta^3 + \zeta^2 + \zeta + 3)] \\
& + \frac{2\alpha^4((\zeta - 4)\zeta - 3) + \alpha^3(\zeta(7\zeta - 43) + 16) - 6\alpha^2(7(\zeta - 2)\zeta + 5) + 8\alpha(8\zeta^2 + 3) - 32\zeta(\zeta + 1)}{2r^{10}} \\
& - \frac{\bar{\alpha}(\alpha((\alpha + 6)\zeta + \alpha - 2) - 8\zeta)}{r^{12}} \Big\} + (\zeta \rightarrow -\zeta)
\end{aligned}$$

$$\begin{aligned}
c_{\gamma\chi_{c1}}^{(+,-,-1)}(r, \alpha, \zeta = x/\xi) &= \frac{4i\mathfrak{C}_{\chi_c}\sqrt{(1-\alpha)(\alpha r^2 - 1)}(\alpha r^2 - 1)}{\alpha(1+\bar{\alpha})^2(r^2 - 1)^2(\zeta + 1 - i0)(\zeta - 1 + i0)(\zeta - \kappa + i0)^2} \times \\
&\times \left\{ \begin{aligned}
&\alpha^3(-(z - 1)^2)(3z + 1) + 4\alpha^2(5z^3 - 7z^2 + 3z - 1) - 4\alpha(11z^3 - 9z^2 + 4z - 2) + 16(2z^3 + z) \\
&- \frac{\alpha^3\bar{z}^2(5z - 1) - 2\alpha^2\bar{z}^2(9z + 5) + 4\alpha z(3z^2 - 11z + 4) + 8(z^3 + 9z^2 + 2z + 2)}{r^2} \\
&+ \frac{2\alpha^2(z^3 - 13z^2 + 15z - 3) + 4\alpha(-2z^3 + 10z^2 + z - 5) + 8(z^3 + 3z^2 + 4z + 2)}{r^4} \\
&+ \frac{4(\alpha(2z^2 - 9z + 3) - 2(2z^2 + z - 1))}{r^6} - \frac{8\bar{z}}{r^8} \end{aligned} \right\} + (\zeta \rightarrow -\zeta)
\end{aligned} \tag{C13}$$

$$\begin{aligned}
d_{\gamma\chi_{c1}}^{(+,-,-1)}(r, \alpha, \zeta = x/\xi) &= \frac{4i\mathfrak{C}_{\chi_c}\sqrt{(1-\alpha)(\alpha r^2 - 1)}(\alpha - 1/r^2)}{\alpha^2(1+\bar{\alpha})(\bar{\alpha} + 1/r^2)(r^2 - 1)^2(\zeta + 1 - i0)(\zeta - 1 + i0)(\zeta - \kappa + i0)} \times \\
&\times \left\{ \begin{aligned}
&\frac{1}{8} \left[(\alpha - 2)\zeta^2 \left(3\alpha - 4 + \frac{\alpha - 2}{r^2} - \frac{2}{r^4} \right) - 2\zeta \left(\alpha - \frac{2}{r^2} \right) \left(\alpha - 3 + \frac{\alpha}{r^2} - \frac{1}{r^4} \right) - \right. \\
&\left. - \left(1 - \frac{1}{r^2} \right) \left(\alpha(\alpha + 4) - 8 - \frac{4\alpha}{r^2} + \frac{4}{r^4} \right) \right] + (\zeta \rightarrow -\zeta)
\end{aligned} \right\}
\end{aligned} \tag{C14}$$

$$\begin{aligned}
c_{\gamma\chi_{c1}}^{(++,0)}(r, \alpha, \zeta = x/\xi) &= -\frac{4i\mathfrak{C}_{\chi_c}}{\alpha^2(1+\bar{\alpha})^2(\bar{\alpha} + 1/r^2)(r^2 - 1)^2(\zeta + 1 - i0)(\zeta - 1 + i0)(\zeta - \kappa + i0)^2} \times \\
&\times \left\{ \begin{aligned}
&(\alpha^6 - 9\alpha^5 + 5\alpha^4 + 70\alpha^3 - 140\alpha^2 + 72\alpha)\zeta^4 + \alpha^7 + 10\alpha^6 + 72\alpha^5 - 195\alpha^4 + 10\alpha^3 + 168\alpha^2 - 64\alpha \\
&+ (35\alpha^7 - 227\alpha^6 + 557\alpha^5 - 650\alpha^4 + 508\alpha^3 - 448\alpha^2 + 224\alpha)\zeta^3 + \zeta^2(-117\alpha^7 + 597\alpha^6 - 1283\alpha^5 \\
&+ 1614\alpha^4 - 1220\alpha^3 + 324\alpha^2 + 88\alpha) + (81\alpha^7 - 301\alpha^6 + 495\alpha^5 - 350\alpha^4 - 120\alpha^3 + 216\alpha^2 - 16\alpha)\zeta \\
&+ \frac{1}{r^2} [(4\alpha^5 - 12\alpha^4 - 8\alpha^3 + 48\alpha^2 - 32\alpha)\zeta^4 + (-44\alpha^6 + 242\alpha^5 - 474\alpha^4 + 314\alpha^3 + 52\alpha^2 - 8\alpha - 80)\zeta^3 \\
&+ (224\alpha^6 - 916\alpha^5 + 1404\alpha^4 - 1286\alpha^3 + 1052\alpha^2 - 408\alpha - 80)\zeta^2 - 8\alpha^6 - 48\alpha^5 - 120\alpha^4 \\
&+ (-220\alpha^6 + 614\alpha^5 - 838\alpha^4 + 686\alpha^3 + 60\alpha^2 - 320\alpha)\zeta + 550\alpha^3 - 332\alpha^2 - 80\alpha + 32] \\
&+ \frac{1}{r^4} [(-5\alpha^4 + 26\alpha^3 - 44\alpha^2 + 24\alpha)\zeta^4 + (31\alpha^5 - 148\alpha^4 + 272\alpha^3 - 216\alpha^2 + 64)\zeta^3 + \\
&+ (-233\alpha^5 + 792\alpha^4 - 760\alpha^3 + 104\alpha^2 - 112\alpha + 224)\zeta^2]
\end{aligned} \right\}
\end{aligned} \tag{C15}$$

$$\begin{aligned}
& + (321\alpha^5 - 620\alpha^4 + 520\alpha^3 - 608\alpha^2 + 256\alpha + 160) \zeta + 25\alpha^5 + 101\alpha^4 - 50\alpha^3 - 484\alpha^2 + 408\alpha] \\
& + \frac{1}{r^6} [(-10\alpha^4 + 42\alpha^3 - 76\alpha^2 + 88\alpha - 48) \zeta^3 + (142\alpha^4 - 470\alpha^3 + 436\alpha^2 + 56\alpha - 176) \zeta^2 \\
& + (-286\alpha^4 + 382\alpha^3 + 76\alpha^2 + 8\alpha - 208) \zeta - 38\alpha^4 - 74\alpha^3 + 212\alpha^2 + 56\alpha - 144] \\
& + \frac{(-40\alpha^3 + 148\alpha^2 - 200\alpha + 96) \zeta^2 + (156\alpha^3 - 224\alpha^2 - 80\alpha + 160) \zeta + 28\alpha^3 - 12\alpha^2 - 88\alpha + 64}{r^8} \\
& + \frac{(-40\alpha^2 + 88\alpha - 48) \zeta - 8\alpha^2 + 24\alpha - 16}{r^{10}} \Big\} + (\zeta \rightarrow -\zeta)
\end{aligned}$$

$$\begin{aligned}
d_{\gamma\chi_{c1}}^{(++,0)}(r, \alpha, \zeta = x/\xi) &= \frac{4i\mathfrak{C}_{\chi_c} r^2}{\alpha^3 (1 + \bar{\alpha})^2 (\bar{\alpha} + 1/r^2)^2 (r^2 - 1)^2 (\zeta + 1 - i0) (\zeta - 1 + i0) (\zeta - \kappa + i0)^2} \times \quad (C16) \\
&\times \left\{ \frac{\bar{\alpha}\alpha^2}{4} [\alpha\bar{\alpha}(2 - \alpha)(\zeta^4 + 1) + (2\alpha^5 - 13\alpha^4 + 31\alpha^3 - 36\alpha^2 + 20\alpha - 4)\zeta^3 \right. \\
&+ (-4\alpha^5 + 18\alpha^4 - 28\alpha^3 + 18\alpha^2 - 4\alpha)\zeta^2 + (2\alpha^5 - 5\alpha^4 + 3\alpha^3 + 4\alpha^2 - 8\alpha + 4)\zeta] + \\
&+ \frac{\alpha}{8r^2} [3(2 - \alpha)\alpha\bar{\alpha}(\alpha^2 - 8\alpha + 8)\zeta^4 + (4\alpha^7 - 47\alpha^6 + 209\alpha^5 - 456\alpha^4 + 562\alpha^3 - 392\alpha^2 + 120\alpha)\zeta^3 \\
&+ (-8\alpha^7 + 95\alpha^6 - 359\alpha^5 + 604\alpha^4 - 468\alpha^3 + 120\alpha^2 + 16\alpha)\zeta^2 \\
&+ (4\alpha^7 - 49\alpha^6 + 127\alpha^5 - 104\alpha^4 - 66\alpha^3 + 200\alpha^2 - 160\alpha + 48)\zeta + \alpha^2\bar{\alpha}^2(\alpha^2 + 6\alpha - 8)] \\
&+ \frac{1}{8r^4} [(-\alpha^6 + 5\alpha^5 + 19\alpha^4 - 106\alpha^3 + 140\alpha^2 - 56\alpha)\zeta^4 + \\
&+ (-11\alpha^7 + 99\alpha^6 - 345\alpha^5 + 574\alpha^4 - 576\alpha^3 + 408\alpha^2 - 144\alpha)\zeta^3 - \alpha^7 - 10\alpha^6 \\
&+ (37\alpha^7 - 309\alpha^6 + 963\alpha^5 - 1438\alpha^4 + 1020\alpha^3 - 196\alpha^2 - 72\alpha)\zeta^2 - 12\alpha^5 + 99\alpha^4 \\
&+ (-25\alpha^7 + 205\alpha^6 - 475\alpha^5 + 450\alpha^4 - 76\alpha^3 - 160\alpha^2 + 112\alpha - 32)\zeta - 102\alpha^3 + 24\alpha^2] \\
&+ \frac{1}{4r^6} [-2\alpha^2\bar{\alpha}(2 - \alpha)\zeta^4 + (6\alpha^6 - 45\alpha^5 + 125\alpha^4 - 133\alpha^3 + 62\alpha^2 - 44\alpha + 24)\zeta^3 + \\
&+ (-32\alpha^6 + 210\alpha^5 - 530\alpha^4 + 683\alpha^3 - 474\alpha^2 + 108\alpha + 24)\zeta^2 + 4\alpha^6 + 14\alpha^5 \\
&+ (30\alpha^6 - 191\alpha^5 + 387\alpha^4 - 375\alpha^3 + 130\alpha^2 + 16\alpha)\zeta - 8\alpha^4 - 77\alpha^3 + 78\alpha^2 - 8\alpha] \\
&+ \frac{1}{4r^8} [-\alpha(2 - \alpha)^3\zeta^4 + (-7\alpha^5 + 44\alpha^4 - 108\alpha^3 + 104\alpha^2 - 32\alpha)\zeta^3 - 25\alpha^5 + \\
&+ (57\alpha^5 - 296\alpha^4 + 536\alpha^3 - 464\alpha^2 + 288\alpha - 96)\zeta^2 - 17\alpha^4 + 54\alpha^3 \\
&+ (-73\alpha^5 + 340\alpha^4 - 500\alpha^3 + 448\alpha^2 - 160\alpha - 32)\zeta + 108\alpha^2 - 120\alpha] \\
&+ \frac{1}{4r^{10}} [(2 - \alpha)^2(2 - \alpha\bar{\alpha})\zeta^3 + (-15\alpha^4 + 67\alpha^3 - 90\alpha^2 + 28\alpha + 8)\zeta^2 \\
&+ (27\alpha^4 - 79\alpha^3 + 22\alpha^2 - 4\alpha + 24)\zeta + 19\alpha^4 - 19\alpha^3 - 10\alpha^2 - 20\alpha + 24] \\
&+ \frac{(2\alpha^3 - 9\alpha^2 + 14\alpha - 8)\zeta^2 + (-7\alpha^3 + 16\alpha^2 + 8\alpha - 16)\zeta - 7\alpha^3 + 15\alpha^2 - 6\alpha}{2r^{12}} \Big\} + (\zeta \rightarrow -\zeta)
\end{aligned}$$

$$\begin{aligned}
c_{\gamma\chi_{c1}}^{(+-,0)}(r, \alpha, \zeta = x/\xi) &= \frac{4i\mathfrak{C}_{\chi_c} (1 - \alpha r^2)}{\alpha (1 + \bar{\alpha})^2 (\bar{\alpha} + 1/r^2) (r^2 - 1)^2 (\zeta + 1 - i0) (\zeta - 1 + i0) (\zeta - \kappa + i0)^2} \times \quad (C17) \\
&\times \left\{ -\bar{\alpha} [-10\alpha(2 - \alpha)^2\zeta^4 + (-12\alpha^5 + 73\alpha^4 - 172\alpha^3 + 236\alpha^2 - 176\alpha + 32)\zeta^3 + \alpha^4 - 8\alpha^3 \right. \\
&+ (24\alpha^5 - 113\alpha^4 + 222\alpha^3 - 196\alpha^2 + 48\alpha)\zeta^2 + (-12\alpha^5 + 39\alpha^4 - 48\alpha^3 - 8\alpha^2 + 16\alpha)\zeta + 16\alpha\bar{\alpha}] + \\
&+ \frac{1}{r^2} [(2\alpha^4 - 12\alpha^3 + 24\alpha^2 - 16\alpha)\zeta^4 + (17\alpha^5 - 98\alpha^4 + 178\alpha^3 - 164\alpha^2 + 144\alpha - 80)\zeta^3 + \\
&+ (-83\alpha^5 + 370\alpha^4 - 708\alpha^3 + 760\alpha^2 - 360\alpha + 16)\zeta^2 + (67\alpha^5 - 190\alpha^4 + 278\alpha^3 - 148\alpha^2 - 16\alpha)\zeta + \\
&- \alpha^5 - 4\alpha^4 + 64\alpha^3 - 56\alpha^2 - 24\alpha + 16] \Big\}
\end{aligned}$$

$$\begin{aligned}
& + \frac{1}{r^4} \left[2\alpha(\alpha-2)^2 \zeta^4 + (-9\alpha^4 + 40\alpha^3 - 44\alpha^2 - 8\alpha + 32) \zeta^3 + (87\alpha^4 - 282\alpha^3 + 340\alpha^2 - 320\alpha + 192) \zeta^2 \right. \\
& \quad \left. + (-131\alpha^4 + 272\alpha^3 - 348\alpha^2 + 168\alpha + 64) \zeta + 5\alpha^4 - 8\alpha^3 - 100\alpha^2 + 120\alpha \right] \\
& + \frac{4}{r^6} \left[(\alpha^3 - 3\alpha^2 + 4\alpha - 4) \zeta^3 + (-11\alpha^3 + 22\alpha^2 + 4\alpha - 20) \zeta^2 + (28\alpha^3 - 29\alpha^2 + 30\alpha - 36) \zeta + \right. \\
& \quad \left. - 2\alpha^3 + 10\alpha^2 + 8\alpha - 20 \right] \\
& + \frac{4((4\alpha^2 - 10\alpha + 8) \zeta^2 + (16 - 13\alpha^2) \zeta + \alpha^2 - 8\alpha + 8)}{r^8} - \frac{4\bar{\alpha}\zeta}{r^{10}} \Bigg\} + \left(\zeta \rightarrow -\zeta \right)
\end{aligned}$$

$$\begin{aligned}
d_{\gamma\chi_{c1}}^{(+,-,0)}(r, \alpha, \zeta = x/\xi) = & - \frac{4i\mathfrak{C}_{\chi_c}}{\alpha^2 (1 + \bar{\alpha})^2 (\bar{\alpha} + 1/r^2)^2 (r^2 - 1)^2 (\zeta + 1 - i0) (\zeta - 1 + i0) (\zeta - \kappa + i0)^2} \times \quad (C18) \\
& \times \left\{ -\frac{\bar{\alpha}\alpha}{8} \left[6\alpha(\alpha-2)^2 \zeta^4 + (4\alpha^5 - 37\alpha^4 + 122\alpha^3 - 194\alpha^2 + 144\alpha - 24) \zeta^3 + \right. \right. \\
& \quad \left. + (-8\alpha^5 + 73\alpha^4 - 194\alpha^3 + 168\alpha^2 - 24\alpha) \zeta^2 + (4\alpha^5 - 35\alpha^4 + 46\alpha^3 - 6\alpha^2) \zeta - \alpha^4 + 4\alpha^3 - 16\alpha\bar{\alpha} \right] + \\
& + \frac{1}{8r^2} \left[2\alpha(2-\alpha)^2 (\alpha^2 + 3\alpha - 3) \zeta^4 + (-13\alpha^6 + 95\alpha^5 - 259\alpha^4 + 392\alpha^3 - 384\alpha^2 + 176\alpha - 16) \zeta^3 \right. \\
& + (43\alpha^6 - 267\alpha^5 + 699\alpha^4 - 866\alpha^3 + 412\alpha^2 - 32\alpha) \zeta^2 + (-31\alpha^6 + 153\alpha^5 - 265\alpha^4 + 120\alpha^3 + 20\alpha^2) \zeta \\
& \quad \left. + \alpha^6 + 5\alpha^5 - 57\alpha^4 + 20\alpha^3 + 64\alpha^2 - 32\alpha \right] \\
& + \frac{1}{4r^4} \left[(9\alpha^5 - 53\alpha^4 + 103\alpha^3 - 94\alpha^2 + 68\alpha - 24) \zeta^3 + (-45\alpha^5 + 198\alpha^4 - 384\alpha^3 + 420\alpha^2 - 176\alpha + 8) \zeta^2 + \right. \\
& \quad \left. + (47\alpha^5 - 151\alpha^4 + 233\alpha^3 - 94\alpha^2 - 20\alpha) \zeta - 3\alpha^5 + 2\alpha^4 + 76\alpha^3 - 64\alpha^2 - 16\alpha + 8 \right] \\
& + \frac{1}{8r^6} \left[2\alpha(2-\alpha)^2 \zeta^4 + (-13\alpha^4 + 60\alpha^3 - 96\alpha^2 + 64\alpha - 16) \zeta^3 + (99\alpha^4 - 322\alpha^3 + 380\alpha^2 - 296\alpha + 96) \zeta^2 + \right. \\
& \quad \left. + (-147\alpha^4 + 300\alpha^3 - 392\alpha^2 + 160\alpha + 16) \zeta + 13\alpha^4 - 48\alpha^3 - 148\alpha^2 + 144\alpha \right] \\
& + \frac{(\alpha-2)(2-\alpha\bar{\alpha}) \zeta^3 + (-15\alpha^3 + 40\alpha^2 - 28\alpha + 4) \zeta^2 + (33\alpha^3 - 37\alpha^2 + 26\alpha - 12) \zeta - 3\alpha^3 + 18\alpha^2 - 12\bar{\alpha}}{2r^8} \\
& + \frac{(4\alpha^2 - 10\alpha + 8) \zeta^2 + (-17\alpha^2 + 12\alpha + 4) \zeta + \alpha^2 - 8\alpha}{2r^{10}} - \frac{2\bar{\alpha}\zeta}{r^{12}} \Bigg\} + \left(\zeta \rightarrow -\zeta \right)
\end{aligned}$$

$$\begin{aligned}
c_{\gamma\chi_{c1}}^{(++,+1)}(r, \alpha, \zeta = x/\xi) = & - \frac{4i\mathfrak{C}_{\chi_c} r^2 \sqrt{(1-\alpha)(\alpha r^2 - 1)}}{\alpha^2 (1 + \bar{\alpha})^2 (\bar{\alpha} + 1/r^2) (r^2 - 1)^2 (\zeta + 1 - i0) (\zeta - 1 + i0) (\zeta - \kappa + i0)^2} \times \quad (C19) \\
& \times \left\{ \alpha\bar{\alpha}^2 \left[(\alpha^3 - 22\alpha^2 + 68\alpha - 40) \zeta^4 - (9\alpha^4 - 62\alpha^3 + 118\alpha^2 - 128\alpha + 56) \zeta^3 - \alpha^3\bar{\alpha} \right. \right. \\
& \quad \left. + (19\alpha^4 - 96\alpha^3 + 142\alpha^2 - 84\alpha + 16) \zeta^2 - \alpha(11\alpha^3 - 34\alpha^2 + 54\alpha - 32) \zeta + (20\alpha^2 - 32\alpha + 16) \right] + \\
& + \frac{\bar{\alpha}}{r^2} \left[-\alpha(\alpha^4 - 15\alpha^3 + 26\alpha^2 + 60\alpha - 88) \zeta^4 - (15\alpha^6 - 93\alpha^5 + 293\alpha^4 - 444\alpha^3 + 524\alpha^2 - 432\alpha + 96) \zeta^3 + \right. \\
& \quad \left. - (29\alpha^6 - 153\alpha^5 + 449\alpha^4 - 688\alpha^3 + 392\alpha^2 + 120\alpha - 96) \zeta^2 \right. \\
& \quad \left. + \alpha(13\alpha^5 - 63\alpha^4 + 107\alpha^3 - 24\alpha^2 - 160\alpha + 80) \zeta + (\alpha^6 + 2\alpha^5 + 64\alpha^4 - 70\alpha^3 - 128\alpha^2 + 144\alpha - 32) \right] \\
& + \frac{1}{r^4} \left[-(8\alpha^4 - 31\alpha^3 + 10\alpha^2 + 52\alpha - 40) \alpha\zeta^4 - 4\bar{\alpha}(11\alpha^5 - 44\alpha^4 + 73\alpha^3 - 19\alpha^2 - 16\alpha - 28) \zeta^3 \right. \\
& \quad \left. - 2(74\alpha^6 - 306\alpha^5 + 589\alpha^4 - 854\alpha^3 + 946\alpha^2 - 488\alpha + 40) \zeta^2 \right. \\
& \quad \left. - 4\bar{\alpha}(25\alpha^5 - 55\alpha^4 + 64\alpha^3 - 7\alpha^2 - 134\alpha + 48) \zeta + 4\alpha^6 + 32\alpha^5 + 219\alpha^4 - 790\alpha^3 + 616\alpha^2 - 16\alpha - 64 \right] \\
& + \frac{1}{r^6} \left[(\alpha-2)^2(9\alpha-10)\alpha\zeta^4 + (-47\alpha^5 + 199\alpha^4 - 336\alpha^3 + 228\alpha^2 + 48\alpha - 96) \zeta^3 + \right. \\
& \quad \left. + (273\alpha^5 - 883\alpha^4 + 848\alpha^3 - 204\alpha^2 + 288\alpha - 320) \zeta^2 \right. \\
& \quad \left. + (-281\alpha^5 + 621\alpha^4 - 684\alpha^3 + 924\alpha^2 - 448\alpha - 128) \zeta - 9\alpha^5 - 154\alpha^4 - 38\alpha^3 + 912\alpha^2 - 872\alpha + 160 \right] \\
& + \frac{2}{r^8} \left[(\alpha-2)(9\alpha-10)(\alpha^2 - \alpha + 2) \zeta^3 - (113\alpha^4 - 351\alpha^3 + 292\alpha^2 + 80\alpha - 136) \zeta^2 + \right.
\end{aligned}$$

$$\begin{aligned}
& \left. \left. + \frac{4 \left[(9\alpha - 10) (2\alpha^2 - 5\alpha + 4) \zeta^2 + \bar{\alpha} (5\alpha + 4) (13\alpha - 16) \zeta - (5\alpha^3 + 16\alpha^2 - 54\alpha + 32) \right]}{r^{10}} - \frac{8\bar{\alpha} [(9\alpha - 10)\zeta + (2 - \alpha)]}{r^{12}} \right\} \right. \\
& + \left(\zeta \rightarrow -\zeta \right)
\end{aligned}$$

$$\begin{aligned}
d_{\gamma\chi_{c1}}^{(+,+1)}(r, \alpha, \zeta = x/\xi) &= \frac{4i\mathfrak{C}_{\chi_c}\sqrt{(1-\alpha)(\alpha r^2-1)}}{\bar{\alpha}\alpha^4(1+\bar{\alpha})^2(\bar{\alpha}+1/r^2)^2(r^2-1)^2(\zeta+1-i0)(\zeta-1+i0)(\zeta-\kappa+i0)^2} \times \quad (C20) \\
&\times \left\{ \begin{aligned}
& \frac{\bar{\alpha}^2\alpha^2}{8} \left[(2-\alpha)(\alpha^2+12\bar{\alpha})\zeta^4 + (9\alpha^4-46\alpha^3+78\alpha^2-80\alpha+40)\zeta^3 - \alpha(19\alpha^3-64\alpha^2+78\alpha-36)\zeta^2 \right. \\
& \quad \left. + (11\alpha^4-18\alpha^3+14\alpha^2+16\bar{\alpha})\zeta + (\alpha^3\bar{\alpha}+4\alpha^2-16\bar{\alpha}) \right] + \\
& + \frac{\bar{\alpha}\alpha}{8r^2} \left[(\alpha-2)\bar{\alpha}(\alpha^3-4\alpha^2-20\alpha+16)\zeta^4 - (3\alpha^6-57\alpha^5+261\alpha^4-472\alpha^3+508\alpha^2-368\alpha+128)\zeta^3 \right. \\
& \quad \left. + (5\alpha^6-129\alpha^5+449\alpha^4-632\alpha^3+360\alpha^2+40\alpha-96)\zeta^2 \right. \\
& \quad \left. - (\alpha^6-75\alpha^5+139\alpha^4-68\alpha^3-128\alpha^2+160\alpha-32)\zeta - (\alpha^6+2\alpha^5+8\alpha^4-86\alpha^3+8\alpha^2+128\alpha-64) \right] \\
& + \frac{1}{8r^4} \left[(\alpha-2)\alpha^2(\alpha^2+4\alpha-4)\zeta^4 + 4(-\alpha^7+18\alpha^6-83\alpha^5+148\alpha^4-143\alpha^3+104\alpha^2-60\alpha+16)\zeta^3 + \right. \\
& \quad \left. + 2(10\alpha^7-166\alpha^6+605\alpha^5-1022\alpha^4+954\alpha^3-456\alpha^2+40\alpha+32)\zeta^2 \right. \\
& \quad \left. - 4\alpha(3\alpha^6-67\alpha^5+165\alpha^4-151\alpha^3-15\alpha^2+130\alpha-64)\zeta \right. \\
& \quad \left. + (-4\alpha^7-8\alpha^6-11\alpha^5+382\alpha^4-584\alpha^3+96\alpha^2+192\alpha-64) \right] \\
& + \frac{1}{8r^6} \left[-(\alpha-2)^2\alpha(\alpha^2-10\alpha+8)\zeta^4 + \alpha(3\alpha^5-51\alpha^4+204\alpha^3-308\alpha^2+224\alpha-64)\zeta^3 + \right. \\
& \quad \left. + (-25\alpha^6+347\alpha^5-1000\alpha^4+1244\alpha^3-896\alpha^2+480\alpha-128)\zeta^2 \right. \\
& \quad \left. + (29\alpha^6-441\alpha^5+920\alpha^4-860\alpha^3+336\alpha^2+160\alpha-128)\zeta \right. \\
& \quad \left. + \alpha(9\alpha^5+34\alpha^4-106\alpha^3-456\alpha^2+936\alpha-416) \right] \\
& + \frac{1}{4r^8} \left[(2-\alpha)(\alpha^2-10\alpha+8)(\alpha^2-\alpha+2)\zeta^3 + (9\alpha^5-119\alpha^4+300\alpha^3-256\alpha^2+24\alpha+32)\zeta^2 + \right. \\
& \quad \left. + (-15\alpha^5+187\alpha^4-250\alpha^3+88\alpha^2-56\alpha+32)\zeta + (-9\alpha^5-9\alpha^4+104\alpha^3+36\alpha^2-216\alpha+96) \right] \\
& + \frac{(-\alpha^2+10\alpha-8)(2\alpha^2-5\alpha+4)\zeta^2 + (5\alpha^4-57\alpha^3+56\alpha^2+32\alpha-32)\zeta + \alpha(5\alpha^3-8\alpha^2-22\alpha+24)}{2r^{10}} \\
& + \frac{\bar{\alpha}[(\alpha^2-10\alpha+8)\zeta-(2-\alpha)\alpha]}{r^{12}} \Big\} + \left(\zeta \rightarrow -\zeta \right)
\end{aligned}$$

$$\begin{aligned}
c_{\gamma\chi_{c1}}^{(+,-,1)}(r, \alpha, \zeta = x/\xi) &= -\frac{4i\mathfrak{C}_{\chi_c}r^2\sqrt{(1-\alpha)(\alpha r^2-1)}}{\alpha(1+\bar{\alpha})^2(\bar{\alpha}+1/r^2)(r^2-1)^2(\zeta+1-i0)(\zeta-1+i0)(\zeta-\kappa+i0)^2} \times \quad (C21) \\
&\times \left\{ \begin{aligned}
& \bar{\alpha}^2 \left[(2-\alpha)^2\alpha\bar{\alpha}^2(4\alpha^2+3\alpha+4)\zeta^3 + (2-\alpha)\alpha^2\bar{\alpha}^2(8\alpha^2+5\alpha+6)\zeta^2 \right. \\
& \quad \left. + \alpha^2\bar{\alpha}^2(4\alpha^3+\alpha^2+8\alpha-8)\zeta + (4-\alpha)\bar{\alpha}^2\alpha^3 \right] + \\
& + \frac{1}{r^2} \left[(2-\alpha)^2\bar{\alpha}\alpha(\alpha+22)\zeta^4 - \bar{\alpha}(4\alpha^6-31\alpha^5+111\alpha^4-229\alpha^3+336\alpha^2-260\alpha+32)\zeta^3 + \right. \\
& \quad \left. + \bar{\alpha}\alpha(8\alpha^5-33\alpha^4+95\alpha^3-223\alpha^2+172\alpha+12)\zeta^2 + \right. \\
& \quad \left. - \bar{\alpha}(4\alpha^6-5\alpha^5+37\alpha^4-35\alpha^3-92\alpha^2+64\alpha-16) - \bar{\alpha}\alpha(3\alpha^4-4\alpha^3-37\alpha^2-12\alpha+24) \right] \\
& + \frac{1}{r^4} \left[(2-\alpha)^2(\alpha^2+6\alpha-8)\alpha\zeta^4 + 2\bar{\alpha}(5\alpha^5-31\alpha^4+76\alpha^3-53\alpha^2+28\alpha-68)\zeta^3 + \right. \\
& \quad \left. + 2(17\alpha^6-107\alpha^5+281\alpha^4-495\alpha^3+561\alpha^2-236\alpha-20)\zeta^2 - 2\alpha^6-11\alpha^5 \right. \\
& \quad \left. + 2\bar{\alpha}(11\alpha^4-41\alpha^3+86\alpha^2-129\alpha-48)\alpha\zeta + 48\alpha^4+106\alpha^3-150\alpha^2-8\alpha+16 \right]
\end{aligned} \right\}
\end{aligned}$$

$$\begin{aligned}
& + \frac{1}{r^6} [(8\alpha^5 - 45\alpha^4 + 101\alpha^3 - 64\alpha^2 - 60\alpha + 64) \zeta^3 + (2 - \alpha) (52\alpha^4 - 165\alpha^3 + 117\alpha^2 - 174\alpha + 168) \zeta^2 + \\
& \quad + \alpha (12\alpha^4 + 4\alpha^3 - 107\alpha^2 - 120\alpha + 212) + (48\alpha^5 - 211\alpha^4 + 351\alpha^3 - 612\alpha^2 + 276\alpha + 144) \zeta + (2 - \alpha)^3 \alpha \zeta^4] \\
& - \frac{2}{r^8} [(2 - \alpha)^2 (\alpha^2 - 2\alpha + 3) \zeta^3 + (2 - \alpha) (17\alpha^3 - 40\alpha^2 - 13\alpha + 38) \zeta^2 + \\
& \quad (27\alpha^4 - 86\alpha^3 + 25\alpha^2 - 100\alpha + 132) \zeta + (13\alpha^4 - 14\alpha^3 - 61\alpha^2 - 8\alpha + 68)] \\
& - \frac{4 [(\alpha - 2)^2 (2\alpha - 3) \zeta^2 + \bar{\alpha} (8\alpha^2 - 13\alpha - 32) \zeta - (6\alpha^3 - 10\alpha^2 - 13\alpha + 16)]}{r^{10}} + \frac{8(\alpha - 3)\bar{\alpha}\zeta - 8\bar{\alpha}^2}{r^{12}} \Big\} + \left(\zeta \rightarrow -\zeta \right)
\end{aligned}$$

$$\begin{aligned}
d_{\gamma\chi_{c1}}^{(+,-,+1)}(r, \alpha, \zeta = x/\xi) &= \frac{4i\mathfrak{C}_{\chi_c}\sqrt{(1-\alpha)(\alpha r^2-1)}}{\alpha^2\bar{\alpha}(1+\bar{\alpha})^2(\bar{\alpha}+1/r^2)(r^2-1)^2(\zeta+1-i0)(\zeta-1+i0)(\zeta-\kappa+i0)} \times \quad (C22) \\
&\times \left\{ \begin{aligned}
& \frac{\bar{\alpha}}{8} [(2 - \alpha) (4\alpha^2 - 9\alpha + 8) \alpha \zeta^2 - 2\bar{\alpha}(2\alpha - 3)\alpha^2 \zeta - (4 - \alpha)\alpha^2] \\
& + \frac{1}{8r^2} [(\alpha - 2)^2 \alpha \zeta^3 + (2 - \alpha) (4\alpha^4 - 3\alpha^3 - 9\alpha^2 + 15\alpha - 4) \zeta^2 + \alpha (4\alpha^4 + 2\alpha^3 - 37\alpha^2 + 52\alpha - 18) \zeta \\
& \quad (3\alpha^4 - 7\alpha^3 + \alpha^2 - 4\alpha + 8)] \\
& + \frac{1}{8r^4} [-(\alpha - 2)^2 \alpha \zeta^3 + (\alpha - 2) (6\alpha^3 - 8\alpha^2 - 3\alpha + 10) \zeta^2 + (-12\alpha^4 + 17\alpha^3 + 20\alpha^2 - 32\alpha - 4) \zeta \\
& \quad + (-2\alpha^4 - 4\alpha^3 + 11\alpha^2 + 4\alpha - 8)] \\
& + \frac{(2 - \alpha) (\alpha^2 - 3\alpha + 3) \zeta^2 + (6\alpha^3 - 11\alpha^2 - 7\alpha + 16) \zeta + (3\alpha^3 - 2\alpha^2 - 4\alpha + 2)}{4r^6} \\
& - \frac{(3 - \alpha)\bar{\alpha}\zeta + \bar{\alpha}^2}{2r^8} \Big\} + \left(\zeta \rightarrow -\zeta \right)
\end{aligned} \right.
\end{aligned}$$

3. Coefficient functions for χ_{c2}

$$\begin{aligned}
c_{\gamma\chi_{c2}}^{(++,-2)}(r, \alpha, \zeta = x/\xi) &= \frac{4\mathfrak{C}_{\chi_c}(1-\alpha)(\alpha r^2-1)r^2}{\alpha^3(1+\bar{\alpha})^2(\bar{\alpha}+1/r^2)(r^2-1)^2(\zeta+1-i0)(\zeta-1+i0)(\zeta-\kappa+i0)^2} \times \quad (C23) \\
&\times \left\{ \begin{aligned}
& \bar{\alpha}\alpha^2 [-(2\alpha^4 - 11\alpha^3 + 20\alpha^2 - 16\alpha + 4) \zeta^3 - (2\alpha^4 - 3\alpha^3 + 4\alpha - 4) \zeta + (2 - \alpha)\alpha (\zeta^4 + 2\bar{\alpha}(2\alpha - 1)\zeta^2 + 1)] \\
& + \frac{1}{r^2} [(\alpha - 4)(2 - \alpha)\bar{\alpha}\alpha(3\alpha - 2)\zeta^4 + \alpha (6\alpha^6 - 41\alpha^5 + 113\alpha^4 - 171\alpha^3 + 176\alpha^2 - 116\alpha + 32) \zeta^3 \\
& \quad - 2\alpha (6\alpha^6 - 33\alpha^5 + 76\alpha^4 - 92\alpha^3 + 54\alpha^2 - 6\alpha - 4) \zeta^2 + \alpha^2 (6\alpha^5 - 25\alpha^4 + 41\alpha^3 - 23\alpha^2 - 8\alpha + 8) \zeta \\
& \quad - \bar{\alpha}\alpha (3\alpha^3 + 8\alpha^2 - 16\alpha + 8)] \\
& + \frac{1}{r^4} [4(\alpha - 2)\bar{\alpha}^2\alpha\zeta^4 - 2 (5\alpha^6 - 28\alpha^5 + 52\alpha^4 - 38\alpha^3 + 36\alpha^2 - 52\alpha + 24) \zeta^3 \\
& \quad + 4 (11\alpha^6 - 47\alpha^5 + 81\alpha^4 - 87\alpha^3 + 54\alpha^2 + 2\alpha - 12) \zeta^2 \\
& \quad - 2\alpha (17\alpha^5 - 46\alpha^4 + 56\alpha^3 - 18\alpha^2 - 48\alpha + 36) \zeta + 4\bar{\alpha} (9\alpha^3 - 7\alpha^2 - 8\alpha + 4)] \\
& + \frac{1}{r^6} [(8\alpha^5 - 37\alpha^4 + 56\alpha^3 - 4\alpha^2 - 56\alpha + 32) \zeta^3 - 2 (28\alpha^5 - 93\alpha^4 + 92\alpha^3 - 74\alpha^2 + 116\alpha - 64) \zeta^2 \\
& \quad + (72\alpha^5 - 145\alpha^4 + 144\alpha^3 - 108\alpha^2 - 72\alpha + 96) \zeta - 2\bar{\alpha}\alpha (5\alpha^2 + 34\alpha - 56) + 2(\alpha - 2)^2\bar{\alpha}\alpha\zeta^4] \\
& + \frac{1}{r^8} [-4(2 - \alpha)\bar{\alpha} (\alpha^2 - \alpha + 2) \zeta^3 + 4 (10\alpha^4 - 29\alpha^3 + 12\alpha^2 + 28\alpha - 20) \zeta^2 \\
& \quad - 4 (19\alpha^4 - 25\alpha^3 + 7\alpha^2 - 32\alpha + 28) \zeta + 16\bar{\alpha} (2\alpha^2 + \alpha - 5)] \\
& \frac{8\bar{\alpha} (2\alpha^2 - 5\alpha + 4) \zeta^2 + 4(3\alpha - 4) (4\alpha^2 + \alpha - 4) \zeta - 8\bar{\alpha}(3\alpha - 4)}{r^{10}} - \frac{16\bar{\alpha}^2\zeta}{r^{12}} \Big\} + \left(\zeta \rightarrow -\zeta \right)
\end{aligned} \right.
\end{aligned}$$

$$\begin{aligned}
d_{\gamma\chi_{c2}}^{(++,-2)}(r, \alpha, \zeta = x/\xi) &= \frac{4\mathfrak{C}_{\chi_c}\bar{\alpha}^2(\alpha r^2 - 1)}{\alpha^4(1 + \bar{\alpha})^2 r^2 (\bar{\alpha} + 1/r^2)^2 (r^2 - 1)^2 (\zeta + 1 - i0)(\zeta - 1 + i0)(\zeta - \kappa + i0)^2} \times \quad (C24) \\
&\times \left\{ \frac{\bar{\alpha}\alpha}{4} [-(\alpha - 2)^2 \zeta^4 - 2(2 - \alpha)(\alpha^3 - 3\alpha^2 + 3\alpha - 3)\zeta^3 - 2(2\alpha^4 - 6\alpha^3 + 7\alpha^2 - 3\alpha - 4)\zeta^2 \right. \\
&\quad + (\alpha^2 + 6\alpha - 4) + 2(\alpha^4 - \alpha^3 + \alpha^2 + \alpha + 2)\zeta] + \\
&\quad + \frac{1}{2r^2} [(\alpha - 2)(2\alpha^4 - 5\alpha^3 + \alpha^2 - \alpha + 2)\zeta^3 + \alpha(6\alpha^4 - 9\alpha^3 + 7\alpha^2 + 9\alpha - 12)\zeta + \\
&\quad + 2(-4\alpha^5 + 13\alpha^4 - 17\alpha^3 + 17\alpha^2 - 6\alpha - 2)\zeta^2 - 4\bar{\alpha}(\alpha + 1)(2\alpha - 1)] \\
&\quad + \frac{1}{4r^4} [(\alpha - 2)^2 \alpha \zeta^4 + 2(2 - \alpha)\alpha(2\alpha^2 - 4\alpha + 1)\zeta^3 + 2(\alpha - 2)(12\alpha^3 - 4\alpha^2 + 3\alpha - 4)\zeta^2 + \\
&\quad + 2(-14\alpha^4 + 14\alpha^3 - 15\alpha^2 + 2\alpha + 8)\zeta - \alpha(5\alpha^2 + 34\alpha - 40)] \\
&\quad + \frac{(\alpha - 2)(\alpha^2 - \alpha + 2)\zeta^3 + 4(2\alpha^2 + 2\alpha - 3) + 2(-5\alpha^3 + 11\alpha^2 - 2\alpha - 2)\zeta^2 + (17\alpha^3 - 7\alpha^2 - 4)\zeta}{2r^6} \\
&\quad \left. \frac{(2\alpha^2 - 5\alpha + 4)\zeta^2 + 2\bar{\alpha}(3\alpha + 2)\zeta - 3\alpha}{r^8} - \frac{2\bar{\alpha}\zeta}{r^{10}} \right\} + \left(\zeta \rightarrow -\zeta \right)
\end{aligned}$$

$$\begin{aligned}
c_{\gamma\chi_{c2}}^{(+-,-2)}(r, \alpha, \zeta = x/\xi) &= -\frac{4\mathfrak{C}_{\chi_c}(1 - \alpha)(\alpha r^2 - 1)^2}{\alpha^2(1 + \bar{\alpha})^2 r^2 (\bar{\alpha} + 1/r^2)(r^2 - 1)(\zeta + 1 - i0)(\zeta - 1 + i0)(\zeta - \kappa + i0)} \times \quad (C25) \\
&\times \left\{ \bar{\alpha}\alpha(2\alpha - 1)[\alpha\zeta + (2 - \alpha)\zeta^2] + \frac{(\alpha - 2)\alpha\zeta^3 - 2(2 - \alpha)\bar{\alpha}\alpha\zeta^2 - 2\bar{\alpha}\alpha(3\alpha - 1)\zeta - (\alpha - 2)^2}{r^2} \right. \\
&\quad \left. \frac{2(\alpha^2 - 2\alpha + 2)\zeta^2 - 2(3\alpha^2 - 2\alpha - 2)\zeta - 2\alpha}{r^4} - \frac{4\bar{\alpha}\zeta}{r^6} \right\} + \left(\zeta \rightarrow -\zeta \right)
\end{aligned}$$

$$d_{\gamma\chi_{c2}}^{(+-,-2)}(r, \alpha, \zeta = x/\xi) = 0 \quad (C26)$$

$$\begin{aligned}
c_{\gamma\chi_{c2}}^{(++,-1)}(r, \alpha, \zeta = x/\xi) &= \frac{4\mathfrak{C}_{\chi_c}r^2\sqrt{(1 - \alpha)(\alpha r^2 - 1)}}{\alpha^3(1 + \bar{\alpha})^2(\bar{\alpha} + 1/r^2)(r^2 - 1)^2(\zeta + 1 - i0)(\zeta - 1 + i0)(\zeta - \kappa + i0)^2} \times \quad (C27) \\
&\times \left\{ \bar{\alpha}\alpha^2[-2(2\alpha^2 - 7\alpha + 4)\zeta^4 - (3\alpha^4 - 20\alpha^3 + 38\alpha^2 - 36\alpha + 12)\zeta^3 + 2(3\alpha^4 - 14\alpha^3 + 18\alpha^2 - 8\alpha + 2)\zeta^2 \right. \\
&\quad - (3\alpha^4 - 8\alpha^3 + 10\alpha^2 - 4\alpha - 4)\zeta + 2(2\alpha^2 - 3\alpha + 2)] + \\
&\quad + \frac{\alpha}{r^2}[2(4 - \alpha)\bar{\alpha}(\alpha^2 - 6\alpha + 4)\zeta^4 + (11\alpha^6 - 71\alpha^5 + 203\alpha^4 - 322\alpha^3 + 362\alpha^2 - 272\alpha + 88)\zeta^3 \\
&\quad - 2(11\alpha^6 - 55\alpha^5 + 133\alpha^4 - 180\alpha^3 + 108\alpha^2 + 4\alpha - 20)\zeta^2 \\
&\quad + \alpha(11\alpha^5 - 39\alpha^4 + 63\alpha^3 - 26\alpha^2 - 42\alpha + 32)\zeta - 2\bar{\alpha}(9\alpha^3 + 4\alpha^2 - 24\alpha + 12)] \\
&\quad + \frac{2}{r^4}[\bar{\alpha}\alpha^2(\alpha^2 - 8)\zeta^4 - (11\alpha^6 - 55\alpha^5 + 103\alpha^4 - 80\alpha^3 + 68\alpha^2 - 96\alpha + 48)\zeta^3 \\
&\quad + 2(22\alpha^6 - 85\alpha^5 + 145\alpha^4 - 176\alpha^3 + 132\alpha^2 - 12\alpha - 24)\zeta^2 \\
&\quad - \alpha(33\alpha^5 - 79\alpha^4 + 95\alpha^3 - 20\alpha^2 - 128\alpha + 96)\zeta + \bar{\alpha}(3\alpha^4 + 51\alpha^3 - 52\alpha^2 - 32\alpha + 16)] \\
&\quad + \frac{1}{r^6}[4(\alpha - 2)^2\alpha\bar{\alpha}\zeta^4 + (19\alpha^5 - 78\alpha^4 + 110\alpha^3 - 12\alpha^2 - 104\alpha + 64)\zeta^3 - 4\alpha\bar{\alpha}(10\alpha^2 + 37\alpha - 66) + \\
&\quad - 2(63\alpha^5 - 190\alpha^4 + 170\alpha^3 - 122\alpha^2 + 212\alpha - 128)\zeta^2 + (151\alpha^5 + 270\alpha^3\bar{\alpha} - 268\alpha^2 - 88\alpha + 192)\zeta] \\
&\quad + \frac{4}{r^8}[2(\alpha - 2)\bar{\alpha}(\alpha^2 - \alpha + 2)\zeta^3 + (23\alpha^4 - 64\alpha^3 + 30\alpha^2 + 52\alpha - 40)\zeta^2 + \\
&\quad - (43\alpha^4 - 52\alpha^3 + 6\alpha^2 - 56\alpha + 56)\zeta + 4\bar{\alpha}(5\alpha^2 + \alpha - 10)] \\
&\quad \left. + \frac{16\bar{\alpha}(2\alpha^2 - 5\alpha + 4)\zeta^2 + 4(27\alpha^3 - 30\alpha^2 - 30\alpha + 32)\zeta - 16\bar{\alpha}(3\alpha - 4)}{r^{10}} - \frac{32\bar{\alpha}^2\zeta}{r^{12}} \right\} + \left(\zeta \rightarrow -\zeta \right)
\end{aligned}$$

$$\begin{aligned}
d_{\gamma\chi_{c2}}^{(++, -1)}(r, \alpha, \zeta = x/\xi) &= \frac{4\mathfrak{C}_{\chi_c}\bar{\alpha}\sqrt{(1-\alpha)(\alpha r^2-1)}}{\alpha^4(1+\bar{\alpha})^2(\bar{\alpha}+1/r^2)^2(r^2-1)^2(\zeta+1-i0)(\zeta-1+i0)(\zeta-\kappa+i0)^2} \times \quad (C28) \\
&\times \left\{ \begin{array}{l} \frac{\bar{\alpha}^2\alpha^2}{4} [2\alpha(2\alpha-3)\zeta^2 - (2-\alpha)\zeta^4 - 2(\alpha^2-2\alpha+2)\zeta^3 - 2(\alpha^2-2\alpha+2)\zeta - (3\alpha-2)] \\ + \frac{\bar{\alpha}\alpha}{8r^2} [(3\alpha^4-9\alpha^3+22\alpha^2-24\alpha+32)\zeta^3 - 2(3\alpha^4-3\alpha^3+14\alpha^2-18\alpha-12)\zeta^2 \\ + (3\alpha^4+3\alpha^3+6\alpha^2+12\alpha+8)\zeta - 2(\alpha^2-4)\zeta^4 - 2(\alpha+2)(7\alpha-4)] \\ + \frac{1}{4r^4} [(5\alpha^5-17\alpha^4+24\alpha^3-10\alpha^2+8\alpha-8)\zeta^3 - 4(-4\alpha^5+8\alpha^4-9\alpha^3+16\alpha^2-8\alpha-2)\zeta^2 \\ + \alpha(11\alpha^4-5\alpha^3+6\alpha^2+22\alpha-32)\zeta - \bar{\alpha}(3\alpha^3+34\alpha^2+8\alpha-8) - (2-\alpha)\bar{\alpha}\alpha^2\zeta^4] \\ + \frac{1}{8r^6} [2(\alpha-2)^2\alpha\zeta^4 - \alpha(11\alpha^3-34\alpha^2+40\alpha-16)\zeta^3 + 2(31\alpha^4-58\alpha^3+18\alpha^2-16\alpha+16)\zeta^2 + \\ + (-63\alpha^4+30\alpha^3-40\alpha^2+16\alpha+32)\zeta - 2\alpha(15\alpha^2+42\alpha-52)] \\ + \frac{(\alpha-2)(2-\alpha)\bar{\alpha}}{2r^8} [\zeta^3 + (-13\alpha^3+26\alpha^2-8\alpha-4)\zeta^2 + (22\alpha^3-7\alpha^2-4\alpha-4)\zeta + 4(3\alpha^2+2\alpha-3) \\ + \frac{2(2\alpha^2-5\alpha+4)\zeta^2 + (-15\alpha^2+6\alpha+8)\zeta - 6\alpha}{2r^{10}} - \frac{2\bar{\alpha}\zeta}{r^{12}}] \end{array} \right\} + (\zeta \rightarrow -\zeta)
\end{aligned}$$

$$\begin{aligned}
c_{\gamma\chi_{c2}}^{(+-, -1)}(r, \alpha, \zeta = x/\xi) &= -\frac{4\mathfrak{C}_{\chi_c}\sqrt{(1-\alpha)^3(\alpha r^2-1)^3}}{\bar{\alpha}\alpha^2(1+\bar{\alpha})^2(\bar{\alpha}+1/r^2)(r^2-1)^2(\zeta+1-i0)(\zeta-1+i0)(\zeta-\kappa+i0)} \times \quad (C29) \\
&\times \left\{ \begin{array}{l} 3\bar{\alpha}\alpha^2(\alpha\zeta + (2-\alpha)\zeta^2) + \frac{(2-\alpha)\alpha^2(5\alpha-4)\zeta^2 + \alpha^2(5\alpha^2+2\alpha-6)\zeta + 2(\alpha-2)\alpha\zeta^3 - 2(\alpha-2)^2}{r^2} \\ + \frac{2(2-\alpha)\alpha\zeta^3 + (5\alpha^3-10\alpha^2+8)\zeta^2 + (-15\alpha^3+8\alpha^2+8)\zeta + 2(\alpha^2-6\alpha+4)}{r^4} \\ + \frac{4\alpha-4(\alpha^2-2\alpha+2)\zeta^2 + 2(7\alpha^2-8)\zeta}{r^6} + \frac{8\bar{\alpha}\zeta}{r^8} \end{array} \right\} + (\zeta \rightarrow -\zeta)
\end{aligned}$$

$$d_{\gamma\chi_{c2}}^{(+-, -1)}(r, \alpha, \zeta = x/\xi) = \frac{\mathfrak{C}_{\chi_c}\zeta\sqrt{(1-\alpha)(\alpha r^2-1)^{3/2}}}{2\alpha^2r^2(r^2-1)^2(\zeta+1-i0)(\zeta-1+i0)} + (\zeta \rightarrow -\zeta) = 0 \quad (C30)$$

$$\begin{aligned}
c_{\gamma\chi_{c2}}^{(++, 0)}(r, \alpha, \zeta = x/\xi) &= \frac{8\bar{\alpha}r^2\mathfrak{C}_{\chi_c}}{\sqrt{6}\alpha^3(1+\bar{\alpha})^2(\bar{\alpha}+1/r^2)(r^2-1)^2(\zeta+1-i0)(\zeta-1+i0)(\zeta-\kappa+i0)^2} \times \quad (C31) \\
&\times \left\{ \begin{array}{l} 2\alpha\bar{\alpha}^2[(\alpha^3-5\alpha^2+12\alpha-16)\zeta^4 + (2\alpha^5-11\alpha^4+24\alpha^3-37\alpha^2+36\alpha-24)\zeta^3 \\ - \alpha(4\alpha^4-14\alpha^3+22\alpha^2-31\alpha+18)\zeta^2 + \alpha(2\alpha^4-3\alpha^3+4\alpha^2-3\alpha+4)\zeta + (\alpha^3+2\alpha^2-10\alpha+8)] + \\ + \frac{\alpha}{r^2}[(\alpha^4-4\alpha^3+16\alpha^2-64\alpha+48)\zeta^4 + 2(5\alpha^6-36\alpha^5+95\alpha^4-153\alpha^3+177\alpha^2-180\alpha+96)\zeta^3 \\ - 2(18\alpha^6-88\alpha^5+169\alpha^4-228\alpha^3+199\alpha^2-26\alpha-60)\zeta^2 \\ + 2\alpha(13\alpha^5-36\alpha^4+43\alpha^3-21\alpha^2-45\alpha+64)\zeta + (21\alpha^4-72\alpha^3-2\alpha^2+124\alpha-56)] \\ + \frac{1}{r^4}[(\alpha^4-9\alpha^3+18\alpha^2+12\alpha-24)\alpha\zeta^4 - 2(5\alpha^6-41\alpha^5+96\alpha^4-98\alpha^3+40\alpha^2-64\alpha+72)\zeta^3 \\ + 2(30\alpha^6-166\alpha^5+281\alpha^4-315\alpha^3+368\alpha^2-176\alpha-72)\zeta^2 \\ - 2(33\alpha^5-107\alpha^4+108\alpha^3-84\alpha^2-84\alpha+204)\alpha\zeta - 5\alpha^5-33\alpha^4+296\alpha^3-276\alpha^2-104\alpha+48] \\ + \frac{1}{r^6}[(6-\alpha)(\alpha-2)^2\alpha\zeta^4 + 2(\alpha^2-2\alpha+2)(3\alpha^3-21\alpha^2+10\alpha+24)\zeta^3 + \alpha(21\alpha^3-54\alpha^2-336\alpha+496) + \\ - 4(13\alpha^5-85\alpha^4+111\alpha^3-27\alpha^2+54\alpha-96)\zeta^2 + 2(43\alpha^5-169\alpha^4+106\alpha^3-150\alpha^2+124\alpha+144)\zeta] \end{array} \right\}
\end{aligned}$$

$$\begin{aligned}
& + \frac{2}{r^8} \left[(\alpha - 6)(2 - \alpha) (2 - \alpha\bar{\alpha}) \zeta^3 + 2 (7\alpha^4 - 54\alpha^3 + 71\alpha^2 + 18\alpha - 60) \zeta^2 + \right. \\
& \quad \left. - (33\alpha^4 - 161\alpha^3 + 10\alpha^2 + 12\alpha + 168) \zeta - 2 (7\alpha^3 - 39\alpha^2 - 6\alpha + 60) \right] \\
& - \frac{4(\alpha - 6) (2\alpha^2 - 5\alpha + 4) \zeta^2 - 32 (\alpha^3 - 6\alpha^2 + 6) \zeta - 4(\alpha - 6)(3\alpha - 4)}{r^{10}} + \frac{8(\alpha - 6)\bar{\alpha}\zeta}{r^{12}} \Big\} + \left(\zeta \rightarrow -\zeta \right)
\end{aligned}$$

$$\begin{aligned}
d_{\gamma\chi_{c2}}^{(++,0)}(r, \alpha, \zeta = x/\xi) = & - \frac{4\bar{\alpha}\mathfrak{C}_{\chi_c}}{\sqrt{6}\alpha^4 (1 + \bar{\alpha})^2 (\bar{\alpha} + 1/r^2)^2 (r^2 - 1)^2 (\zeta + 1 - i0) (\zeta - 1 + i0) (\zeta - \kappa + i0)^2} \times \quad (C32) \\
& \times \left\{ \frac{(2 - \alpha)\alpha^2}{4} \left[-2 (\alpha^5 - 6\alpha^4 + 13\alpha^3 - 15\alpha^2 + 10\alpha - 4) \zeta^3 - 2\alpha(2 - \alpha) (2\alpha^3 - 4\alpha^2 + 3\alpha - 2) \zeta^2 \right. \right. \\
& \quad + (2 - \alpha) (\alpha^2 + 2\alpha - 2) - 2\alpha (\alpha^4 - 2\alpha^3 + \alpha^2 + \alpha - 2) \zeta + (2 - \alpha) (\alpha^2 + 2\bar{\alpha}) \zeta^4 \Big] + \\
& + \frac{\alpha}{2r^2} \left[(2 - \alpha) (2\alpha^5 - 13\alpha^4 + 24\alpha^3 - 25\alpha^2 + 18\alpha - 10) \zeta^3 - (\alpha - 2)^2 (1 - \alpha\bar{\alpha}) \zeta^4 - \alpha (\alpha^2 + 6\bar{\alpha}) (3\alpha^2 - 2\bar{\alpha}) \right. \\
& \quad + (8\alpha^6 - 50\alpha^5 + 108\alpha^4 - 109\alpha^3 + 59\alpha^2 - 4\alpha - 16) \zeta^2 - \alpha (6\alpha^5 - 25\alpha^4 + 30\alpha^3 - 11\alpha^2 - 14\alpha + 18) \zeta \Big] \\
& + \frac{1}{2r^4} \left[(\alpha - 2) (\alpha^5 - 11\alpha^4 + 16\alpha^3 - 12\alpha^2 + 6\alpha - 4) \zeta^3 + 2\bar{\alpha} (5\alpha^5 - 32\alpha^4 + 44\alpha^3 - 24\alpha^2 + 20\alpha + 4) \zeta^2 \right. \\
& \quad + \alpha (13\alpha^5 - 61\alpha^4 + 62\alpha^3 - 20\alpha^2 - 30\alpha + 40) \zeta + (3\alpha^4 - 52\alpha^3 + 44\alpha^2 + 16\alpha - 8) + (\alpha - 2)^2 \alpha^2 \zeta^4 \Big] \\
& + \frac{1}{2r^6} \left[-(\alpha - 2)^2 \alpha \zeta^4 + 2(\alpha - 2)\alpha (3\alpha^2 - 4\alpha + 3) \zeta^3 + (4\alpha^5 - 56\alpha^4 + 111\alpha^3 - 64\alpha^2 + 28\alpha - 16) \zeta^2 + \right. \\
& \quad \left. + 2 (-6\alpha^5 + 39\alpha^4 - 29\alpha^3 + 11\alpha^2 - 2\alpha - 8) \zeta + 8\alpha (\alpha^2 - 8\bar{\alpha}) \right] \\
& + \frac{(2 - \alpha) (2 - \alpha\bar{\alpha}) \zeta^3 - 2\bar{\alpha} (7\alpha^2 - 8\alpha - 2) \zeta^2 - 2 (5\alpha^2 - 6\bar{\alpha}) + (2\alpha^4 - 31\alpha^3 + 13\alpha^2 + 4\alpha + 4) \zeta}{r^8} \\
& \left. + \frac{2 (8\alpha^2 - 3\alpha - 4) \zeta - 2 (2\alpha^2 - 5\alpha + 4) \zeta^2 + 6\alpha}{r^{10}} + \frac{4\bar{\alpha}\zeta}{r^{12}} \right\} + \left(\zeta \rightarrow -\zeta \right)
\end{aligned}$$

$$\begin{aligned}
c_{\gamma\chi_{c2}}^{(+-,0)}(r, \alpha, \zeta = x/\xi) = & - \frac{8\mathfrak{C}_{\chi_c} (\alpha r^2 - 1)}{\sqrt{6}\alpha^2 (1 + \bar{\alpha})^2 (\bar{\alpha} + 1/r^2)^2 (r^2 - 1)^2 (\zeta + 1 - i0) (\zeta - 1 + i0) (\zeta - \kappa + i0)^2} \times \quad (C33) \\
& \times \left\{ 2\bar{\alpha}\alpha \left[\bar{\alpha} (2\alpha^4 - \alpha^3 + \alpha + 2) \zeta - (\alpha - 2)^2 \alpha \zeta^4 - \alpha (\alpha^2 + 3\alpha - 3) + \bar{\alpha} (2\alpha^4 - 9\alpha^3 + 12\alpha^2 - 9\alpha + 6) \zeta^3 \right. \right. \\
& \quad + \alpha (4\alpha^4 - 14\alpha^3 + 16\alpha^2 - 9\alpha + 5) \zeta^2 \Big] + \\
& + \frac{1}{r^2} \left[2\alpha\bar{\alpha} (3\alpha^4 - 17\alpha^3 + 30\alpha^2 - 24\alpha + 10) \zeta^3 + 2\alpha (14\alpha^5 - 64\alpha^4 + 107\alpha^3 - 84\alpha^2 + 37\alpha - 8) \zeta^2 \right. \\
& \quad + 2\bar{\alpha} (11\alpha^5 - 17\alpha^4 + 6\alpha^3 + 2\alpha^2 + 6\alpha - 12) \zeta - \alpha (19\alpha^3 - 11\alpha^2 - 26\alpha + 20) + (\alpha - 3)(\alpha - 2)^2 \alpha \zeta^4 \Big] \\
& + \frac{1}{r^4} \left[(3 - \alpha)(\alpha - 2)^2 \alpha \zeta^4 + 4(\alpha - 3) (\alpha^2 - 2\alpha + 2) (\alpha^2 - \alpha - 1) \zeta^3 - 4 (8\alpha^5 - 36\alpha^4 + 54\alpha^3 - 31\alpha^2 + 12\alpha - 6) \zeta^2 \right. \\
& \quad + 4 (11\alpha^5 - 29\alpha^4 + 23\alpha^3 - \alpha^2 - 12\alpha + 6) \zeta + 5\alpha^4 + 37\alpha^3 + -52\alpha^2 - 12\alpha + 24 \Big] \\
& - \frac{2}{r^6} \left[(\alpha - 3)(\alpha - 2) (\alpha^2 - \alpha + 2) \zeta^3 - 2(\alpha - 2) (5\alpha^3 - 12\alpha^2 + 9) \zeta^2 + (21\alpha^4 - 54\alpha^3 + 29\alpha^2 - 12\alpha + 12) \zeta + \right. \\
& \quad \left. + 2 (4\alpha^3 + 3\alpha^2 - 15\alpha + 6) \right] \\
& - \frac{4(\alpha - 3) (2\alpha^2 - 5\alpha + 4) \zeta^2 + 8\bar{\alpha} (3\alpha^2 - 5\alpha - 6) \zeta - 4\alpha(3\alpha - 5)}{r^8} + \frac{8(\alpha - 3)\bar{\alpha}\zeta}{r^{10}} \right\} + \left(\zeta \rightarrow -\zeta \right)
\end{aligned}$$

$$\begin{aligned}
d_{\gamma\chi_{c2}}^{(+-,0)}(r, \alpha, \zeta = x/\xi) = & \frac{4\mathfrak{C}_{\chi_c} (\alpha - 1/r^2)}{\sqrt{6}\alpha^2 (1 + \bar{\alpha})^2 (\bar{\alpha} + 1/r^2)^2 (r^2 - 1)^2 (\zeta + 1 - i0) (\zeta - 1 + i0) (\zeta - \kappa + i0)^2} \times \quad (C34) \\
& \times \left\{ \frac{\bar{\alpha}}{4} \left[(\alpha - 2)^2 \alpha \zeta^4 - 2(2 - \alpha) (\alpha^4 - 4\alpha^3 + 6\alpha^2 - 6\alpha + 1) \zeta^3 - 2\alpha (2\alpha^4 - 8\alpha^3 + 13\alpha^2 - 9\alpha - 1) \zeta^2 \right. \right. \\
& \quad \left. + 2 (\alpha^5 - 2\alpha^4 + 2\alpha^3 + 3\alpha - 2) \zeta + \alpha (\alpha^2 + 6\alpha - 6) \right]
\end{aligned}$$

$$\begin{aligned}
& + \frac{1}{2r^2} [(\alpha - 2)(2\alpha^4 - 7\alpha^3 + 7\alpha^2 - 5\alpha + 2)\zeta^3 + 2(-4\alpha^5 + 17\alpha^4 - 31\alpha^3 + 33\alpha^2 - 16\alpha + 2)\zeta^2 \\
& \quad \alpha(6\alpha^4 - 15\alpha^3 + 17\alpha^2 + \alpha - 8)\zeta - 4\bar{\alpha}(\alpha + 1)(2\alpha - 1)] \\
& + \frac{1}{4r^4} [(\alpha - 2)^2\alpha\zeta^4 + 2(2 - \alpha)\bar{\alpha}^2(2\alpha - 1)\zeta^3 + 2(12\alpha^4 - 38\alpha^3 + 41\alpha^2 - 27\alpha + 8)\zeta^2 \\
& \quad + 2(-14\alpha^4 + 27\alpha^3 - 32\alpha^2 + 11\alpha + 2)\zeta - \alpha(5\alpha^2 + 34\alpha - 34)] \\
& + \frac{(\alpha - 2)(2 - \alpha\bar{\alpha})\zeta^3 + 2\bar{\alpha}\alpha(5\alpha - 8)\zeta^2 + (17\alpha^3 - 19\alpha^2 + 12\alpha - 4)\zeta + 8(\alpha^2 + \alpha - 1)}{2r^6} \\
& \left. + \frac{(2\alpha^2 - 5\alpha + 4)\zeta^2 + 2\bar{\alpha}(3\alpha + 1)\zeta - 3\alpha}{r^8} - \frac{2\bar{\alpha}\zeta}{r^{10}} \right\} + (\zeta \rightarrow -\zeta)
\end{aligned}$$

$$\begin{aligned}
c_{\gamma\chi_{c2}}^{(++,+1)}(r, \alpha, \zeta = x/\xi) = & -\frac{4\mathfrak{C}_{\chi_c} r^2 \sqrt{(1 - \alpha)(\alpha r^2 - 1)}}{\alpha(1 + \bar{\alpha})^2(\bar{\alpha} + 1/r^2)(r^2 - 1)^2(\zeta + 1 - i0)(\zeta - 1 + i0)(\zeta - \kappa + i0)^2} \times \quad (C35) \\
& \times \left\{ \begin{aligned}
& \bar{\alpha}\alpha^2[-2(\alpha - 4)\bar{\alpha}\zeta^4 - (\alpha^4 - 2\alpha^3 + 2\alpha^2 + 4\alpha - 4)\zeta^3 + 2(\alpha^4 - 4\alpha^2 + 4\alpha - 2)\zeta^2 \\
& \quad - (\alpha^4 + 2\alpha^3 - 10\alpha^2 + 12\alpha - 4)\zeta + 2\bar{\alpha}(3\alpha - 2)] + \\
& - \frac{1}{r^2}[4\alpha(5\alpha^2 - 12\alpha + 8)\zeta^4 + \alpha(7\alpha^6 - 41\alpha^5 + 113\alpha^4 - 188\alpha^3 + 230\alpha^2 - 200\alpha + 88)\zeta^3 \\
& \quad - 2\alpha(7\alpha^6 - 25\alpha^5 + 49\alpha^4 - 74\alpha^3 + 54\alpha^2 + 4\alpha - 20)\zeta^2 \\
& \quad + \alpha^2(7\alpha^5 - 9\alpha^4 + 5\alpha^3 + 12\alpha^2 - 38\alpha + 32)\zeta + 4\alpha(-4\alpha^3\bar{\alpha} - 9\alpha^2 + 16\alpha - 6)] \\
& + \frac{2}{r^4}[-\alpha(\alpha^4 - 5\alpha^3 + 3\alpha^2 + 8\alpha - 8)\zeta^4 + (7\alpha^6 - 35\alpha^5 + 71\alpha^4 - 76\alpha^3 + 68\alpha^2 - 72\alpha + 48)\zeta^3 \\
& \quad - 2(14\alpha^6 - 51\alpha^5 + 84\alpha^4 - 111\alpha^3 + 100\alpha^2 - 24\alpha - 24)\zeta^2 + \alpha(21\alpha^5 + 39\alpha^3\bar{\alpha} + 4\alpha^2 + 96\bar{\alpha})\zeta \\
& \quad + (3\alpha^5 + 31\alpha^4 - 83\alpha^3 + 36\alpha^2 + 40\alpha - 16)] \\
& + \frac{1}{r^6}[-(\alpha^2 + 2\alpha - 2)(11\alpha^3 - 26\alpha^2 - 4\alpha + 32)\zeta^3 + 2(39\alpha^5 - 128\alpha^4 + 130\alpha^3 - 90\alpha^2 + 148\alpha - 128)\zeta^2 \\
& \quad + (176\alpha^4 - 95\alpha^5 - 166\alpha^3 + 188\alpha^2 - 8\alpha - 192)\zeta + 2(\alpha - 2)^3\alpha\zeta^4 - 2\alpha(15\alpha^3 + 22\alpha^2 - 146\alpha + 132)] \\
& + \frac{4}{r^8}[(\alpha - 2)^2(2 - \alpha\bar{\alpha})\zeta^3 - (13\alpha^4 - 44\alpha^3 + 32\alpha^2 + 32\alpha - 40)\zeta^2 + (26\alpha^4 - 43\alpha^3 + 6\alpha^2 - 28\alpha + 56)\zeta \\
& \quad + 2(6\alpha^3 - 9\alpha^2 - 12\alpha + 20)] \\
& + \frac{8(\alpha - 2)(2\alpha^2 - 5\alpha + 4)\zeta^2 - 4(15\alpha^3 - 28\alpha^2 - 14\alpha + 32)\zeta - 8(\alpha - 2)(3\alpha - 4)}{r^{10}} + \frac{16(2 - \alpha)\bar{\alpha}\zeta}{r^{12}} \Big\} \\
& + (\zeta \rightarrow -\zeta)
\end{aligned} \right.
\end{aligned}$$

$$\begin{aligned}
d_{\gamma\chi_{c2}}^{(++,+1)}(r, \alpha, \zeta = x/\xi) = & \frac{4\mathfrak{C}_{\chi_c} \sqrt{(1 - \alpha)(\alpha r^2 - 1)}}{\bar{\alpha}\alpha^4(1 + \bar{\alpha})^2(\bar{\alpha} + 1/r^2)^2(r^2 - 1)^2(\zeta + 1 - i0)(\zeta - 1 + i0)(\zeta - \kappa + i0)^2} \times \quad (C36) \\
& \times \left\{ \begin{aligned}
& \frac{\bar{\alpha}^2\alpha^2}{8}[2(2 - \alpha)\bar{\alpha}\zeta^4 + (3\alpha^4 - 16\alpha^3 + 28\alpha^2 - 24\alpha + 8)\zeta^3 - 2\alpha(3\alpha^3 - 10\alpha^2 + 10\alpha - 2)\zeta^2 + \\
& \quad + (3\alpha^4 - 4\alpha^3 - 8\bar{\alpha})\zeta - 2\bar{\alpha}(\alpha + 2)] + \\
& + \frac{\bar{\alpha}\alpha}{8r^2}[(10\alpha^5 - 59\alpha^4 + 121\alpha^3 - 138\alpha^2 + 96\alpha - 32)\zeta^3 - 2(16\alpha^5 - 65\alpha^4 + 95\alpha^3 - 50\alpha^2 - 6\alpha + 12)\zeta^2 \\
& \quad + (22\alpha^5 - 47\alpha^4 + 29\alpha^3 + 22\alpha^2 - 36\alpha + 8)\zeta + 2(2 - \alpha)\bar{\alpha}(3\alpha - 2)\zeta^4 - 2\bar{\alpha}(3\alpha - 2)(3\alpha + 4)] \\
& + \frac{1}{8r^4}[2(2 - \alpha)\bar{\alpha}\alpha^2\zeta^4 + (11\alpha^6 - 66\alpha^5 + 134\alpha^4 - 148\alpha^3 + 116\alpha^2 - 64\alpha + 16)\zeta^3 - 2\bar{\alpha}(37\alpha^3 - 26\alpha^2 - 16\alpha + 8) \\
& \quad + \alpha(63\alpha^5 - 178\alpha^4 + 174\alpha^3 - 124\alpha + 64)\zeta + 2(-31\alpha^6 + 142\alpha^5 - 264\alpha^4 + 248\alpha^3 - 112\alpha^2 + 8\alpha + 8)\zeta^2] \\
& + \frac{1}{8r^6}[-\alpha(8\alpha^4 - 39\alpha^3 + 62\alpha^2 - 48\alpha + 16)\zeta^3 + 2(30\alpha^5 - 111\alpha^4 + 162\alpha^3 - 126\alpha^2 + 64\alpha - 16)\zeta^2 +
\end{aligned} \right.
\end{aligned}$$

$$\begin{aligned}
& + (-92\alpha^5 + 219\alpha^4 - 202\alpha^3 + 64\alpha^2 + 48\alpha - 32) \zeta - 2(\alpha - 2)^2 \bar{\alpha} \alpha \zeta^4 + 2\alpha \bar{\alpha} (5\alpha^2 + 62\alpha - 52)] \\
& + \frac{1}{2r^8} [(2 - \alpha) \bar{\alpha} (\alpha^2 - \alpha + 2) \zeta^3 + (-10\alpha^4 + 31\alpha^3 - 30\alpha^2 + 4\alpha + 4) \zeta^2 + (20\alpha^4 - 33\alpha^3 + 15\alpha^2 - 8\alpha + 4) \zeta \\
& \quad - 4\bar{\alpha} (2\alpha^2 + 4\alpha - 3)] \\
& + \frac{6\alpha \bar{\alpha} - 2\bar{\alpha} (2\alpha^2 - 5\alpha + 4) \zeta^2 - (12\alpha^3 - 15\alpha^2 - 6\alpha + 8) \zeta}{2r^{10}} + \frac{2\bar{\alpha}^2 \zeta}{r^{12}} \Big\} + \left(\zeta \rightarrow -\zeta \right)
\end{aligned}$$

$$\begin{aligned}
c_{\gamma\chi_{c2}}^{(+-,+1)}(r, \alpha, \zeta = x/\xi) = & -\frac{4\mathfrak{C}_{\chi_c} r^2 \sqrt{(1-\alpha)(\alpha r^2 - 1)}}{\alpha (1+\bar{\alpha})^2 (\bar{\alpha} + 1/r^2) (r^2 - 1)^2 (\zeta + 1 - i0) (\zeta - 1 + i0) (\zeta - \kappa + i0)^2} \times \quad (C37) \\
& \times \left\{ \begin{aligned}
& \bar{\alpha} \alpha^2 (2 - \alpha) [\alpha^2 \zeta + 2(2 - \alpha) \alpha \zeta^2 + (2 - \alpha)^2 \zeta^3] \\
& + \frac{\alpha}{r^2} [(9\alpha^5 - 51\alpha^4 + 109\alpha^3 - 130\alpha^2 + 88\alpha - 16) \zeta^3 - 2\alpha (9\alpha^4 - 35\alpha^3 + 57\alpha^2 - 50\alpha + 14) \zeta^2 \\
& \quad + 4(\alpha - 2)^2 \alpha \zeta^4 + (9\alpha^5 - 19\alpha^4 + 25\alpha^3 - 2\alpha^2 + 4\alpha - 8) \zeta + 4\alpha (\alpha^2 - 3\bar{\alpha})] \\
& + \frac{2}{r^4} [(\alpha - 2)^2 \alpha \zeta^4 - \alpha (7\alpha^4 - 33\alpha^3 + 45\alpha^2 - 28\alpha + 16) \zeta^3 + 2\alpha (16\alpha^4 - 52\alpha^3 + 63\alpha^2 - 43\alpha + 4) \zeta^2 \\
& \quad - (25\alpha^5 - 37\alpha^4 + 37\alpha^3 + 8\alpha^2 + 4\alpha - 8) \zeta - \alpha (19\alpha^2 + 6\alpha - 12)] \\
& + \frac{1}{r^6} [-2(\alpha - 2)^2 \alpha \zeta^4 + (9\alpha^4 - 32\alpha^3 + 28\alpha^2 - 16) \zeta^3 - 2 (37\alpha^4 - 90\alpha^3 + 56\alpha^2 - 32\alpha + 8) \zeta^2 + \\
& \quad + (101\alpha^4 - 104\alpha^3 + 100\alpha^2 + 40\alpha - 16) \zeta + 2 (5\alpha^3 + 40\alpha^2 - 4\alpha - 8)] \\
& + \frac{4 ((2 - \alpha) (\alpha^2 - \alpha + 2) \zeta^3 + (11\alpha^3 - 20\alpha^2 - 2\alpha + 12) \zeta^2 - (24\alpha^3 - 9\alpha^2 + 10\alpha - 4) \zeta - 2(\alpha + 2)(4\alpha - 1))}{r^8} + \\
& - \frac{8 (2\alpha^2 - 5\alpha + 4) \zeta^2 - 4 (13\alpha^2 - 8) \zeta - 24\alpha}{r^{10}} + \frac{16\bar{\alpha}\zeta}{r^{12}} \Big\} + \left(\zeta \rightarrow -\zeta \right)
\end{aligned} \right.
\end{aligned}$$

$$d_{\gamma\chi_{c2}}^{(+-,+1)}(r, \alpha, \zeta = x/\xi) = \frac{\zeta \sqrt{(1-\alpha)(\alpha r^2 - 1)} (\alpha \bar{\alpha} + \alpha r^2 - 1)}{2\bar{\alpha} \alpha^2 (\zeta + 1 - i0) (\zeta - 1 + i0) r^2 (r^2 - 1)^2} + \left(\zeta \rightarrow -\zeta \right) = 0 \quad (C38)$$

$$\begin{aligned}
c_{\gamma\chi_{c2}}^{(++,+2)}(r, \alpha, \zeta = x/\xi) = & \frac{4\mathfrak{C}_{\chi_c} (1 - \alpha) (\alpha r^2 - 1) r^2}{\alpha^2 (1 + \bar{\alpha})^2 (\bar{\alpha} + 1/r^2) (r^2 - 1)^2 (\zeta + 1 - i0) (\zeta - 1 + i0) (\zeta - \kappa + i0)^2} \times \quad (C39) \\
& \times \left\{ \begin{aligned}
& \bar{\alpha} \alpha^2 [-(2 - \alpha) \alpha \zeta^4 + (2\alpha^4 - 11\alpha^3 + 20\alpha^2 - 16\alpha + 4) \zeta^3 - 2(2 - \alpha) \bar{\alpha} \alpha (2\alpha - 1) \zeta^2 + \\
& \quad + (2\alpha^4 - 3\alpha^3 + 4\alpha - 4) \zeta - (2 - \alpha) \alpha] \\
& + \frac{1}{r^2} [(\alpha - 2) \alpha (\alpha^3 + \alpha^2 + 2\alpha - 8) \zeta^4 + \alpha (2\alpha^6 - 11\alpha^5 + 23\alpha^4 - 37\alpha^3 + 44\alpha^2 - 44\alpha + 32) \zeta^3 + \alpha^5 - \alpha^4 - 4\alpha^3 \\
& \quad + 2(2 - \alpha) \alpha (2\alpha^5 + \alpha^4 - 6\alpha^3 + 2\alpha^2 + 4\alpha + 2) \zeta^2 + \alpha^2 (2\alpha^5 + 5\alpha^4 - 17\alpha^3 + 15\alpha^2 - 4\alpha + 8) \zeta + 16\alpha^2 - 8\alpha] \\
& + \frac{1}{r^4} [2(2 - \alpha) \alpha (\alpha^2 - 2) \zeta^4 + -2 (\alpha^6 - 8\alpha^5 + 20\alpha^4 - 34\alpha^3 + 36\alpha^2 - 28\alpha + 24) \zeta^3 + 4 (3\alpha^6 - 13\alpha^5 + 20\alpha^4) \zeta^2 \\
& \quad + 4 (22\alpha^2 \bar{\alpha} - 10\alpha - 12) \zeta^2 - 2\alpha (5\alpha^5 - 6\alpha^4 + 6\alpha^2 - 16\alpha + 36) \zeta + 2(2 - \alpha) (\alpha^3 - 10\alpha^2 - 6\alpha + 4)] \\
& + \frac{1}{r^6} [2(\alpha - 2)^2 \alpha \zeta^4 + (-7\alpha^4 + 16\alpha^3 - 4\alpha^2 - 24\alpha + 32) \zeta^3 - 2 (4\alpha^5 - 31\alpha^4 + 52\alpha^3 - 42\alpha^2 + 52\alpha - 64) \zeta^2 + \\
& \quad + (16\alpha^5 - 51\alpha^4 + 40\alpha^3 - 28\alpha^2 + 24\alpha + 96) \zeta - 2\alpha (3\alpha^2 + 30\alpha - 56)] \\
& + \frac{4 [(\alpha - 2) (\alpha^2 - \alpha + 2) \zeta^3 - (9\alpha^3 - 14\alpha^2 - 8\alpha + 20) \zeta^2 - (2\alpha^4 - 16\alpha^3 + 7\alpha^2 - 4\alpha + 28) \zeta + 2 (3\alpha^2 + 2\alpha - 10)]}{r^8} \\
& + \frac{4 [2 (2\alpha^2 - 5\alpha + 4) \zeta^2 - (11\alpha^2 - 16) \zeta - 2(3\alpha - 4)]}{r^{10}} - \frac{16\bar{\alpha}\zeta}{r^{12}} \Big\} + \left(\zeta \rightarrow -\zeta \right)
\end{aligned} \right.
\end{aligned}$$

$$\begin{aligned}
d_{\gamma\chi_{c2}}^{(++,+2)}(r, \alpha, \zeta = x/\xi) = & -\frac{4\mathfrak{C}_{\chi_c}\bar{\alpha}}{\alpha^2(1+\bar{\alpha})^2(\bar{\alpha}+1/r^2)^2(r^2-1)^2(\zeta+1-i0)(\zeta-1+i0)(\zeta-\kappa+i0)^2} \times \quad (C40) \\
& \times \left\{ \frac{\bar{\alpha}\alpha}{4} [(\alpha-2)^2\zeta^4 - 2(2-\alpha)(\alpha^3-3\alpha^2+3\alpha-3)\zeta^3 - 2(2\alpha^4-6\alpha^3+6\alpha^2-\alpha-4)\zeta^2 \right. \\
& \quad + 2(\alpha^4-\alpha^3-\alpha^2+5\alpha-2)\zeta + (3\alpha^2+2\alpha-4)] + \\
& \quad + \frac{1}{2r^2} [(\alpha-2)(2\alpha^4-7\alpha^3+7\alpha^2-5\alpha+2)\zeta^3 + 2(-4\alpha^5+15\alpha^4-21\alpha^3+15\alpha^2-2\alpha-2)\zeta^2 + \\
& \quad + \alpha(6\alpha^4-11\alpha^3+5\alpha^2+13\alpha-12)\zeta - 4\bar{\alpha}(\alpha+1)(2\alpha-1)] \\
& \quad + \frac{1}{4r^4} [(\alpha-2)^2\alpha\zeta^4 + 2(2-\alpha)\bar{\alpha}^2\alpha\zeta^3 + 2(\alpha-2)(10\alpha^3-13\alpha^2+11\alpha-4)\zeta^2 + \\
& \quad 2(-13\alpha^4+20\alpha^3-15\alpha^2-6\alpha+8)\zeta + \alpha(\alpha^2-46\alpha+40)] \\
& \quad + \frac{(\alpha-2)(\alpha^2-\alpha+2)\zeta^3 + 2\bar{\alpha}(3\alpha^2-4\alpha-2)\zeta^2 + (13\alpha^3-11\alpha^2+8\alpha-4)\zeta + 4(\alpha^2+4\alpha-3)}{2r^6} + \\
& \quad \left. \frac{(2\alpha^2-5\alpha+4)\zeta^2 + 4\bar{\alpha}(\alpha+1)\zeta - 3\alpha}{r^8} - \frac{2\bar{\alpha}\zeta}{r^{10}} \right\} + (\zeta \rightarrow -\zeta)
\end{aligned}$$

$$\begin{aligned}
c_{\gamma\chi_{c2}}^{(+-,+2)}(r, \alpha, \zeta = x/\xi) = & \frac{4\mathfrak{C}_{\chi_c}(1-\alpha)(\alpha r^2-1)r^2}{\alpha^2(1+\bar{\alpha})^2(\bar{\alpha}+1/r^2)(r^2-1)^2(\zeta+1-i0)(\zeta-1+i0)(\zeta-\kappa+i0)^2} \times \quad (C41) \\
& \times \left\{ \bar{\alpha}\alpha^2(2\alpha-1)[\alpha^2\zeta + 2(2-\alpha)\alpha\zeta^2 + (2-\alpha)^2\zeta^3] \right. \\
& \quad + \frac{1}{r^2} [-5(\alpha-2)^2\alpha^2\zeta^4 - \alpha(6\alpha^5-37\alpha^4+87\alpha^3-115\alpha^2+80\alpha-12)\zeta^3\alpha^2(5\alpha^2+8\alpha-8) \\
& \quad + 2\alpha^2(6\alpha^4-29\alpha^3+56\alpha^2-45\alpha+8)\zeta^2 - \alpha^2(2\alpha-1)(3\alpha^3-9\alpha^2+7\alpha+8)\zeta] \\
& \quad + \frac{1}{r^4} [-(\alpha-2)^2\bar{\alpha}\alpha\zeta^4 + 2\alpha(4\alpha^4-20\alpha^3+26\alpha^2-19\alpha+18)\zeta^3 - 2\alpha^2(20\alpha^3-73\alpha^2+109\alpha-78)\zeta^2 \\
& \quad + 2(16\alpha^5-34\alpha^4+38\alpha^3+9\alpha^2+2\alpha-4)\zeta + \alpha(\alpha^3+35\alpha^2+4\alpha-12)] \\
& \quad + \frac{1}{r^6} [(\alpha-2)^2\alpha\zeta^4 + (-4\alpha^4+15\alpha^3-8\alpha^2-8\alpha+8)\zeta^3 + 4(10\alpha^4-25\alpha^3+22\alpha^2-20\alpha+2)\zeta^2 + \\
& \quad + (-60\alpha^4+83\alpha^3-104\alpha^2-40\alpha+8)\zeta - 11\alpha^3-64\alpha^2+4\alpha+8] \\
& \quad + \frac{2(\alpha-2)(\alpha^2-\alpha+2)\zeta^3 - 4(5\alpha^3-7\alpha^2-5\alpha+6)\zeta^2 + 2(25\alpha^3-9\alpha^2+28\alpha-4)\zeta + 4(7\alpha^2+11\alpha-2)}{r^8} \\
& \quad \left. + \frac{4[(2\alpha^2-5\alpha+4)\zeta^2 - (6\alpha^2+3\alpha-4)\zeta - 5\alpha]}{r^{10}} - \frac{8\bar{\alpha}\zeta}{r^{12}} \right\} + (\zeta \rightarrow -\zeta)
\end{aligned}$$

$$\begin{aligned}
d_{\gamma\chi_{c2}}^{(+-,+2)}(r, \alpha, \zeta = x/\xi) = & -\frac{4\mathfrak{C}_{\chi_c}\bar{\alpha}}{\alpha^2(1+\bar{\alpha})^2(\bar{\alpha}+1/r^2)^2(r^2-1)^2(\zeta+1-i0)(\zeta-1+i0)(\zeta-\kappa+i0)^2} \times \quad (C42) \\
& \times \left\{ \frac{\alpha}{4} [(\alpha-2)^2\alpha\zeta^4 + 2(\alpha^2-2\alpha+2)[(\alpha-2)(\alpha^2-3\alpha+1)\zeta^3 + (\alpha^3-\alpha^2-\alpha+2)\zeta] \right. \\
& \quad - 2(2\alpha^4-10\alpha^3+19\alpha^2-14\alpha+2)\alpha\zeta^2 + \alpha^3] + \\
& \quad - \frac{1}{2r^2} [(\alpha-2)^2\alpha\zeta^4 - (2-\alpha)(2\alpha^4-9\alpha^3+13\alpha^2-11\alpha+1)\zeta^3 - \alpha(8\alpha^4-38\alpha^3+70\alpha^2-49\alpha+5)\zeta^2 \\
& \quad + (6\alpha^5-17\alpha^4+19\alpha^3-3\alpha^2-3\alpha+2)\zeta + \alpha(3\alpha^2+\bar{\alpha})] \\
& \quad + \frac{(\alpha-2)(\alpha^3+4\alpha\bar{\alpha}-4)\zeta^3 - 2\alpha(5\alpha^3-22\alpha^2+39\alpha-24)\zeta^2 + \alpha(13\alpha^3-34\alpha^2+36\alpha-4)\zeta + 6\alpha^2}{2r^4} \\
& \quad \left. \frac{(2-\alpha)\zeta^3 + (4\alpha^3-16\alpha^2+31\alpha-16)\zeta^2 - (12\alpha^3-28\alpha^2+27\alpha+2)\zeta - 7\alpha}{2r^6} + \frac{2[(\alpha^2+2\bar{\alpha})\zeta - \zeta^2+1]}{r^8} \right\} + (\zeta \rightarrow -\zeta)
\end{aligned}$$

-
- [1] M. Diehl, T. Feldmann, R. Jakob and P. Kroll, Nucl. Phys. B **596**, 33 (2001) [Erratum-ibid. B **605**, 647 (2001)] [arXiv:hep-ph/0009255].
- [2] K. Goeke, M. V. Polyakov and M. Vanderhaeghen, Prog. Part. Nucl. Phys. **47**, 401 (2001) [arXiv:hep-ph/0106012].
- [3] M. Diehl, Phys. Rept. **388**, 41 (2003) [arXiv:hep-ph/0307382].
- [4] M. Guidal, H. Moutarde and M. Vanderhaeghen, “*Generalized Parton Distributions in the valence region from Deeply Virtual Compton Scattering*,” Rept. Prog. Phys. **76** (2013), 066202 [arXiv:1303.6600 [hep-ph]].
- [5] D. Boer, M. Diehl, R. Milner, R. Venugopalan, W. Vogelsang, D. Kaplan, H. Montgomery, S. Vigdor, A. Accardi and E. C. Aschenauer, *et al.* “*Gluons and the quark sea at high energies: Distributions, polarization, tomography*,” [arXiv:1108.1713 [nucl-th]].
- [6] H. Dutrieux, C. Lorcé, H. Moutarde, P. Szajner, A. Trawinski and J. Wagner, “*Phenomenological assessment of proton mechanical properties from deeply virtual Compton scattering*,” Eur. Phys. J. C **81**, no.4, 300 (2021) [arXiv:2101.03855 [hep-ph]].
- [7] V. Burkert, L. Elouadrhiri, A. Afanasev, J. Arrington, M. Contalbrigo, W. Cosyn, A. Deshpande, D. Glazier, X. Ji and S. Liuti, *et al.* “*Precision Studies of QCD in the Low Energy Domain of the EIC*,” [arXiv:2211.15746 [nucl-ex]].
- [8] R. Abdul Khalek *et al.* “*Science Requirements and Detector Concepts for the Electron-Ion Collider: EIC Yellow Report*,” [arXiv:2103.05419 [physics.ins-det]].
- [9] A. Accardi *et al.*, Eur. Phys. J. A **52**, no. 9, 268 (2016) [arXiv:1212.1701 [nucl-ex]].
- [10] K. Kumericki, S. Liuti and H. Moutarde, “*GPD phenomenology and DVCS fitting: Entering the high-precision era*,” Eur. Phys. J. A **52** (2016) no.6, 157 [arXiv:1602.02763 [hep-ph]].
- [11] V. Bertone, H. Dutrieux, C. Mezrag, H. Moutarde and P. Szajner, “*Deconvolution problem of deeply virtual Compton scattering*,” Phys. Rev. D **103**, no.11, 114019 (2021) [arXiv:2104.03836 [hep-ph]].
- [12] E. Moffat, A. Freese, I. Cloët, T. Donohoe, L. Gamberg, W. Melnitchouk, A. Metz, A. Prokudin and N. Sato, “*Shedding light on shadow generalized parton distributions*,” Phys. Rev. D **108**, no.3, 036027 (2023) [arXiv:2303.12006 [hep-ph]].
- [13] Y. Guo, X. Ji, M. G. Santiago, K. Shiells and J. Yang, “*Generalized parton distributions through universal moment parameterization: non-zero skewness case*,” JHEP **05**, 150 (2023) [arXiv:2302.07279 [hep-ph]].
- [14] G. Duplančić, S. Nabeebaccus, K. Passek-Kumerički, B. Pire, L. Szymanowski and S. Wallon, “*Accessing chiral-even quark generalised parton distributions in the exclusive photoproduction of a $\gamma\pi^\pm$ pair with large invariant mass in both fixed-target and collider experiments*,” [arXiv:2212.00655 [hep-ph]].
- [15] G. Duplančić, K. Passek-Passek-Kumerički, B. Pire, L. Szymanowski and S. Wallon, JHEP 11 (2018) 179 [arXiv:1809.08104 [hep-ph]].
- [16] R. Boussarie, B. Pire, L. Szymanowski and S. Wallon, JHEP 02 (2017) 054 [erratum: JHEP **10** (2018), 029] [arXiv:1609.03830 [hep-ph]].
- [17] W. Cosyn and B. Pire, Phys. Rev. D **103** (2021) 114002 [arXiv:2103.01411 [hep-ph]].
- [18] A. Pedrak, B. Pire, L. Szymanowski and J. Wagner, Phys. Rev. D **101** (2020) 114027 [arXiv:2003.03263 [hep-ph]].
- [19] B. Pire, L. Szymanowski and S. Wallon, Phys. Rev. D **101** (2020) 074005 [arXiv:1912.10353 [hep-ph]].
- [20] A. Pedrak, B. Pire, L. Szymanowski and J. Wagner, Phys. Rev. D **96** (2017) 074008 [arXiv:1708.01043 [hep-ph]].
- [21] M. El Beiyad, B. Pire, M. Segond, L. Szymanowski and S. Wallon, Phys. Lett. B **688** (2010) 154 [arXiv:1001.4491 [hep-ph]].
- [22] D.Y. Ivanov, B. Pire, L. Szymanowski and O.V. Teryaev, Phys. Lett. B **550** (2002) 65 [arXiv:hep-ph/0209300].
- [23] G. Duplančić, S. Nabeebaccus, K. Passek-Kumerički, B. Pire, L. Szymanowski and S. Wallon, “*Accessing GPDs through the exclusive photoproduction of a photon-meson pair with a large invariant mass*,” [arXiv:2212.01034 [hep-ph]].
- [24] J. W. Qiu and Z. Yu, “*Extracting transition generalized parton distributions from hard exclusive pion-nucleon scattering*,” Phys. Rev. D **109**, no.7, 074023 (2024) [arXiv:2401.13207 [hep-ph]].
- [25] J. W. Qiu and Z. Yu, “*Extraction of the Parton Momentum-Fraction Dependence of Generalized Parton Distributions from Exclusive Photoproduction*,” Phys. Rev. Lett. **131**, no.16, 161902 (2023) [arXiv:2305.15397 [hep-ph]].
- [26] K. Deja, V. Martinez-Fernandez, B. Pire, P. Szajner and J. Wagner, “*Phenomenology of double deeply virtual Compton scattering in the era of new experiments*,” Phys. Rev. D **107**, no.9, 094035 (2023) [arXiv:2303.13668 [hep-ph]].
- [27] M. Siddikov and I. Schmidt, “*Exclusive production of quarkonia pairs in collinear factorization framework*,” Phys. Rev. D **107** (2023) no.3, 034037 [arXiv:2212.14019 [hep-ph]].
- [28] M. Siddikov and I. Schmidt, “*Exclusive photoproduction of D-meson pairs with large invariant mass*,” Phys. Rev. D **108** (2023) no.9, 096031 [arXiv:2309.09748 [hep-ph]].
- [29] J.-W. Qiu and Z. Yu, “*Exclusive production of a pair of high transverse momentum photons in pion-nucleon collisions for extracting generalized parton distributions*”, [arXiv:2205.07846 [hep-ph]].
- [30] J.-W. Qiu and Z. Yu, “*Single diffractive hard exclusive processes for the study of generalized parton distributions*”, [arXiv:2210.07995 [hep-ph]].
- [31] G. Duplan, S. Nabeebaccus, K. Passek-Kumerički, B. Pire, J. Schönleber, L. Szymanowski and S. Wallon, [arXiv:2401.17656 [hep-ph]].
- [32] S. Nabeebaccus, J. Schönleber, L. Szymanowski and S. Wallon, [arXiv:2311.09146 [hep-ph]].
- [33] M. Siddikov, “*Exclusive photoproduction of $\eta_c\gamma$ pairs with large invariant mass*,” Phys. Rev. D **110**, no.5, 056043 (2024) [arXiv:2408.01822 [hep-ph]].
- [34] J. G. Korner and G. Thompson, Phys. Lett. B **264**, 185 (1991).
- [35] M. Neubert, “*Heavy quark symmetry*,” Phys. Rept. **245** (1994), 259-396 [arXiv:hep-ph/9306320 [hep-ph]].

- [36] G. T. Bodwin, E. Braaten and G. P. Lepage, Phys. Rev. D **51**, 1125 (1995) Erratum: [Phys. Rev. D **55**, 5853 (1997)] [hep-ph/9407339].
- [37] F. Maltoni, M. L. Mangano and A. Petrelli, Nucl. Phys. B **519**, 361 (1998) [hep-ph/9708349].
- [38] N. Brambilla, E. Mereghetti and A. Vairo, Phys. Rev. D **79**, 074002 (2009) Erratum: [Phys. Rev. D **83**, 079904 (2011)] [arXiv:0810.2259 [hep-ph]].
- [39] Y. Feng, J. P. Lansberg and J. X. Wang, Eur. Phys. J. C **75**, no. 7, 313 (2015) [arXiv:1504.00317 [hep-ph]].
- [40] N. Brambilla *et al.*; Eur. Phys. J. C**71**, 1534 (2011).
- [41] P. L. Cho and A. K. Leibovich, Phys. Rev. D **53**, 6203 (1996) [hep-ph/9511315].
- [42] P. L. Cho and A. K. Leibovich, Phys. Rev. D **53**, 150 (1996) [hep-ph/9505329].
- [43] S. Benić, A. Dumitru, A. Kaushik, L. Motyka and T. Stobel, Phys. Rev. D **110** (2024) 1, 014025 [arXiv:2402.19134 [hep-ph]].
- [44] S. J. Brodsky, H. C. Pauli and S. S. Pinsky, “*Quantum chromodynamics and other field theories on the light cone*,” Phys. Rept. **301** (1998), 299-486 [arXiv:hep-ph/9705477 [hep-ph]].
- [45] S. V. Goloskokov and P. Kroll, Eur. Phys. J. C **65**, 137 (2010) [arXiv:0906.0460 [hep-ph]].
- [46] H. Mäntysaari, K. Roy, F. Salazar and B. Schenke, Phys. Rev. D **103**, no.9, 094026 (2021) [arXiv:2011.02464 [hep-ph]].
- [47] J. Collins, “*Foundations of Perturbative QCD*,” Camb. Monogr. Part. Phys. Nucl. Phys. Cosmol. **32**, 1-624 (2011), Cambridge University Press, 2011, ISBN 978-1-009-40184-5, 978-1-009-40183-8, 978-1-009-40182-1, doi:10.1017/9781009401845.
- [48] C. F. von Weizsäcker, “*Radiation emitted in collisions of very fast electrons*,” Z. Phys. **88**, 612 (1934).
- [49] E. J. Williams, “*Correlation of certain collision problems with radiation theory*,” Kong. Dan. Vid. Sel. Mat. Fys. Medd. **13N4**, 1 (1935).
- [50] V. M. Budnev, I. F. Ginzburg, G. V. Meledin and V. G. Serbo, “*The Two photon particle production mechanism. Physical problems. Applications. Equivalent photon approximation*,” Phys. Rept. **15** (1975), 181-281.
- [51] A. V. Belitsky, D. Mueller and A. Kirchner, Nucl. Phys. B **629**, 323 (2002) [arXiv:hep-ph/0112108].
- [52] A. V. Belitsky and A. V. Radyushkin, Phys. Rept. **418**, 1 (2005) [arXiv:hep-ph/0504030].
- [53] S. V. Goloskokov and P. Kroll, Eur. Phys. J. C **50**, 829 (2007) [hep-ph/0611290].
- [54] S. V. Goloskokov and P. Kroll, Eur. Phys. J. C **53**, 367 (2008) [arXiv:0708.3569 [hep-ph]].
- [55] S. V. Goloskokov and P. Kroll, Eur. Phys. J. C **59** (2009) 809 [arXiv:0809.4126 [hep-ph]].
- [56] S. V. Goloskokov and P. Kroll, Eur. Phys. J. A **47**, 112 (2011) [arXiv:1106.4897 [hep-ph]].
- [57] G. P. Lepage and S. J. Brodsky, “*Exclusive processes in perturbative quantum chromodynamics*”, Phys. Rev. D **22** (1980) 2157.
- [58] S. Navas *et al.* [Particle Data Group], Phys. Rev. D **110**, 030001 (2024).
- [59] M. Ablikim *et al.* [BESIII], “*Measurements of the branching fractions of $\chi_c \rightarrow K^+ K^- \pi^0$, $K_S^0 K^\pm \pi^\mp$, $2(\pi^+ \pi^- \pi^0)$, and $p\bar{p}$* ,” Phys. Rev. D **100** (2019) no.1, 012003 [arXiv:1903.05375 [hep-ex]].
- [60] J. Czyzowski, J. Kwiecinski, L. Motyka, and M. Sadzikowski, Phys. Lett. B 398, 400 (1997); 411, 402 (1997).
- [61] R. Engel, D. Y. Ivanov, R. Kirschner, and L. Szymanowski, Eur. Phys. J. C **4**, 93 (1998).
- [62] A. Dumitru, T. Stobel, Phys. Rev. D **99**, 094038 (2019).
- [63] J. Bartels, Nucl. Phys. B175, 365 (1980); T. Jaroszewicz, Acta Phys. Polon. B **11**, 965 (1980); J. Kwiecinski and M. Praszalowicz, Phys. Lett. 94B, 413 (1980).
- [64] L. Lukaszuk and B. Nicolescu, Lett. Nuovo Cim. **8**, 405 (1973); D. Joynson, E. Leader, B. Nicolescu, and C. Lopez, Nuovo Cimento A **30**, 345 (1975).
- [65] C. Ewerz, arXiv:hep-ph/0306137.
- [66] S. Benic, D. Horvatic, A. Kaushik, and E. A. Vivoda, “*Exclusive χ_c production from small-x evolved Odderon at a electron-ion collider*,” Phys. Rev. D **108** (2023) 7, 074005. [arXiv:2306.10626 [hep-ph]].
- [67] G. Antchev *et al.* (TOTEM Collaboration), arXiv:1812.08610.
- [68] V. M. Abazov *et al.* (D0 Collaboration), Phys. Rev. D **86**, 012009 (2012).
- [69] A. Accardi, P. Achenbach, D. Adhikari, A. Afanasev, C. S. Akondi, N. Akopov, M. Albaladejo, H. Albataineh, M. Albrecht and B. Almeida-Zamora, *et al.* “*Strong Interaction Physics at the Luminosity Frontier with 22 GeV Electrons at Jefferson Lab*,” [arXiv:2306.09360 [nucl-ex]].
- [70] J. P. Ma and Z. G. Si, “*NRQCD Factorization for Twist-2 Light-Cone Wave-Functions of Charmonia*,” Phys. Lett. B **647** (2007), 419-426 [arXiv:hep-ph/0608221 [hep-ph]].
- [71] X. P. Wang and D. Yang, “*The leading twist light-cone distribution amplitudes for the S-wave and P-wave quarkonia and their applications in single quarkonium exclusive productions*,” JHEP **06** (2014), 121 [arXiv:1401.0122 [hep-ph]].
- [72] W. Wang, J. Xu, D. Yang and S. Zhao, “*Relativistic corrections to light-cone distribution amplitudes of S-wave B_c mesons and heavy quarkonia*,” JHEP **12** (2017), 012 [arXiv:1706.06241 [hep-ph]].
- [73] V.M. Braun and I.B. Filyanov, Z. Phys. C **48** (1990) 239,
- [74] P. Ball, JHEP **01** (1999) 010.
- [75] P. Ball and V.M. Braun, Phys. Rev. D **54** (1996) 2182.
- [76] P. Ball, V. M. Braun, Y. Koike and K. Tanaka, Nucl. Phys. B **529** (1998) 323.
- [77] P. Ball and V.M. Braun, Nucl. Phys. B **543** (1999) 201.
- [78] I. Babiarz, R. Pasechnik, W. Schaefer and A. Szczurek, JHEP **06** (2020), 101 [arXiv:2002.09352 [hep-ph]].
- [79] M. Diehl, T. Gousset and B. Pire, “*Polarization in deeply virtual meson production*,” [arXiv:hep-ph/9909445 [hep-ph]].
- [80] X. D. Ji, J. Phys. G **24**, 1181 (1998) [arXiv:hep-ph/9807358].
- [81] D. Yu. Ivanov, A. Schafer, L. Szymanowski and G. Krasnikov, Eur. Phys. J. C **34** (2004) 297, [arXiv:hep-ph/0401131].
- [82] E. Braaten and J. Lee, “*Exclusive Double Charmonium Production from $e^+ e^-$ Annihilation into a Virtual Photon*,” Phys. Rev. D **67** (2003), 054007 [erratum: Phys. Rev. D **72** (2005), 099901] [arXiv:hep-ph/0211085 [hep-ph]].